The complex genetic architecture of shoot growth

natural variation in *Arabidopsis thaliana*

Marchadier*, Hanemian*, Tisné*, Bach, Bazakos, Gilbault, Haddadi, Virlouvet, Loudet
* co-first authors

Institut Jean-Pierre Bourgin, INRA, AgroParisTech, CNRS, Université Paris-Saclay, 78000, Versailles, France

ABSTRACT

One of the main outcome of quantitative genetics approaches to natural variation is to reveal the genetic architecture underlying the phenotypic space. Complex genetic architectures are described as including numerous loci (or alleles) with small-effect and/or low-frequency in the populations, interactions with the genetic background, environment or age... Linkage or association mapping strategies will be more or less sensitive to this complexity, so that we still have an unclear picture of its extent. By combining high-throughput phenotyping under two environmental conditions with classical QTL mapping approaches in multiple *Arabidopsis thaliana* segregating populations as well as advanced near isogenic lines construction and survey, we have attempted to push back the limits of our understanding of quantitative phenotypic variation. Integrative traits such as those related to vegetative growth used in this work (highlighting either cumulative growth, growth rate or morphology) all showed complex and dynamic genetic architecture with respect to the segregating population and condition. The more resolutive our mapping approach, the more complexity we uncover, with several instances of QTLs visible in near isogenic lines but not detected with the initial QTL mapping, indicating that our phenotyping resolution was less limiting than the mapping resolution with respect to the underlying genetic architecture. In an ultimate approach to resolve this complexity, we intensified our phenotyping effort to target specifically a 3Mb-region known to segregate for a major quantitative trait gene, using a series of selected lines recombined every 100kb. We discovered that at least 3 other independent QTLs had remained hidden in this region, some with trait- or condition-specific effects, or opposite allelic effects. If we were to extrapolate the figures obtained on this specific region in this particular cross to the genome- and species-scale, we would predict hundreds of causative loci of detectable phenotypic effect controlling these growth-related phenotypes.

INTRODUCTION

Fine-tuning plant growth throughout development and in response to environmental limitations is a decisive process to optimize fitness and population survival in the wild. As a sessile organism, plants have to cope with environmental fluctuations and evolved a wide range of responses. This is well illustrated by their great phenotypic plasticity and their ability to colonize very diverse habitats, through intraspecific genetic diversity as revealed in most pathways [1]. Aerial and below-ground growth represent a balance between resource investment in the structures and resource acquisition (respectively photosynthesis and water / nutrient uptake). Thus, growth is a highly complex trait controlled by many genes with constitutive or more specific roles depending on developmental stage, tissue, timing, environment… [2-7]. In this context, plant growth can be considered as a model complex trait to increase our knowledge in the genetics of adaptation/evolution, as well as to improve plant performance.

Forward mutant analysis plays a central role in plant biology to blindly identify gene functions associated with a phenotype [8], but sometimes remains limiting to reveal genes with modest phenotypic effect, or when addressing genes from redundant families. With regard to growth and stress tolerance, these limitations are likely to be relevant given the multigenic nature of growth phenotypes, the low mean effect at each locus and/or epistatic interaction they involve [9, 10]. Thus, the use of naturally-occurring variation through quantitative genetic approaches designed to map quantitative trait loci (QTLs) is interesting notably to complement the search for alleles selected during evolution which may not be brought out with classical loss-of-function approaches. Linkage mapping and genome-wide association lead to the identification of large amount of alleles involved in intraspecific phenotype variation from different plant species [1, 11].

With the drop of sequencing and genotyping costs, phenotyping clearly is the limiting factor for quantitative genetics approaches [12]. However the complexity of the genetic architecture of a given trait, which depends on the contribution and the number of loci controlling a trait and their interactions with the genetic background and the environment, has direct consequences on how much phenotyping remains limiting. Highly heritable traits with a limited number of contributing loci (in a given segregating material, or at the species scale) are more likely to be well understood than more complex traits. For instance, a large part of the phenotypic variation for flowering time in *Arabidopsis thaliana* maps to a limited number of loci [13-16], including *FRIGIDA* and *FLC* genes [17-19] and thus has a relatively simple genetic architecture, although many more loci make smaller contributions -at least in some environments- and allelic heterogeneity also interferes [15, 16, 20, 21]. By contrast, traits like fitness or growth can be

expected to have a more complex basis as they integrate many upstream traits, and consequently many genes, each prone to residual variation and heterogeneity. Smaller contributions from individual loci means that, although one can still estimate total heritabilities, the accuracy and throughput of phenotyping will be limiting to confirm individual QTLs' contributions. Heritabilities for flowering time-related traits will often be above 80%, while biomass accumulation or fitness' heritabilities are essentially found in the range 20-60% [22-27].

Another factor that will influence the genetic complexity of a trait is its response to the environment through phenotypic plasticity [28]. Part of the environmental fluctuations may be controlled in an experimental design, while another part may contribute to the residuals / noise. Whether the sensitivity of a pathway or trait to the environment depends on the number and architecture of the contributing loci remains an open question, however the relationships between higher plasticity and lower heritability are described [26]. Water availability is an environmental factor that varies through space and time and shows great heterogeneity which certainly constrains plant growth and shapes plant distribution in nature and in agricultural systems. Prevalence of drought episode is expected to increase with global climate change making the understanding of plant response to drought one of the major challenge of the next decades [29, 30]; this includes deciphering the genetic basis for variation in mechanisms such as drought escape, avoidance and tolerance [31]. Hence, this environmental parameter is definitely a good candidate to understand the genetic architecture of GxE. However, drought is both difficult to control and hard to predict, because of interactions with almost all other factors in the environment (temperature, air flow, light...) and interplay with other constraints (especially nutrient-related or osmotic). The development of robotic phenotyping tools throughout the community makes it now feasible to acquire traits on hundreds or thousands of plants in precisely controlled and reproducible conditions [32-35], pushing a bit further one of the main limitation for a better decomposition of the genetic architecture of these complex traits.

Still, regarding plant growth variation in nature, mainly genomic regions with relatively large effect were identified in Arabidopsis and were often related to development, immunity or major hormones (for instance [36-43]). A limited number of non-theoretical studies seem to confirm that many genes with smaller effect –potentially involving epistasis and linked loci– would be responsible for part of the phenotypic variation of such complex traits (for instance [44-46]).

Here, we undertook a precise analysis of plant growth genetic architecture under both optimal watering condition and mild drought stress, using a classical linkage mapping approach on 4 biparental segregating populations [47]. As a dynamic trait, we chose to follow growth during

the vegetative phase using a high-throughput phenotyping robot (the *Phenoscope* [34]; https://phenoscope.versailles.inra.fr/) to map major- to small- effect QTLs as well as their interaction with drought stress. Zooming in on the loci, we use near-isogenic lines to validate these QTLs and reveal in more detail the genetics behind a single QTL peak. We then focus more precisely on a region where a major Quantitative Trait Gene (QTG) is segregating (= *CRY2*, a known polymorphic actor with major pleiotropic phenotypic consequences), and show that other loci with additive or opposite effect are also present in its vicinity, illustrating the complexity of growth genetic architecture.

RESULTS

Characterization of shoot growth-related phenotypes

The four RIL sets used in this study (BurxCol, CvixCol, BlaxCol, YoxCol) were conducted under well-watered (WW) and moderate water deficit (WD) conditions on our high-throughput phenotyping platform. Ensuring that growth occurs in a highly controlled and homogeneous environment, the Phenoscope records a number of image-based quantitative traits describing shoot development (@Figure 1). Taking daily pictures gave access to cumulative (Projected Rosette Area, PRA) and dynamics (Relative Expansion Rate, RER) growth parameters for individual plants (@Figure 1C&D) as well as other descriptive or derived traits (rosette morphology and RGB colour components) [48]. A principal component analysis (PCA) was performed using all picture-based phenotypes at the final day of the experiment, 29 Days After Sowing (DAS; hence 'PRA29' etc) and relative expansion rate calculated between 16 and 29 DAS (RER16-29; @Figure 2). The first axis explained a major part of the total variance, essentially through final rosette size (PRA29) and expansion rate (RER16-29). However, PRA29 and RER16-29 variables were not perfectly correlated, with genotypes exhibiting moderate PRA29 despite high RER16-29. The red (Red29) and green (Green29) components colour phenotypes mainly contributed to the second axis and were positively correlated, and both were negatively correlated with compactness at 29DAS (Compactness29) which was the main trait contributing to the third axis. Individual projection showed that the first axis strongly structured the individuals according to the watering treatment (WW versus WD) while the axes 2 and 3 represented cross (RIL set) effects, differentiating CvixCol and BurxCol (axis 2) and BlaxCol (axis 3) from the other RIL sets. PRA29, RER16-29 and Compactness29 are complementary growth phenotypes that were investigated further in this study to quantify different aspects of shoot development variation: final projected rosette area is a cumulative proxy for biomass and photosynthetically-active surface, rosette compactness is an informative

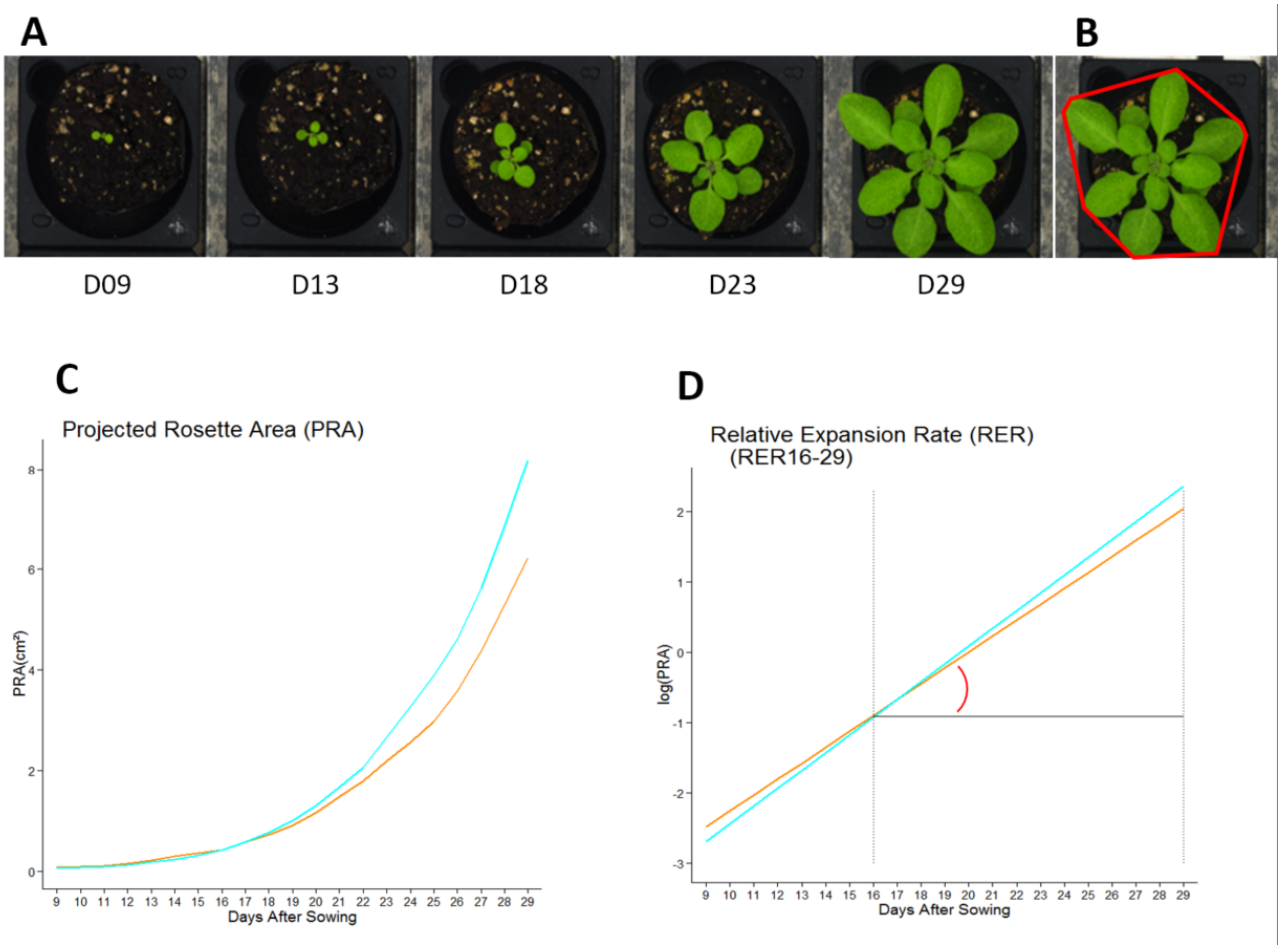

Figure 1: Extracting phenotypic information from zenithal images

A: Pictures of plants on the Phenoscope at different selected days after sowing

B: Representation of the rosette-encompassing convex hull (red shape) used to calculate the compactness (here illustrated at day 29)

C: Growth kinetics obtained by extracting the projected rosette area from the daily images.

D: Relative Expansion Rate calculated between two dates (for instance RER16-29 was integrated from day 16 to 29)

C and D: Blue: 'WW' = Well Watered (soil water content at 60%); Orange: 'WD' = Water Deficit (soil water content at 30%)

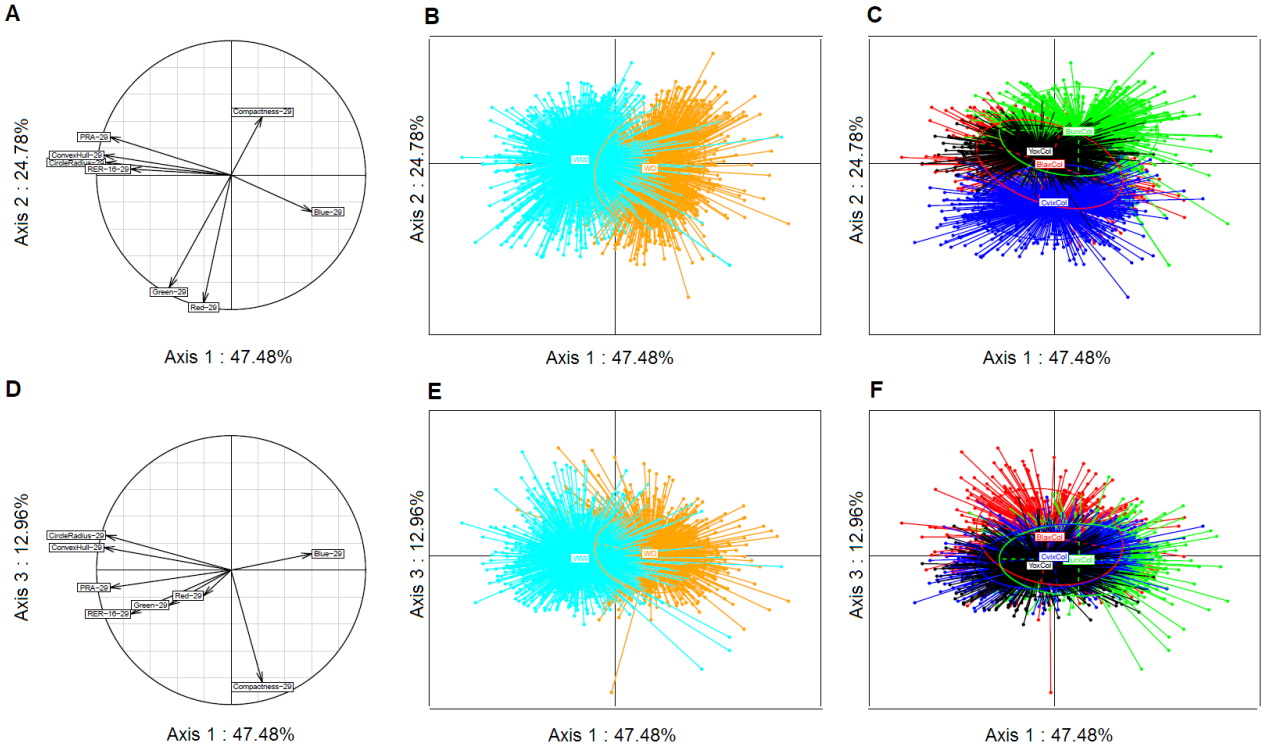

Figure 2: Principal component analysis of phenotypic traits

A to C show the results of the PCA based on plan 1-2.

D to F show the results of the PCA based on plan 1-3.

A and D: circles of correlations with projected variables on the 2D plan.

B and E: individual lines (RILs) projected on the 2D plans, clustered and colored according to the watering conditions as indicated.

C and F: individual lines (RILs) projected on the 2D plans, clustered and colored according to the RIL set as indicated.

parameter -rather stable through time- describing the rosette morphology, and relative expansion rate highlights the dynamics of growth.

Phenotypic distribution among the RILs compared to their parents (@Suppl. Figure S1) revealed extensive transgressive segregation for most of the traits and the crosses studied. As expected, mild drought stress (WD) condition impacted the distribution of the RILs for PRA29 and RER16-29 with generally reduced values for both traits. Interestingly, compactness distribution was much more robust to stress, which indicated that overall the morphology of the rosette is less affected by mild drought. In order to estimate the part of phenotypic variation that is explained by genetic factors for each traits, heritabilities were calculated (@Suppl. Table S1) and were essentially low for RER (except in BurxCol where they were high), intermediate for cumulative PRA and generally high for Compactness (this trait is certainly less sensitive to shifts in developmental stage that could be induced, for instance, by small changes in germination time). Overall, heritabilities were also lower in stress conditions than in control, as if the stress was inducing noisier phenotypic variations.

According to ANOVA analyses (@Suppl. Table S2), all traits and RIL sets showed significant variation according to both the watering condition (WD versus WW) and the genotype (within each RIL set), except for Compactness29 response to stress in BlaxCol. There were also weaker but significant biological replicates' effects (i.e. independent Phenoscope experiments), but less genotype x experiment interactions (with the exception of PRA and RER traits in BlaxCol for instance). PRA is more prone to genotype x experiment interactions than other traits, especially in CvixCol and YoxCol. Genotype x condition interactions are often milder than genotype or condition effects, and overall compactness –or YoxCol– show much less genotype x condition interactions than other traits/sets.

The phenotypic values of each RIL were then corrected for inter-experiment differences (indicated by the significant biological replicates' effect).

QTL mapping-based shoot growth genetic architecture

Our experimental design allowed the identification of many QTLs for all combinations of traits, conditions and RIL sets, and also for the GxE interaction term using genotype x condition effects from the ANOVA model for each trait (@Figure 3 and @Suppl. Table S3). Globally 112 QTLs were identified all along the genome when conditions are studied independently (62 under WW + 50 under WD) likely corresponding to at least 18 independent loci, yielding an average of ~4.7 QTLs per modality of cross x trait x condition. QTL hotspots across RIL sets and traits were identified for instance at the beginning of chromosome 1, at the bottom of chromosome 2 and 5. These hotspots include very highly significant QTLs with LOD scores above 10, and up to 32. Chromosome 3 appeared to show less significant QTLs in all crosses,

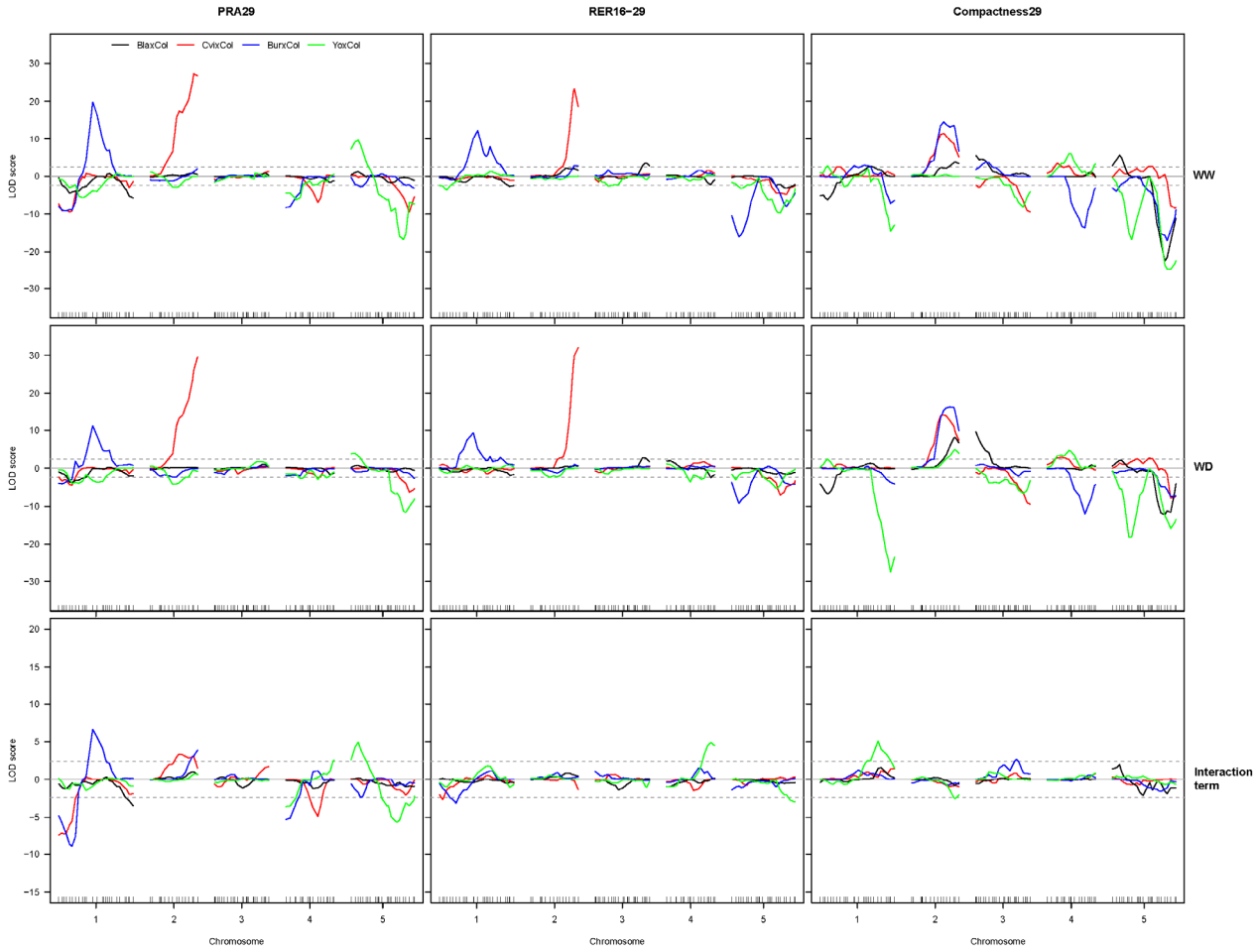

Figure 3: QTL mapping for 4 RIL sets, 3 traits and 2 conditions

QTL maps obtained from four RIL sets (BlaxCol in black; CvixCol in red; BurxCol in blue; YoxCol in green) using three phenotypes (PRA29, RER16-29 and Compactness29), generated independently in two conditions (top panels: WW; middle panels: WD) and from the genotype x environment interaction term in the model (bottom panels: Interaction term). LOD score values above (below) the X axis indicate that the Col allele increases (decreases) trait value with respect to the other parental allele. Significance threshold (LOD=2.4) is shown as dotted lines. The parameters of the significant QTLs detected are listed in @Suppl. Table S3.

especially for PRA29 and RER16-29. Individual QTL contributions to phenotypic variance (R^2) ranged from 1 up to 30%, with the typical L-shaped distribution of effect. Using empirical significance boundaries according to the observed distribution of QTLs effects, ~10% of the QTLs could be considered as showing major effects and significance (R2>10% and/or LOD>15); ~25% of the QTLs could be considered as showing intermediate effects and significance (5%<R2<10% and/or 7<LOD<15); the remaining 2/3rd of the QTLs could be considered as showing minor effects and significance R2<5% and/or LOD<7). Many more potential QTLs not listed here were only suggestive with LOD score peaks just below our threshold (<2.4 LOD).

Most of the QTL profiles are stable across the 2 watering conditions, especially for the major-effect loci. However, QTLs specific for one condition were detected, e.g for RER16-29 under WD in YoxCol on chromosome 4, and at the top of chromosome 1 under WW. We also mapped QTLs for the interaction term with the drought treatment, yielding another 19 QTLs (@Figure 3 and @Suppl. Table S3). These essentially emphasize large effect QTLs showing a modulation of their effect in response to stress (especially for PRA, see chromosome 1 and 5), with no real new loci revealed. For RER16-29 in YoxCol, this would confirm the interaction of the above-mentioned locus on chromosome 4 (although its exact location is questionable), but not for the one at the top of chromosome 1. There may be some power issues when comparing across conditions due to lower heritabilities of traits under WD.
Although derived from PRA29, Compactness29 showed an independent genetic basis, as exemplified by the major peaks on the bottom of chromosome 4 in BurxCol or 5 in BlaxCol. Although contributing to RER16-29, PRA29 does not always share the same contributing loci, for instance on the top of chromosome 1 in CvixCol and BurxCol. Other more complex cross x trait patterns are apparent, like at the bottom of chromosome 2 where a major QTL for Compactness29 in three of the four RIL sets seems to colocalize with a significant PRA29 and RER16-29 QTL (in the same direction), but only in one cross. It may be that these Compactness29 QTLs are actually independant in each RIL set.

A two-dimensions search for epistatic interactions was performed across all traits, conditions and RIL sets (@Suppl. Figure S2). Overall, the BurxCol and CvixCol RIL sets showed more significant epistasis compared to the two other sets. Interestingly, pairwise interactions controlling growth phenotypes are overall quite different depending on RIL set and growth phenotypes. Shared epistasis effects are potentially detected in both watering conditions: they appear as symetrical across the diagonal on @Suppl. Figure S2. One of the most significant epistatic interaction was observed between 2 loci on the top and bottom of chromosome 4 in the BurxCol cross (@Suppl. Figure S2; highest significance for RER16-29 in WW). Positions

and directions of effect match perfectly with the previously published SG3 x SG3i interaction known to segregate in this cross [49]. Based on its significance, another relevant interaction (*p*-value=0.01 in WW and *p*-value=0.03 in WD) was observed for PRA29 in the BlaxCol cross between the bottom of chromosomes 4 and 5 (@Figure 4). The effect of the bottom of chromosome 5 QTL on PRA29 is observed only when RILs carry Bla alleles at the bottom of chromosome 4. As a consequence of this epistasis, these QTLs appear barely significant in single QTL scans (@Figure 3).

We also performed dynamic QTL detection on daily-recorded traits (PRA and Compactness) to reveal the evolution of QTL effect throughout the experiment on the Phenoscope: these interactive QTL profiles can be accessed at http://www.inra.fr/vast/PhenoDynamic.htm
Most of the PRA QTLs observed after 29 days of growth correspond to locus that become gradually significant across the experiment and are essentially not time-specific. These are most likely contrasted allelic effect on growth that cumulate their effect over time. There are only a few exceptions for PRA, like the bottom of chromosome 5 locus segregating in BlaxCol which remains significant only until 13DAS and thereafter is canceled out. For Compactness, the picture is rather different with numerous examples of QTLs that are essentially significant around specific time-points, even sometimes in successive waves of significance (BlaxCol, bottom of chromosome 5 : QTL peaking at Days 11, 17 and 27 –providing that this is a unique locus).

In order to take advantage of the different crosses to Col-0 in our experimental setup, QTL mapping was performed on the whole dataset using MCQTL tool to compare allelic effects in a multicross design and potentially reveal shared QTLs. The combined QTL maps obtained (@Figure 5 for PRA29 and @Suppl. Figure S3 for RER16-29 and Compactness29) highlight 10 independent loci, including at least 4 regions with contrasting allelic effect on PRA29: for instance, the middle of chromosome 1 region shows contrasted phenotypic consequences in different crosses, particularly when comparing Bur and Yo alleles (with respect to Col). At this scale, it can be difficult to distinguish between different alleles at the same QTL and different QTLs. Conversely, combining the information of multiple crosses sometimes allows to predict narrower QTL intervals than with the initial QTL mapping, enabling the detection of distinct linked loci, for instance for PRA on the bottom half of chromosome 2; a location where the dynamic QTL analysis for PRA in CvixCol was already showing signs of 2 different segregating loci with slightly distinct dynamics over time. Another striking example is for Compactness on chromosome 5, with neighbouring QTLs predicted to show opposite allelic effects (e.g. BlaxCol).

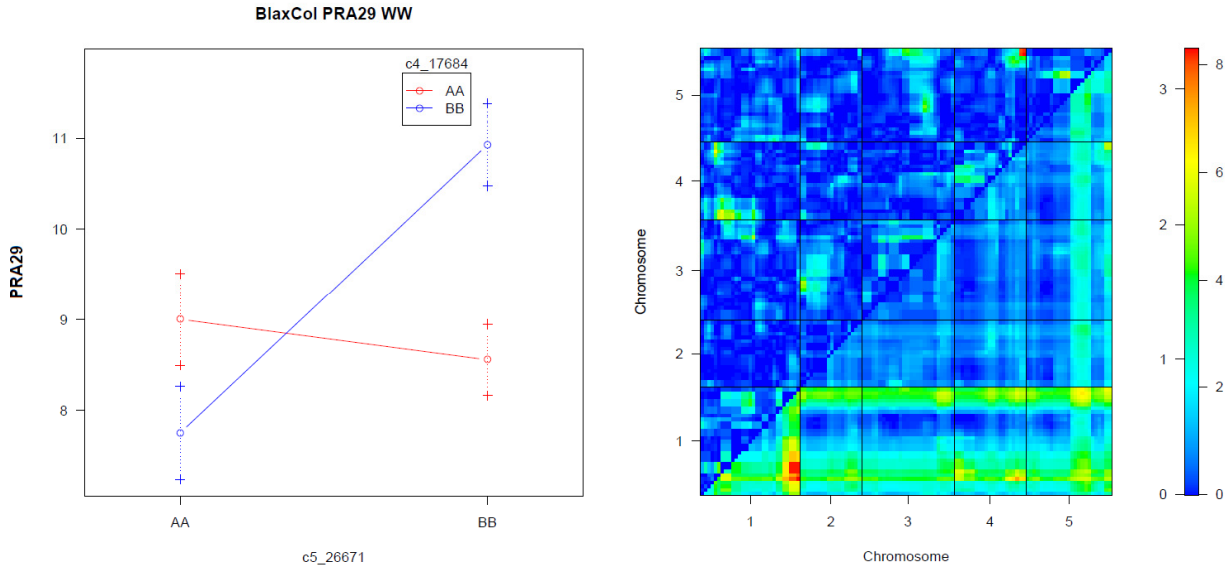

Figure 4: A significant epistatic interaction for PRA29 in BlaxCol

A significant epistatic effect on PRA29 between the bottom of chromosomes 4 and 5 segregating in the BlaxCol RIL set. Results shown in WW condition. The interaction plot (left panel) represents the average RIL phenotype (in cm2) for each allelic combination ('AA' = homozygous Col, 'BB' = homozygous Bla). Right panel: heatmaps representing the LOD score of the full model with additive and interaction effects (triangle below diagonal) and that of the interaction effects only (triangle above diagonal) for PRA29 in BlaxCol. The color scales for significance (LOD) are indicated on the right.

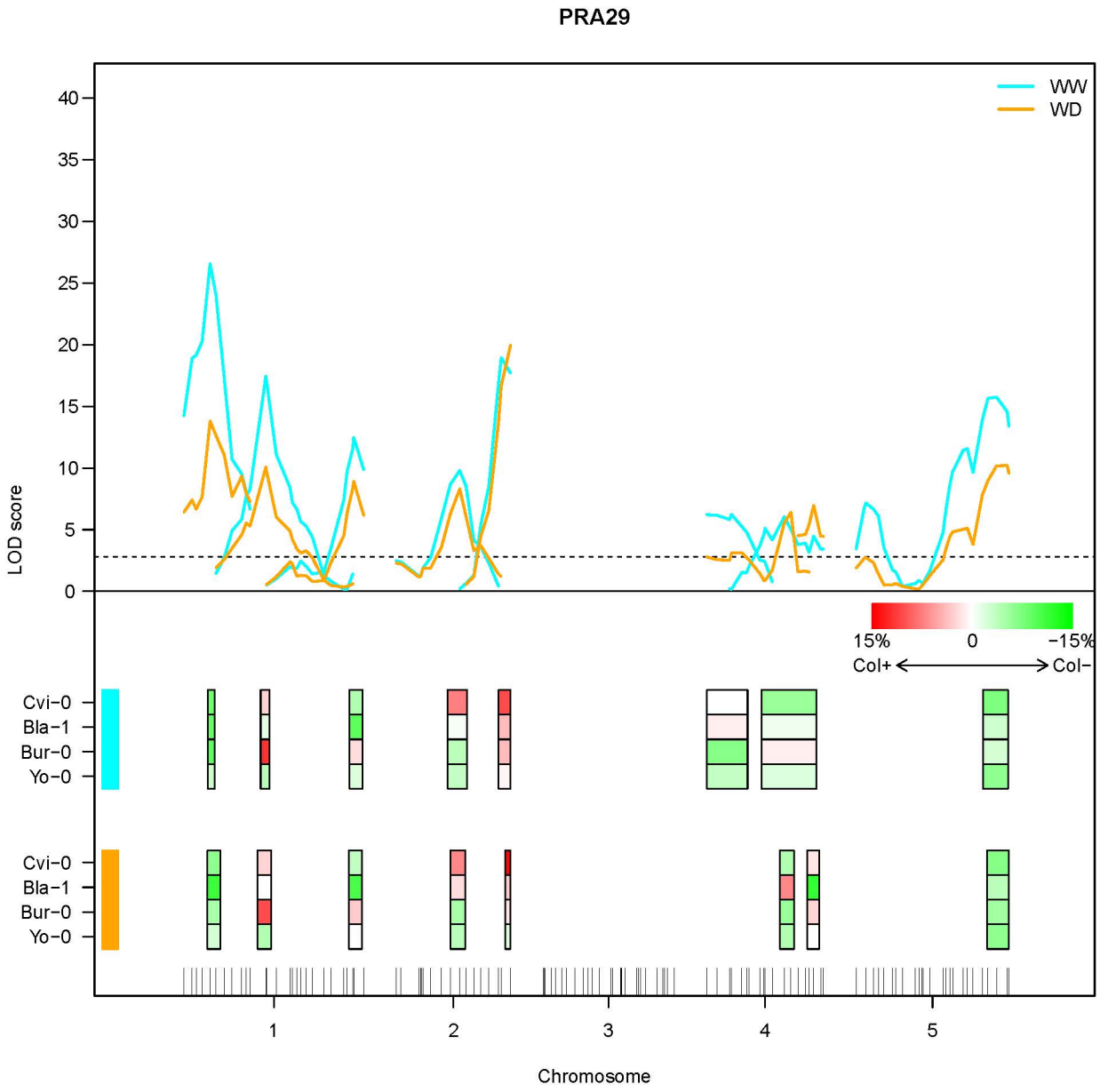

Figure 5: Multi-cross QTL analysis for PRA29

The upper panel of the figure represents the LOD scores calculated by the MCQTL method along the genetic map in WW (blue) and WD (orange) conditions. Each QTL is depicted by a LOD score profile which peak is represented by colored boxes on the lower panel of the figure (WW conditions above and WD conditions below). The color of the box indicates the deviation of the trait value for the Cvi, Bla, Bur or Yo alleles relative to the Col allele as indicated. Chromosome 3 shows no significant combined QTLs for PRA29. This figure shows results obtained for trait PRA29 only; other traits are in @Suppl. Figure S3.

Near isogenic lines-based shoot growth genetic architecture:

To confirm and investigate further the complexity of the genetic architecture of these traits, we used near-isogenic lines to mendelize QTLs and assess in more details the role of smaller chromosomal regions. Using 81 independent Heterogeneous Inbred Families (HIFs) scattered across the genome or chosen to decompose candidate regions in specific crosses [50], we tested a total of 79 QTL effects from the 24 modalities of RIL set x trait x condition (@Figure 6 for PRA29; @Suppl. Figure S4 for RER16-29 and Compactness29). Globally, 60% of the HIFs with a segregating region covering a candidate region previously identified showed significant effect with consistent direction, thus validating the QTL. Larger effect QTL were more often validated in HIF, with ~75% of the tested major or intermediate effect QTLs confirmed, compared to ~50% of the minor effect QTL. Specifically for PRA29 trait in the two conditions studied (@Figure 6), 28 QTL were assessed with at least one HIF, among which 17 (60%) were confirmed. Some (minor-effect) QTL x condition interactions detected in the RIL set were also significantly confirmed using HIF, such as the top of chromosome 5 locus in BurxCol which has significance (PRA29) only under WW.

Many factors can explain that a QTL is not validated in an HIF (beyond an unreliable phenotype): the QTL could be mislocalised by QTL mapping (thus, out of the HIF segregating region), the QTL could be under epistatic interaction with another locus (thus, a specific HIF may not represent the adequate genetic background), or the HIF harbours a more complex genotype than expected at the segregating region, such as a double recombined region (thus, the HIF doesn't actually allow to test the whole region). This makes the comparison between HIFs difficult, even in the same cross, and negative HIF results should particularly be interpreted carefully. In this context, the rate of QTL validation obtained here is rather satisfying.

We are also interested in positive HIF results that were not predicted by the QTL mapping. This was particularly possible in regions with high HIF coverage and shows that several LOD score peaks were explained by more than one underlying QTL, as also suggested by the MCQTL analysis. A good example lies in the CvixCol cross, where the bottom half of chromosome 4 seemed to control PRA29 as a single locus in the initial QTL analysis (@Figure 3) and is now subdivided in at least 2 independent loci with opposite allelic effects after the HIF analysis. Another example segregates in YoxCol at the top of chromosome 3 where two QTL with opposite-effect on Compactness29 under WW conditions seem to localise closely according to the HIFs (@Suppl. Figure S4) but wasn't detected at all in the QTL mapping at 29DAS (@Figure 3) and only remained significant at intermediate stages around 16DAS according to the dynamic analysis. The initial QTL mapping may have lacked power (= RILs) to detect these complex patterns, either due to the confusing effect of linked loci, or the confusing effect of epistasis, or both.

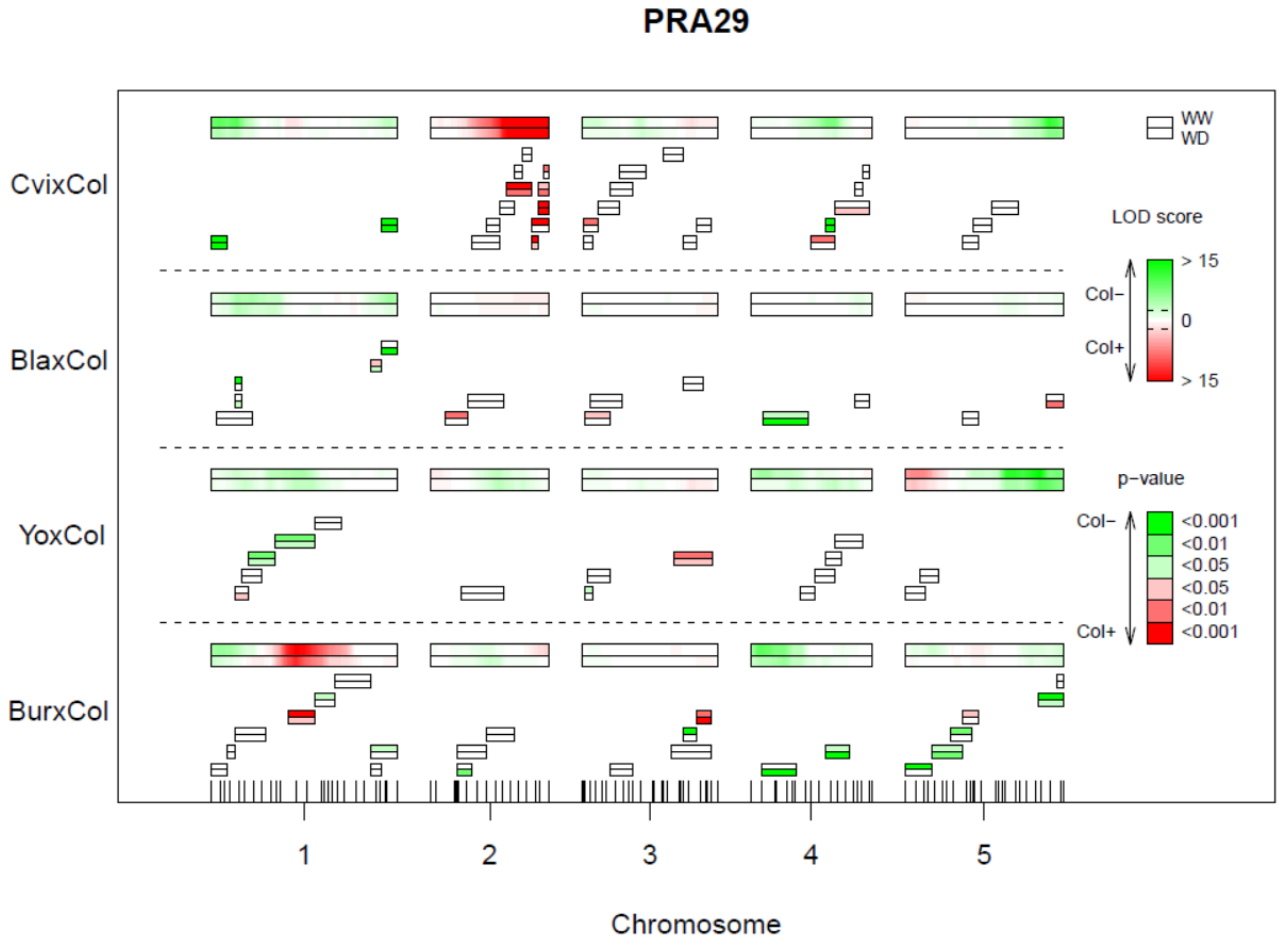

Figure 6: Near isogenic lines-based validation of QTLs for PRA29

QTL mapping results (same LOD score profiles as @Figure 3) are shown as LOD score heatmaps (see color scale on the right) for each RIL set, across long twin boxes representing the 5 chromosomes (the upper frame is for WW, the lower frame is for WD conditions). Below each chromosome are series of short twin boxes representing individual HIFs segregating region, used to test phenotypes associated with specific regions (for each twin box the upper frame is for WW, the lower frame is for WD). The significance and the direction of the difference between Col-fixed HIF lines and alternate parental allele-fixed HIF lines are indicated by the p-value color scale as indicated. Details of each HIF used here are gathered in a deposited dataset [50]. This figure shows results obtained for trait PRA29 only; other traits are in @Suppl. Figure S4.

Finally, we can occasionally exploit the localisation of the segregating region(s) of the tested HIFs to narrow down the candidate QTL region, like for a PRA29 QTL in CvixCol at the bottom of chromosome 2 which is narrowed down to the extremity of the chromosome and shown to be distinct (= confirmed in non-overlapping HIFs) from another nearby QTL segregating in the same cross (with allelic effect in the same direction), as predicted by the multicross analysis above. Here again the dynamic analysis also helped to distinguish these loci based on their effect through time. Still, the 'precision' remains approximately at the Mb level at this stage.

To tackle further the question of the complexity of the genetic architecture at a higher resolution than with simple HIFs, we decided to systematically dissect a region of 3Mb at the very beginning of chromosome 1 in CvixCol: in this region all previous approaches have predicted a single QTL with intermediate to major effect significance on PRA29 (@Figure 3), which was confirmed in an HIF (@Figure 6). This HIF was used to zoom in on the region across 30 bins (stairs) of ~100kb, defined by successive recombination breakpoints (@Suppl. Table S4) and phenotypically evaluated individually in the same conditions as above (an approach coined 'microStairs'). We selected this interval to test if a region harbouring a large-effect growth QTL may typically also include independent loci, maybe of smaller effect or hidden by the main QTL. A pairwise comparison of their growth phenotypes allows to test the impact of Cvi versus Col alleles over relatively short physical intervals of expected average size 100kb, with a maximum ~200kb, depending on recombination breakpoints location and marker interval. We either compared only the 2 successive recombinants ('stair by stair'), or we took advantage of the support from all pairwise comparisons ('staircase') to increase our power to detect QTL (@Figure 7 for PRA29 and @Suppl. Figure S5 for RER16-29 and Compactness29).

The strongest phenotypic effect for PRA29 in WW and WD (but also –to a lesser extent– for RER16-29 in WD) was fine-mapped down to the stair between recombinants 111 and 112, covering potentially a physical interval (bin) extending to the maximum between 1.070 and 1.291 Mb (an interval including 54 genes). In the middle of this region lies the obvious candidate gene *CRYPTOCHROME 2* (At1g04400; *CRY2*, a blue-light photoreceptor; @Suppl. Table S5) that is known to harbour a functional variant in Cvi (a single amino-acid change) and impact plant photomorphogenic development especially in short days [51, 52]. This is a good test case of our approach, as it is very likely that *CRY2* is primarily responsible for the growth difference overall observed in this HIF.

Still, on either side of this locus, a few other QTLs also affect growth, underlying a much more complex genetic architecture than expected after the initial HIF results: in both watering conditions, a milder PRA29 QTL, with opposite allelic effect than CRY2, was detected in the stair defined by recombinants 115 and 116 (1.495 to 1.703 Mb positions). Another PRA29 QTL was predicted in the bin 125/126 (2.509 to 2.710 Mb). For Compactness29 specifically under

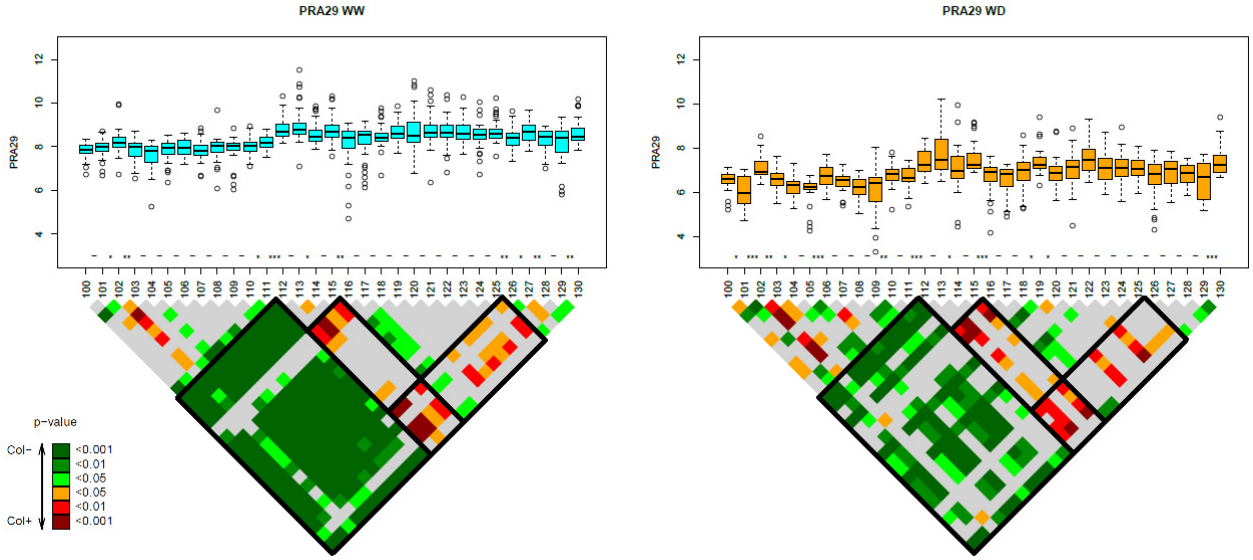

Figure 7: Dissection of a genomic region in CvixCol for PRA29 ('microStairs' approach)

The upper panels' are boxplots indicating phenotypic values observed for each of the 31 successive recombinant lines along the 3Mb region studied (details of each line used here are in @Suppl. Table S4). Significant differences between successive lines (stairs) are indicated along the X axis with '*' (p-value < 0.05), '**' (p-value < 0.01), '***' (p-value < 0.001) or '-' for no significant difference. The lower panel shows a triangular matrix gathering the significance of all pairwise comparisons between lines (see the p-value color scale also indicating the direction of the allelic effect). Blocks of significance ('staircase') are interpreted and highlighted in black-framed boxes. This figure shows results obtained for trait PRA29 only (in 2 conditions), PRA is expressed in cm2; other traits are in @Suppl. Figure S5.

WD treatment, *CRY2* did not seem to be causal and the causative locus for the observed HIF phenotype would most likely be in the bin 118/119 (1.801 to 2.027 Mb); this QTL was not clear from the initial QTL analysis for this trait on Day 29 (@Suppl. Figure S4), but appeared significant earlier in the experiment (cf dynamic analyses for CvixCol around 14DAS and later). There are probably even more loci, especially at the very beginning of the region for PRA29 (stairs between recombinant 101 and 104 at least), but we reach the limits of our experimental design and phenotyping precision to be able to conclude accurately, with either too complex genetic architecture in this region or not enough recombinant lines to robustly support each intervals' effect.

We then looked for high impact polymorphisms (premature stop codon, frameshift or non-synonymous mutations) likely affecting gene function between Col-0 and Cvi-0 within the most promising bins to find out candidate genes. Because of the numerous non-synonymous changes between these accessions (@Suppl. Table S5), we decided to arbitrarily filter the genes with the criteria of at least 3 non-synonymous mutations to increase our chance to detect genes with altered function or degenerated sequences after loss-of-function mutations.

Within the bin 115/116 lie at least 2 interesting candidates (among those with functional annotations):

URIDINE DIPHOSPHATE GLYCOSYLTRANSFERASE 74E2 (At1g05680; *UGT74E2*) is an auxin glycosyltransferase whose overexpression was shown to modify plant morphology and the size of the petioles, to delay flowering, and to increase drought tolerance [53]. The gene is also known for ample natural variation in expression, including potentially cis-acting variants [54]: http://www.bioinformatics.nl/AraQTL/multiplot/?query=AT1G05680.

GLUTAMATE RECEPTOR 3.4 (At1g05200; *GLR3.4*) is a calcium-dependent abiotic stimuli-responsive gene [55] expressed throughout the plant and impacting at least lateral root initiation [56]. It harbours several non-synonymous variants in Cvi-0 (compared to Col-0), but also higher expression in Col-0 as shown by several local-eQTLs in different crosses (http://www.bioinformatics.nl/AraQTL/multiplot/?query=AT1G05200) confirmed to be cis-regulated through Allele-Specific Expression assay [57] (reported in @Suppl. Table S6).

Within the bin 125/126 lie at least 2 interesting candidates:

AT1G08130 encodes *DNA LIGASE 1* (*LIG1*), a ligase involved in DNA repair, which mutation causes severe growth defects [58]. Its expression is also known to be controlled by a local-eQTL (most likely cis-acting) in LerxCvi:

http://www.bioinformatics.nl/AraQTL/multiplot/?query=AT1G08130

AT1G08410 is *DROUGHT INHIBITED GROWTH OF LATERAL ROOTS* 6 (*DIG6*), encoding a large 60S subunit nuclear export GTPase 1 that impacts several developmental processes regulated by auxin, including growth [59].

Further work is required to prove any link between the observed phenotypic variation and these candidate genes.

DISCUSSION

Owing to its fine regulation throughout development and in interaction with the environment, plant growth represents a highly complex trait potentially controlled by numerous factors and interactions. Little is known on the actual genetic architecture of plant growth natural variation, with essentially a few genes of major effect being identified until now and only a few exceptions of more complex genetics revealed [44]. Association genetics hold great promise to dissect the underlying molecular bases of complex traits [12], however one can wonder if the genetic architecture of highly integrative traits like growth or fitness is amenable to genome-wide association studies (GWAS) at the species scale: GWAS especially lacks power to decompose traits controlled by many loci of small effects, particularly if the underlying alleles have moderate or low frequency in the populations. For instance when exploiting worldwide collections of accessions, very little (if any) significant associations for growth parameters were found [60], even when using very anti-conservative thresholds [2, 61] or using morphological parameters with higher heritabilities [62]. Even with more targeted growth traits like root cell length, Meijon *et al.* did not detect any significant signal above the threshold, although the first peak just below the threshold identified a causal gene [63]. Overall, it is argued that linkage and GWA studies are complementary in the loci that they are able to reveal, depending on the genetic architecture of the trait in the population considered (e.g. [21, 64]). Here, by studying four different crosses to the reference Col-0, we find many cross-specific loci, especially of mild effects, several of which might correspond to low frequency-alleles that would not likely be pictured in GWAS (not enough power due to low frequency x effect size).

Whether linkage or association mapping, these approaches are both similarly phenotyping-intensive and prone to interaction with uncontrolled environmental parameters (increasingly so with the scale of the experiments). Using our high-throughput phenotyping robots to grow individual plants under tightly controlled conditions, we intended to dissect the genetic basis of plant growth under optimal and limiting watering conditions, to a level of accuracy rarely reached so far. We focused on vegetative growth from days 8 to 29 (after sowing) and selected three non fully-correlated variables allowing to characterize plant growth dynamically: rosette area (PRA), relative growth rate (RER) and compactness. PRA is a typical cumulative trait: what is observed on day n is not independent from what has occured from day 1 to n-1.

Compactness, which basically represents a measure of PRA normalised by rosette width, is rather independent on cumulative phenomenons and hence shows much more age-specific QTLs; this is particularly striking when comparing the dynamic analyses for these traits. Finally RER integrates growth rates over a specific period of time, and is independent from plant size (= relative). Because estimated during the exponential phase of growth, RER is very much similar to what is obtained by fitting exponential models to the PRA data and exploiting model parameters [2].

Hence, growth-related phenotypes, depending on how they are exploited, will present different genetic architectures throughout age, with individual loci making different contributions to cumulative or age-specific traits. It has previously been shown that heritabilities for growth-related traits change over time [6, 65], suggesting that QTLs are more or less likely to act at specific time points. For instance, studying growth dynamics in maize [66, 67] and root tip growth in Arabidopsis [68] allowed to identify marker-trait associations that would not be detectable by considering the cumulative trait only at a single (final) time point. At the other end of time-resolution for growth, going into much more details of the dynamics (several images per day) may result in noisy raw data requiring further treatment before exploiting, for example due to projected growth estimates interfering with circadian leaf movements [65].

Our work has been performed under two environmental conditions, a control condition and one that moderately limits growth due to water (but not nutrient) availability [34], i.e. a mild drought treatment. The QTL profiles obtained at the genomic scale are very robust to mild drought with most of the large effect QTL showing no clear signs of interaction with water availability in our conditions. Some of them still change their level of significance with conditions, but it is difficult to know if this is a real interaction with drought, a change in trait variance under stress, or a change in the rest of the genetic architecture of the trait (which will impact the significance of individual QTL). Condition-specific QTLs detected here always are of small effect, which also raises the question of the power of these comparisons across different conditions/experiments due to false negative in mapping QTL. Still, this result (a relatively smaller part of the phenotypic variation is plastic rather than constitutive) is similar to what was found previously for instance in linkage [69] and association mapping [61], showing an overlap in the network of genes that regulate plant size under control and mild drought conditions [60]. Drought stress might have pleiotropic effects on different tightly interrelated phenotypic traits and impose strong constraints on them, reducing trait variability [31]. Of course, this may highly depend on the type of stress (intensity, stage of application, stability...) that is applied. Here, we chose a mild stress intensity, to remain physiologically relevant and avoid the squeezing of trait variation concomitant to strong stress levels. Also, our robot is compensating (twice a day) the

individual plant size effect on transpiration that may otherwise artificially increase stress intensity according to intrinsic plant size difference.

One advantage of using a star-like cross design, increasingly used in nested association mapping (NAM) populations, is to combine the power of individual crosses and take advantage of the comparison of multiple alleles, with respect to the reference allele in order to identify allelic variants more efficiently [70-73]. These could correspond to variants originating from Col-0 or to shared allelic variants among the other parents (same direction of the allelic effect in all crosses), or to allelic series (other parents could have divergent direction/intensity of effect with respect to the reference parent). This multi-population study has confirmed the effect of several loci across traits and environments, with particular power for compactness, and in some instances already allows to predict that independent loci actually underlie major peaks. However, this approach is still limited by the mapping resolution which makes it difficult to distinguish shared variants from linked loci.

Considering the precision of our phenotyping (which has an impact on the part of phenotypic variation that is amenable to genetic dissection), the need for higher-resolution approaches to better describe the trait's genetic architecture is obvious here. If the architecture of variation in our crosses is more complex than just a limited number of loci independently segregating for intermediate or major effects, then the density of recombination observed in a simple RIL set will not allow to decipher the full architecture [74, 75]. We first went deeper in resolution by phenotyping numerous pairs of near-isogenic lines (actually, HIFs) that each interrogate a specific portion of a chromosome (2-3Mb on average) in an otherwise fixed genetic background. This nicely confirms a majority of loci but also shows some effects that were unexpected after the initial QTL mapping results, already indicating more complex genetic architecture than anticipated; this includes single peaks splitting up in independent loci or complex patterns of linkage versus pleiotropy (when comparing different traits) and linkage versus GxE (when comparing traits in different conditions). It seems that QTL colocalisation among crosses (linkage versus shared variants) is also often questioned, although this requires to be able to compare multiple HIFs and they may not be directly comparable due to interactions with the genetic background. The difficulties to identify genes responsible for complex phenotypes also depends on their involvement in epistatic interactions. HIFs are particularly sensitive to epistasis (compared to traditional NILs) as they each harbour a different genetic background, which means that they allow epistasis to be interrogated providing that one can test enough independent HIFs, otherwise they have to be compared with care.
Epistatic interactions are detected in all crosses / traits (although not always with very high significance) even when the trait heritability or variation is not so high in a cross, illustrating

another factor of the complex genetic architecture. Some interactions seem to be condition-specific, but power issues are likely to be limiting in understanding these patterns of GxGxE. Furthermore, HIF have an expected candidate segregating region of several Mb usually, so our observations are likely just a glimpse at the real complexity of growth as it is known that linkage and epistasis is also active at a very local scale [44].

Still, the sensitivity of our approach here is validated by the detection of QTL colocalising with several already-known QTG expected to segregate in our crosses, like *CRY2* as discussed above [52, 76], *MPK12* which would explain nicely the bottom of chromosome 2 QTL in CvixCol [77, 78], or SG3 detected here through its epistasis with SG3i in BurxCol [49, 79].

To avoid genome-wide epistasis and better reveal local-scale architecture, we have investigated in further details a single HIF background for a specific 3Mb region containing a known QTG of large and pleiotropic effect (*CRY2*) in an original approach. Our analysis reveals that there are at least 3 other QTGs in this interval controlling one of the traits in at least one condition. For PRA29, the picture seems to be even more complex with traces of at least one more locus; here, it seems that phenotyping accuracy becomes again limiting after all. Obviously these loci with opposite allelic effects, different patterns of pleiotropy and interaction with the environment, and just a few hundreds of kb from each other, remain cryptic in simple QTL mapping. This major result of local-scale independent complex genetic architecture for different traits and conditions should lead us to a lot of caution when interpreting colocalising QTLs from different traits / conditions / age, as these may very well be independent loci rather than a single pleiotropic locus, as shown here for PRA and Compactness. If we were to extrapolate the figures obtained on this specific region in this particular cross to the genome- and species-scale, we would expect hundreds of causative loci of detectable phenotypic effect controlling these growth-related phenotypes. One way to approach these individual loci would be to decompose their independent signature based on different dynamics or underlying traits (transcriptomics, metabolomics...) in a 'systems genetics' strategy [54, 60, 80].

Complex genetic architecture as revealed in this study has consequences on quantitative genetics experimental design and interpretation, arguing in favor of linkage mapping or GWAS depending on the balance between genetic complexity due to linked loci (where association is expected to behave better than linkage mapping) and genetic complexity due to small effect/rare alleles (where association will behave poorly). Other intermediate experimental designs like multiparental populations or nested-association mapping should bring more power [12, 81]. Resolution is improved by pushing recombination densities to its limits and it was shown to help resolve more complex genetic architecture in yeast [82]. In plants, using 'hyper-

recombinant' mutations to generate new segregating populations could also be a strategy in the future [83].

MATERIALS AND METHODS

Genetic material. Recombinant Inbred Lines (RILs): The 4 RIL sets used for this work were generated at the Versailles Arabidopsis Stock Center, France (http://publiclines.versailles.inra.fr/) and described previously [47]. Versailles stock center ID are indicated as 'xxxAV' and 'xxRV' for Accessions and RILs respectively). They are derived from crosses between the following pairs of accessions :

RIL set 'BlaxCol' (ID = 2RV): Bla-1 (76AV) x Col-0 (186AV) / 259 RILs

RIL set 'CvixCol' (ID = 8RV): Cvi-0 (166AV) x Col-0 / 358 RILs

RIL set 'BurxCol' (ID = 20RV): Bur-0 (172AV) x Col-0 / 283 RILs

RIL set 'YoxCol' (ID = 23RV): Yo-0 (250AV) x Col-0 / 358 RILs

Heterogeneous Inbred Families (HIFs): HIFs have been selected in each RIL set to cover several regions of the genome, some of which are expected to segregate for QTLs while others were chosen at random locations. As described previously [84] they are derived from the progeny of one RIL which is heterozygous only at the locus of interest. Hence, one HIF family is composed of 2 or 3 lines fixed for one parental allele at the segregating region and 2 or 3 lines fixed for the alternate parental allele at the segregating region, in an otherwise identical genetic background. Each HIF (ID = 'xxHVyyy') is named after the RIL ID ('xxRVyyy') from which it has been generated ('xx' is the ID of the RIL set, 'yyy' is the ID of the RIL): for example the family 2HV142 is fixed from the RIL 2RV142. The tentative QTL validation is based on the phenotypic comparison of these fixed lines within the HIF family. The complete dataset gathering genotypic information on the RILs used to generate HIFs has been submitted to INRA institutional data repository (https://data.inra.fr) [50], with the genotypic conventions and ID from the Versailles Arabidopsis Stock Center (http://publiclines.versailles.inra.fr/).

microStairs: The progeny of CvixCol RIL 8RV294 (also used to generate HIF family 8HV294), segregating for the first 3Mb of chromosome 1, has been screened to detect recombined individuals. 4000 individuals were genotyped with markers at the edge of the heterozygous region and then 29 evenly distributed recombinants were selected using markers spaced every ~100kb. These recombinants were genotyped and fixed for the remaining segregating region in such a way that they each differ genotypically from the next recombinant by a ~100kb bin on average (@Suppl. Table S4). This is similar to the approach taken by Koumproglou *et al.* [85], but at a much finer scale, hence the name '*microStairs*'.

Phenotyping: Phenotyping was performed on the Phenoscope robots as previously described [34] (https://phenoscope.versailles.inra.fr/). Every RIL set and their respective parental accessions have been phenotyped in 2 independent Phenoscope experiments (= biological replicates), except for CvixCol (3 biological replicates). In short, the peatmoss plugs' soil water content (SWC) is gradually adjusted for each plant individually as a fraction of the initially-saturated plug weight. We worked at 2 watering conditions: 60% SWC for non-limiting conditions (called 'WW' for well watered) and 30% SWC for mildly growth-limiting watering conditions (called 'WD' for water deficit). The growth room is set at a 8 hours short-days photoperiod (230 µmol m-2 sec-1) with days at 21°C/65%RH and nights at 17°C/65%RH. A picture of each individual plant is taken every day at the same day-time and a semi-automatic segmentation process (with some manual corrections when required) is performed to extract leaf pixels. From this we exploit different traits: Projected Rosette Area (PRA), circle radius, convex hull area, average Red, Green and Blue components (leaf pixels, RGB colour scale), and derived phenotypic traits are calculated, such as the compactness (ratio PRA / convex hull area) and the Relative Expansion Rate (RER) over specific time windows (@Figure 1), as previously described [34]. The complete raw phenotypic dataset has been submitted to INRA institutional data repository (https://data.inra.fr) [48]. Principal component analysis (PCA) was performed using the ade4 R package based on phenotypic data from all the RIL sets in WW and WD conditions. For QTL detection and further analyses, the phenotypic values were corrected for experiment effects. Corrected phenotypic values were calculated using the intercept (µ), the condition (α), genotype (γ), and genotype*condition (σ) effects of the following model :

$$Y_{ijkl} \sim \mu + \alpha_i + \beta_j + \gamma_k + \delta_{ij} + \lambda_{jk} + \sigma_{ik} + \varepsilon_{ijkl}$$

where Y_{ijkl} : phenotype; μ : mean; α_i : effect of the condition; β_j : effect of the experiment; γ_k :effect of the genotype; δ_{ij} :effect of the interaction condition*experiment; λ_{jk} :effect of the interaction experiment*genotype; σ_{ik} :effect of the interaction condition*genotype; ε_{ijkl} : residuals.

Note that one of the replicates of the CvixCol phenotypic data was already analysed for QTL mapping -with a different statistical model- in Tisné *et al.* [34].

Similarly, the set of near isogenic lines (microStairs) were phenotyped and analysed from 3 full biological replicates in independent Phenoscope experiments.

QTL MQM: QTL detections were performed using Multiple QTL Mapping algorithm (MQM) implemented in the R/qtl package [86, 87] using a backward selection of cofactors. At first, genotype missing data were augmented, then one marker every three markers were selected and used as cofactors. Important markers were selected through backward elimination. Finally,

a QTL was moved along the genome using these pre-selected markers as cofactors, except for the markers in the 25.0 cM window around the region of interest. QTL were identified based on the most informative model through maximum likelihood. According to permutation tests results, a universal LOD threshold of 2.4 was chosen for all QTL maps. Interactive QTL maps for time-course series were generated using the R/qtl charts package [88]. All QTL positions were projected on the consensus genetic map of the 4 crosses built with R/qtl. A joint genotype dataset was constructed with 'A' alleles coding Col alleles (the common parent), 'B' alleles for non-Col alleles, and monomorphic markers in a cross coded as missing. The linkage groups were considered known from the individual maps and the physical position of markers, and a first marker order was calculated using orderMarkers function. In case of conflicting marker order between individual, physical and consensus maps, the function switch.order was used to retain the most probable order (i.e with the lowest number of recombination).

Epistatic interactions: Epistatic interactions were identified using the scantwo function of the R/qtl package. LOD scores were calculated for additive, interaction and full models. LOD score and p-values were calculated for all pairwise combination of markers, except for adjacent markers. Effect plots for the pairs of markers were drawn using the R/qtl package.

QTL mapping in the multi-cross design: QTL mapping in the multi-cross design was performed with the MCQTL package [89]. The model was described as additive (no dominance effect) and connected (Col-0 centered design) and the following 3 steps process was applied. Step 1: thresholds were calculated by variable on the whole genome using 1000 resampling replicates (PRA29_WW = 3.73; PRA29_WD = 3.84; RER16-29_WW = 5.22; RER16-29_WD = 3.95; Compactness29_WW = 3.64 Compactness29_WD = 3.30). Step 2: QTL detection was performed using iQTLm method with a threshold of 4. To perform this detection, cofactors were automatically chosen by backward selection with a threshold of 2.8 among a skeleton with a minimal inter distance of 10cM. Search for QTL was not allowed within +/-10cM window surrounding the QTL to avoid linked genetic regions. Step 3: model estimations were performed for each variable and condition using the parameters previously described and the QTL position identified at the QTL detection step.

Fine dissection of a genomic region 'microStairs': The phenotypes of the recombined HIFs lines were modeled using the following linear equation :

$Y_{ij} \sim \mu + \alpha_i + \beta_j + \varepsilon_{ij}$

where Y_{ij} is the value of the phenotype; μ is the mean of the phenotype; α_i is the effect of the stair (bin) i; β_j is the effect of the line j and ε_{ij} is the residuals. An anova was performed

with this model and the p-value of the stair effects were adjusted by a Benjamini-Hochberg correction.

Polymorphic candidate genes (Cvi versus Col) were listed for each PRA29 'microStairs' significant interval according to variants listed on the 1001Genomes website (http://1001genomes.org/), through the Polymorph1001 tool. Differentially cis-regulated variants were extracted from Cvi/Col Allele-Specific Expression (ASE) data [57] and from CvixCol local-eQTLs data [90] across the whole region.

ACKNOWLEDGMENTS

We thank Yann Serrand for the supervision of the *Phenoscope*, we thank Francisco Cubillos, Cécile Grondin, Isabelle Gy and Mathieu Canut for the selection of recombinants from 8HV294. We also thank Laurence Moreau for her help in performing multi-cross analyses. We thank José Jiménez-Gómez for discussions on statistical analyses of the 'microStairs' experiment. This work was supported by funding from the European Commission Framework Programme 7, ERC Starting Grant 'DECODE'/ERC-2009-StG-243359 to O.L. and Agence Nationale de la Recherche (ANR) grant '2Complex'/ANR-09-BLAN-0366 to O.L. The IJPB benefits from the support of the LabEx Saclay Plant Sciences-SPS (ANR-10-LABX-0040-SPS).

DATASETS

> Two datasets have been submitted to INRA Dataverse repository (https://data.inra.fr) :

- Raw phenotypic data obtained on the Arabidopsis RILs with the Phenoscope robots [48]

This dataset gathers the main raw phenotypic data obtained and exploited in Marchadier, Hanemian, Tisné *et al.* (2018). It contains data from 4 RIL sets across 9 Phenoscope experiments.

For each Phenoscope experiment, Recombinant Inbred Line (RIL) and Condition ('WW' = Well Watered / 'WD' = Water Deficit), the data set indicates the phenotypic value for 6 traits at 21 successive time points. 'Trait.XX' = Trait at XX days after sowing, with 'XX' = 09 to 29 and 'Trait' = PRA (Projected Rosette Area; in cm2), GreenMean / RedMean / BlueMean (rosette pixels' colour components; arbitrary unit), ConvexHullArea (area of the convex hull encompassing the rosette; in cm2) and CircleRadius (radius of the smallest circle

encompassing the rosette; in cm). RIL set IDs and RIL IDs are according to Publiclines http://publiclines.versailles.inra.fr/rils/index

- Genotypic description of the near isogenic lines (HIFs) used for QTL validation and significance of the observed segregating phenotypes [50]

Each row represents a single HIF and the genotype of the F7 RIL it originates from is indicated along the chromosomes with RIL ID, markers and genotypic conventions from Publiclines http://publiclines.versailles.inra.fr/rils/index (i.e. 'A' = Col allele; 'B' = alternate parental allele; 'C' = heterozygous). The region highlighted in yellow is the segregating region that is tested in the HIF family through several fixed lines for each parental allele. For each of the 3 growth traits (Compactness29 = rosette compactness 29 days after sowing; PRA29 = Projected Rosette Area 29 days after sowing; RER16-29 = Relative rosette Expansion Rate between days 16 and 29 after sowing) in 2 conditions ('WW' = Well Watered / 'WD' = Water Deficit), whenever significant, the p-value of the comparison between allelic lines ('Pval') and the direction of the allelic effect ('sign' calculated as [Col-Xxx] where Xxx is the alternate parental allele) are indicated in the last columns of the table.

> A specific webpage is associated with this work to display interactive graphes for dynamic QTL analyses at http://www.inra.fr/vast/PhenoDynamic.htm

REFERENCES

1. Alonso-Blanco C and Mendez-Vigo B (2014) Genetic architecture of naturally occurring quantitative traits in plants: an updated synthesis. *Current opinion in plant biology* 18: 37-43
2. Bac-Molenaar JA, Vreugdenhil D, Granier C, and Keurentjes JJ (2015) Genome-wide association mapping of growth dynamics detects time-specific and general quantitative trait loci. *Journal of experimental botany* 66: 5567-5580
3. Bouteille M, Rolland G, Balsera C, Loudet O, and Muller B (2012) Disentangling the intertwined genetic bases of root and shoot growth in Arabidopsis. *PLoS ONE* 7: e32319
4. Geng Y, Wu R, Wee CW, Xie F, Wei X, Chan PM, Tham C, Duan L, and Dinneny JR (2013) A spatio-temporal understanding of growth regulation during the salt stress response in Arabidopsis. *The Plant cell* 25: 2132-2154
5. Schmid M, Davison TS, Henz SR, Pape UJ, Demar M, Vingron M, Scholkopf B, Weigel D, and Lohmann JU (2005) A gene expression map of Arabidopsis thaliana development. *Nature Genetics* 37: 501-506
6. Zhang X, Hause RJ, Jr., and Borevitz JO (2012) Natural Genetic Variation for Growth and Development Revealed by High-Throughput Phenotyping in *Arabidopsis thaliana*. *G3* 2: 29-34

7. Clauw P, Coppens F, De Beuf K, Dhondt S, Van Daele T, Maleux K, Storme V, Clement L, Gonzalez N, and Inze D (2015) Leaf responses to mild drought stress in natural variants of Arabidopsis. *Plant physiology* 167: 800-816
8. Provart NJ*, et al.* (2016) 50 years of Arabidopsis research: highlights and future directions. *The New Phytologist* 209: 921-944
9. Gonzalez N and Inze D (2015) Molecular systems governing leaf growth: from genes to networks. *Journal of Experimental Botany* 66: 1045-1054
10. Vanhaeren H, Gonzalez N, Coppens F, De Milde L, Van Daele T, Vermeersch M, Eloy NB, Storme V, and Inze D (2014) Combining growth-promoting genes leads to positive epistasis in Arabidopsis thaliana. *eLife* 3: e02252
11. Trontin C, Tisné S, Bach L, and Loudet O (2011) What does Arabidopsis natural variation teach us (and does not teach us) about adaptation in plants? *Current Opinion in Plant Biology* 14: 225-231
12. Bazakos C, Hanemian M, Trontin C, Jimenez-Gomez JM, and Loudet O (2017) New Strategies and Tools in Quantitative Genetics: How to Go from the Phenotype to the Genotype. *Annual review of plant biology* 68: 435-455
13. Alonso-Blanco C, Aarts MG, Bentsink L, Keurentjes JJ, Reymond M, Vreugdenhil D, and Koornneef M (2009) What has natural variation taught us about plant development, physiology, and adaptation? *The Plant Cell* 21: 1877-1896
14. Grillo MA, Li C, Hammond M, Wang L, and Schemske DW (2013) Genetic architecture of flowering time differentiation between locally adapted populations of Arabidopsis thaliana. *The New phytologist* 197: 1321-1331
15. Salome PA, Bomblies K, Laitinen RA, Yant L, Mott R, and Weigel D (2011) Genetic architecture of flowering-time variation in *Arabidopsis thaliana*. *Genetics* 188: 421-433
16. Tabas-Madrid D, Mendez-Vigo B, Arteaga N, Marcer A, Pascual-Montano A, Weigel D, Xavier Pico F, and Alonso-Blanco C (2018) Genome-wide signatures of flowering adaptation to climate temperature: Regional analyses in a highly diverse native range of Arabidopsis thaliana. *Plant, cell & environment*
17. Johanson U, West J, Lister C, Michaels SD, Amasino RM, and Dean C (2000) Molecular analysis of *FRIGIDA*, a major determinant of natural variation in Arabidopsis flowering time. *Science* 290: 344-347
18. Michaels SD and Amasino RM (1999) *FLOWERING LOCUS C* encodes a novel MADS domain protein that acts as a repressor of flowering. *The Plant Cell* 11: 949-956
19. Shindo C, Aranzana MJ, Lister C, Baxter C, Nicholls C, Nordborg M, and Dean C (2005) Role of FRIGIDA and FLOWERING LOCUS C in determining variation in flowering time of Arabidopsis. *Plant physiology* 138: 1163-1173
20. Atwell S*, et al.* (2010) Genome-wide association study of 107 phenotypes in Arabidopsis thaliana inbred lines. *Nature* 465: 627-31
21. Brachi B, Faure N, Horton M, Flahauw E, Vazquez A, Nordborg M, Bergelson J, Cuguen J, and Roux F (2010) Linkage and association mapping of *Arabidopsis thaliana* flowering time in nature. *PLoS Genetics* 6: e1000940
22. El-Lithy ME, Clerkx EJ, Ruys GJ, Koornneef M, and Vreugdenhil D (2004) Quantitative trait locus analysis of growth-related traits in a new Arabidopsis recombinant inbred population. *Plant Physiology* 135: 444-458
23. Loudet O, Chaillou S, Camilleri C, Bouchez D, and Daniel-Vedele F (2002) Bay-0 x Shahdara recombinant inbred line population: a powerful tool for the genetic dissection of complex traits in Arabidopsis. *Theoretical and Applied Genetics* 104: 1173-1184
24. Loudet O, Chaillou S, Merigout P, Talbotec J, and Daniel-Vedele F (2003) Quantitative Trait Loci analysis of nitrogen use efficiency in Arabidopsis. *Plant Physiology* 131: 345-358
25. Tisné S, Schmalenbach I, Reymond M, Dauzat M, Pervent M, Vile D, and Granier C (2010) Keep on growing under drought: genetic and developmental bases of the response of rosette area using a recombinant inbred line population. *Plant, Cell & Environment* 33: 1875-1887

26. Tonsor SJ, Elnaccash TW, and Scheiner SM (2013) Developmental instability is genetically correlated with phenotypic plasticity, constraining heritability, and fitness. *Evolution* 67: 2923-2935
27. Dittmar EL, Oakley CG, Agren J, and Schemske DW (2014) Flowering time QTL in natural populations of Arabidopsis thaliana and implications for their adaptive value. *Molecular ecology* 23: 4291-4303
28. El-Soda M, Malosetti M, Zwaan BJ, Koornneef M, and Aarts MG (2014) Genotype x environment interaction QTL mapping in plants: lessons from Arabidopsis. *Trends in plant science* 19: 390-398
29. Kooyers NJ (2015) The evolution of drought escape and avoidance in natural herbaceous populations. *Plant science* 234: 155-162
30. Exposito-Alonso M, Vasseur F, Ding W, Wang G, Burbano HA, and Weigel D (2018) Genomic basis and evolutionary potential for extreme drought adaptation in Arabidopsis thaliana. *Nature ecology & evolution* 2: 352-358
31. Juenger TE (2013) Natural variation and genetic constraints on drought tolerance. *Current Opinion in Plant Biology* 16: 274-281
32. Granier C, Aguirrezabal L, Chenu K, Cookson SJ, Dauzat M, Hamard P, Thioux J-J, Rolland G, Bouchier-Combaud S, Lebaudy A, Muller B, Simonneau T, and Tardieu F (2006) PHENOPSIS, an automated platform for reproducible phenotyping of plant responses to soil water deficit in *Arabidopsis thaliana* permitted the identification of an accession with low sensitivity to soil water deficit. *The New Phytologist* 169: 623–635
33. Skirycz A*, et al.* (2011) Survival and growth of Arabidopsis plants given limited water are not equal. *Nature Biotechnology* 29: 212-214
34. Tisné S, Serrand Y, Bach L, Gilbault E, Ben Ameur R, Balasse H, Voisin R, Bouchez D, Durand-Tardif M, Guerche P, Chareyron G, Da Rugna J, Camilleri C, and Loudet O (2013) Phenoscope: an automated large-scale phenotyping platform offering high spatial homogeneity. *The Plant Journal* 74: 534-544
35. Walter A, Scharr H, Gilmer F, Zierer R, Nagel KA, Ernst M, Wiese A, Virnich O, Christ MM, Uhlig B, Junger S, and Schurr U (2007) Dynamics of seedling growth acclimation towards altered light conditions can be quantified via GROWSCREEN: a setup and procedure designed for rapid optical phenotyping of different plant species. *The New Phytologist* 174: 447-455
36. Barboza L, Effgen S, Alonso-Blanco C, Kooke R, Keurentjes JJ, Koornneef M, and Alcazar R (2013) Arabidopsis semidwarfs evolved from independent mutations in GA20ox1, ortholog to green revolution dwarf alleles in rice and barley. *Proceedings of the National Academy of Sciences of the United States of America* 110: 15818-15823
37. Bomblies K, Lempe J, Epple P, Warthmann N, Lanz C, Dangl JL, and Weigel D (2007) Autoimmune response as a mechanism for a Dobzhansky-Muller-type incompatibility syndrome in plants. *PLoS Biology* 5: e236
38. Loudet O, Michael TP, Burger BT, Le Mette C, Mockler TC, Weigel D, and Chory J (2008) A zinc knuckle protein that negatively controls morning-specific growth in *Arabidopsis thaliana*. *Proceedings of the National Academy of Sciences of the United States of America* 105: 17193-17198
39. Masle J, Gilmore SR, and Farquhar GD (2005) The ERECTA gene regulates plant transpiration efficiency in Arabidopsis. *Nature* 436: 866-870
40. Mouchel CF, Briggs GC, and Hardtke CS (2004) Natural genetic variation in Arabidopsis identifies *BREVIS RADIX*, a novel regulator of cell proliferation and elongation in the root. *Genes & Development* 18: 700-714
41. Sureshkumar S, Todesco M, Schneeberger K, Harilal R, Balasubramanian S, and Weigel D (2009) A genetic defect caused by a triplet repeat expansion in *Arabidopsis thaliana*. *Science* 323: 1060-1063
42. Todesco M*, et al.* (2010) Natural allelic variation underlying a major fitness trade-off in *Arabidopsis thaliana*. *Nature* 465: 632-636

43. Trontin C, Kiani S, Corwin JA, Hematy K, Yansouni J, Kliebenstein DJ, and Loudet O (2014) A pair of receptor-like kinases is responsible for natural variation in shoot growth response to mannitol treatment in *Arabidopsis thaliana*. *The Plant Journal* 78: 121-133
44. Kroymann J and Mitchell-Olds T (2005) Epistasis and balanced polymorphism influencing complex trait variation. *Nature* 435: 95-98
45. Prinzenberg AE, Barbier H, Salt DE, Stich B, and Reymond M (2010) Relationships between growth, growth response to nutrient supply, and ion content using a recombinant inbred line population in Arabidopsis. *Plant Physiology* 154: 1361-1371
46. Lemmon ZH and Doebley JF (2014) Genetic dissection of a genomic region with pleiotropic effects on domestication traits in maize reveals multiple linked QTL. *Genetics* 198: 345-353
47. Simon M, Loudet O, Durand S, Bérard A, Brunel D, Sennesal F-X, Durand-Tardif M, Pelletier G, and Camilleri C (2008) QTL mapping in five new large RIL populations of *Arabidopsis thaliana* genotyped with consensus SNP markers. *Genetics* 178: 2253-2264
48. Loudet O (2018) "Raw phenotypic data obtained on the Arabidopsis RILs with the Phenoscope robots (Marchadier, Hanemian, Tisné et al., 2018)", https://doi.org/10.15454/OCOP9B, Portail Data Inra, V1
49. Vlad D, Rappaport F, Simon M, and Loudet O (2010) Gene transposition causing natural variation for growth in *Arabidopsis thaliana*. *PLoS Genetics* 6: e1000945
50. Loudet O (2018) "Genotypic description of the near isogenic lines (HIFs) used for QTL validation and significance of the observed segregating phenotypes (Marchadier, Hanemian, Tisné et al., 2018)", https://doi.org/10.15454/EORHL8, Portail Data Inra, V1.
51. Botto JF, Alonso-Blanco C, Garzaron I, Sanchez RA, and Casal JJ (2003) The Cape Verde Islands allele of cryptochrome 2 enhances cotyledon unfolding in the absence of blue light in Arabidopsis. *Plant Physiology* 133: 1547-1456
52. El-Din El-Assal S, Alonso-Blanco C, Peeters AJ, Raz V, and Koornneef M (2001) A QTL for flowering time in Arabidopsis reveals a novel allele of *CRY2*. *Nature Genetics* 29: 435-440
53. Tognetti VB, Van Aken O, Morreel K, Vandenbroucke K, van de Cotte B, De Clercq I, Chiwocha S, Fenske R, Prinsen E, Boerjan W, Genty B, Stubbs KA, Inze D, and Van Breusegem F (2010) Perturbation of indole-3-butyric acid homeostasis by the UDP-glucosyltransferase UGT74E2 modulates Arabidopsis architecture and water stress tolerance. *The Plant cell* 22: 2660-2679
54. Nijveen H, Ligterink W, Keurentjes JJ, Loudet O, Long J, Sterken MG, Prins P, Hilhorst HW, de Ridder D, Kammenga JE, and Snoek BL (2017) AraQTL - workbench and archive for systems genetics in *Arabidopsis thaliana*. *The Plant Journal* 89: 1225-1235
55. Meyerhoff O, Muller K, Roelfsema MR, Latz A, Lacombe B, Hedrich R, Dietrich P, and Becker D (2005) AtGLR3.4, a glutamate receptor channel-like gene is sensitive to touch and cold. *Planta* 222: 418-427
56. Vincill ED, Clarin AE, Molenda JN, and Spalding EP (2013) Interacting glutamate receptor-like proteins in Phloem regulate lateral root initiation in Arabidopsis. *The Plant Cell* 25: 1304-1313
57. Cubillos FA, Stegle O, Grondin C, Canut M, Tisne S, Gy I, and Loudet O (2014) Extensive *cis*-regulatory variation robust to environmental perturbation in Arabidopsis. *The Plant Cell* 26: 4298-4310
58. Waterworth WM, Kozak J, Provost CM, Bray CM, Angelis KJ, and West CE (2009) DNA ligase 1 deficient plants display severe growth defects and delayed repair of both DNA single and double strand breaks. *BMC plant biology* 9: 79
59. Zhao H, Lu S, Li R, Chen T, Zhang H, Cui P, Ding F, Liu P, Wang G, Xia Y, Running MP, and Xiong L (2015) The Arabidopsis gene DIG6 encodes a large 60S subunit nuclear export GTPase 1 that is involved in ribosome biogenesis and affects multiple auxin-regulated development processes. *Journal of experimental botany* 66: 6863-6875

60. Clauw P, Coppens F, Korte A, Herman D, Slabbinck B, Dhondt S, Van Daele T, De Milde L, Vermeersch M, Maleux K, Maere S, Gonzalez N, and Inze D (2016) Leaf Growth Response to Mild Drought: Natural Variation in Arabidopsis Sheds Light on Trait Architecture. *The Plant Cell*
61. Bac-Molenaar JA, Granier C, Keurentjes JJ, and Vreugdenhil D (2016) Genome-wide association mapping of time-dependent growth responses to moderate drought stress in Arabidopsis. *Plant, cell & environment* 39: 88-102
62. Kooke R, Kruijer W, Bours R, Becker F, Kuhn A, van de Geest H, Buntjer J, Doeswijk T, Guerra J, Bouwmeester H, Vreugdenhil D, and Keurentjes JJ (2016) Genome-Wide Association Mapping and Genomic Prediction Elucidate the Genetic Architecture of Morphological Traits in Arabidopsis. *Plant physiology* 170: 2187-2203
63. Meijon M, Satbhai SB, Tsuchimatsu T, and Busch W (2014) Genome-wide association study using cellular traits identifies a new regulator of root development in Arabidopsis. *Nature genetics* 46: 77-81
64. Rishmawi L, Buhler J, Jaegle B, Hulskamp M, and Koornneef M (2017) Quantitative trait loci controlling leaf venation in Arabidopsis. *Plant, cell & environment* 40: 1429-1441
65. Flood PJ, Kruijer W, Schnabel SK, van der Schoor R, Jalink H, Snel JF, Harbinson J, and Aarts MG (2016) Phenomics for photosynthesis, growth and reflectance in Arabidopsis thaliana reveals circadian and long-term fluctuations in heritability. *Plant methods* 12: 14
66. Zhang X, Huang C, Wu D, Qiao F, Li W, Duan L, Wang K, Xiao Y, Chen G, Liu Q, Xiong L, Yang W, and Yan J (2017) High-Throughput Phenotyping and QTL Mapping Reveals the Genetic Architecture of Maize Plant Growth. *Plant physiology* 173: 1554-1564
67. Muraya MM, Chu J, Zhao Y, Junker A, Klukas C, Reif JC, and Altmann T (2017) Genetic variation of growth dynamics in maize (Zea mays L.) revealed through automated non-invasive phenotyping. *The Plant Journal* 89: 366-380
68. Moore CR, Johnson LS, Kwak IY, Livny M, Broman KW, and Spalding EP (2013) High-throughput computer vision introduces the time axis to a quantitative trait map of a plant growth response. *Genetics* 195: 1077-1086
69. Mojica JP, Mullen J, Lovell JT, Monroe JG, Paul JR, Oakley CG, and McKay JK (2016) Genetics of water use physiology in locally adapted Arabidopsis thaliana. *Plant Science* 251: 12-22
70. Blanc G, Charcosset A, Mangin B, Gallais A, and Moreau L (2006) Connected populations for detecting quantitative trait loci and testing for epistasis: an application in maize. *Theoretical and Applied Genetics* 113: 206-224
71. Nice LM, Steffenson BJ, Brown-Guedira GL, Akhunov ED, Liu C, Kono TJ, Morrell PL, Blake TK, Horsley RD, Smith KP, and Muehlbauer GJ (2016) Development and Genetic Characterization of an Advanced Backcross-Nested Association Mapping (AB-NAM) Population of Wild x Cultivated Barley. *Genetics* 203: 1453-1467
72. Yu J, Holland JB, McMullen MD, and Buckler ES (2008) Genetic design and statistical power of nested association mapping in maize. *Genetics* 178: 539-551
73. Brenton ZW, Cooper EA, Myers MT, Boyles RE, Shakoor N, Zielinski KJ, Rauh BL, Bridges WC, Morris GP, and Kresovich S (2016) A Genomic Resource for the Development, Improvement, and Exploitation of Sorghum for Bioenergy. *Genetics* 204: 21-33
74. Huang YF, Madur D, Combes V, Ky CL, Coubriche D, Jamin P, Jouanne S, Dumas F, Bouty E, Bertin P, Charcosset A, and Moreau L (2010) The genetic architecture of grain yield and related traits in Zea maize L. revealed by comparing intermated and conventional populations. *Genetics* 186: 395-404
75. Studer AJ and Doebley JF (2011) Do large effect QTL fractionate? A case study at the maize domestication QTL teosinte branched1. *Genetics* 188: 673-681
76. Sanchez-Bermejo E, Zhu W, Tasset C, Eimer H, Sureshkumar S, Singh R, Sundaramoorthi V, Colling L, and Balasubramanian S (2015) Genetic Architecture of Natural Variation in Thermal Responses of Arabidopsis. *Plant physiology* 169: 647-659

77. Des Marais DL, Auchincloss LC, Sukamtoh E, McKay JK, Logan T, Richards JH, and Juenger TE (2014) Variation in MPK12 affects water use efficiency in Arabidopsis and reveals a pleiotropic link between guard cell size and ABA response. *Proceedings of the National Academy of Sciences of the United States of America* 111: 2836-2841
78. Jakobson L*, et al.* (2016) Natural Variation in Arabidopsis Cvi-0 Accession Reveals an Important Role of MPK12 in Guard Cell CO2 Signaling. *PLoS biology* 14: e2000322
79. Michael TP, Jupe F, Bemm F, Motley ST, Sandoval JP, Lanz C, Loudet O, Weigel D, and Ecker JR (2018) High contiguity Arabidopsis thaliana genome assembly with a single nanopore flow cell. *Nature communications* 9: 541
80. Civelek M and Lusis AJ (2014) Systems genetics approaches to understand complex traits. *Nature reviews. Genetics* 15: 34-48
81. de Koning DJ and McIntyre LM (2017) Back to the Future: Multiparent Populations Provide the Key to Unlocking the Genetic Basis of Complex Traits. *Genetics* 206: 527-529
82. She R and Jarosz DF (2018) Mapping Causal Variants with Single-Nucleotide Resolution Reveals Biochemical Drivers of Phenotypic Change. *Cell* 172: 478-490
83. Fernandes JB, Seguela-Arnaud M, Larcheveque C, Lloyd AH, and Mercier R (2018) Unleashing meiotic crossovers in hybrid plants. *Proceedings of the National Academy of Sciences of the United States of America* 115: 2431-2436
84. Loudet O, Gaudon V, Trubuil A, and Daniel-Vedele F (2005) Quantitative trait loci controlling root growth and architecture in *Arabidopsis thaliana* confirmed by heterogeneous inbred family. *Theoretical and Applied Genetics* 110: 742-753
85. Koumproglou R, Wilkes TM, Townson P, Wang XY, Beynon J, Pooni HS, Newbury HJ, and Kearsey MJ (2002) STAIRS: a new genetic resource for functional genomic studies of Arabidopsis. *The Plant Journal* 31: 355-364
86. Broman KW, Wu H, Sen S, and Churchill GA (2003) R/qtl: QTL mapping in experimental crosses. *Bioinformatics* 19: 889-890
87. Arends D, Prins P, Jansen RC, and Broman KW (2010) R/qtl: high-throughput multiple QTL mapping. *Bioinformatics* 26: 2990-2992
88. Broman KW (2015) R/qtlcharts: interactive graphics for quantitative trait locus mapping. *Genetics* 199: 359-361
89. Jourjon MF, Jasson S, Marcel J, Ngom B, and Mangin B (2005) MCQTL: multi-allelic QTL mapping in multi-cross design. *Bioinformatics* 21: 128-130
90. Cubillos FA, Yansouni J, Khalili H, Balzergue S, Elftieh S, Martin-Magniette ML, Serrand Y, Lepiniec L, Baud S, Dubreucq B, Renou JP, Camilleri C, and Loudet O (2012) Expression variation in connected recombinant populations of *Arabidopsis thaliana* highlights distinct transcriptome architectures. *BMC Genomics* 13: 117

>>> SUPPLEMENTARY MATERIAL

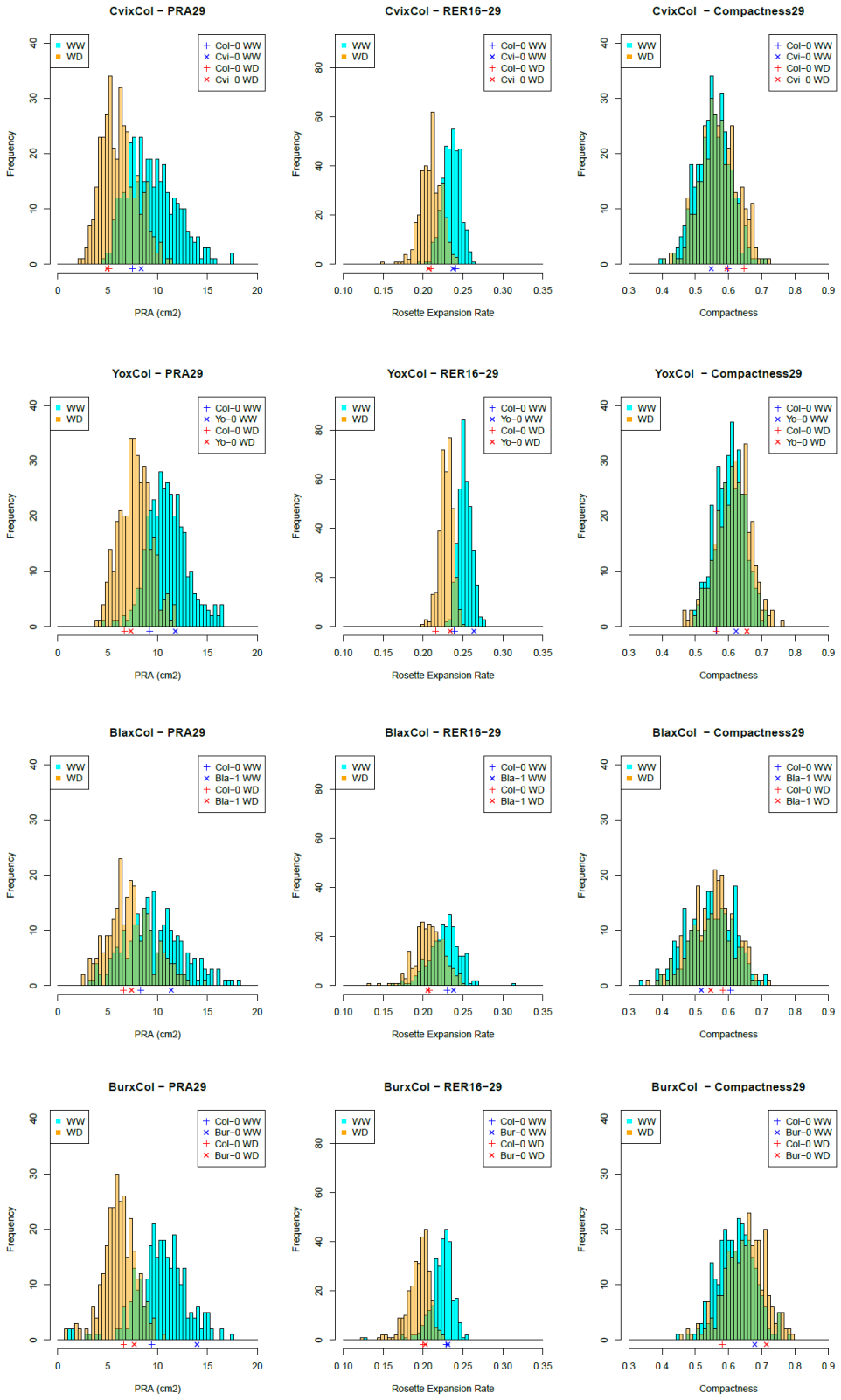

Supplementary Figure S1: Distributions of the mean phenotypic values across RILs

Frequency histograms showing the distributions of the PRA29, RER16-29 and Compactness29 traits within each of the four RIL sets in well watered (WW: blue) and water deficit (WD: orange) conditions. Phenotypic values for parental accessions from these specific experiments are indicated by blue (WW) and red (WD) ticks (see inset for legend) just above the x axes.

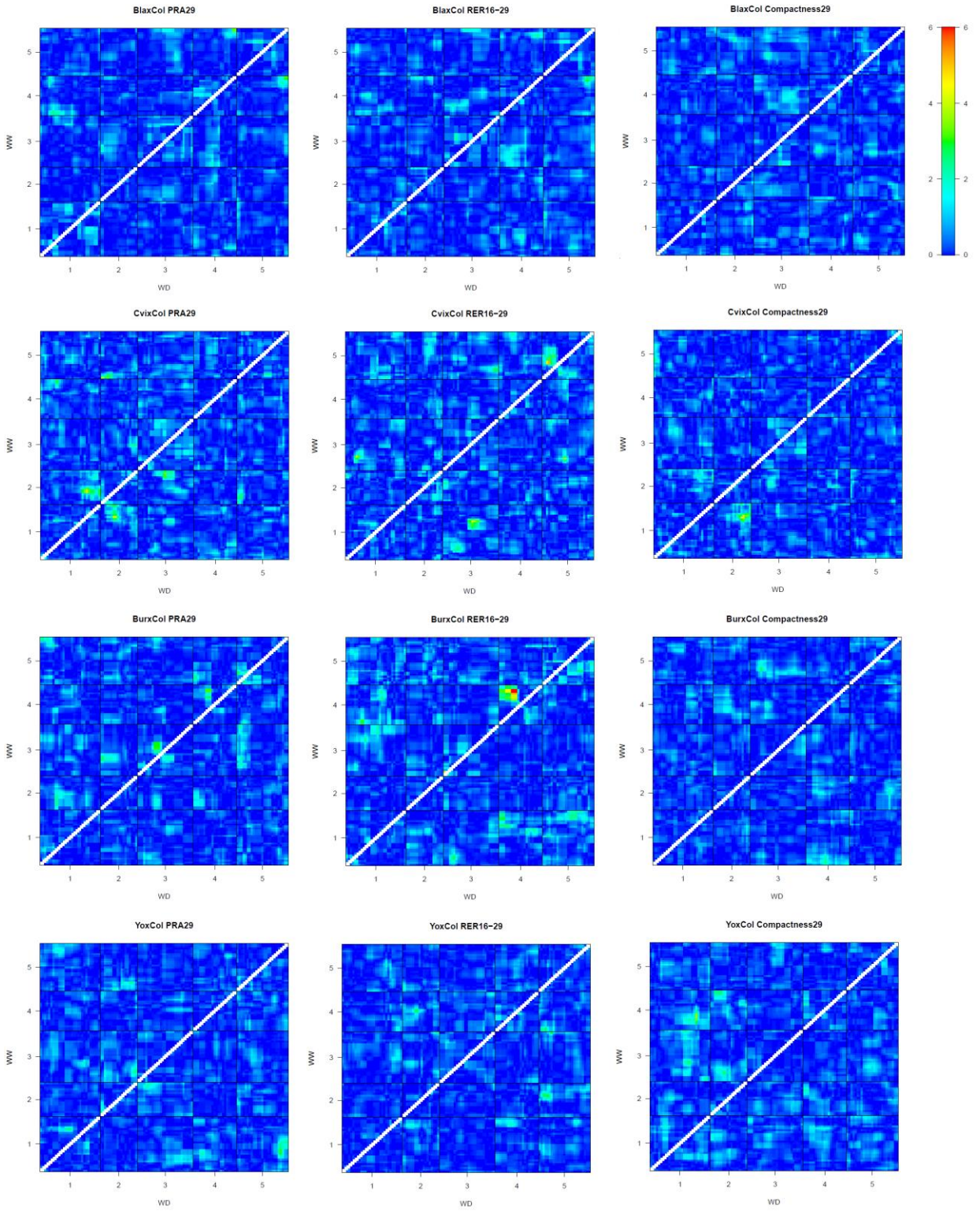

Supplementary Figure S2: 2D scans for epistasis

Heatmaps representing the LOD score of the interaction effects between all pairs of loci for 4 RIL sets, 3 traits, in 2 conditions. Each heatmap shows the pairwise interaction effects obtained in control condition WW (triangle above diagonal) and in water deficit condition WD (triangle below diagonal). The color scale (LOD score values) shared among all heatmaps is indicated on the right (note that it is different from the scale of @Figure 4). Diagonal values are canceled and enlarged to exclude pairs of adjacent markers from the test.

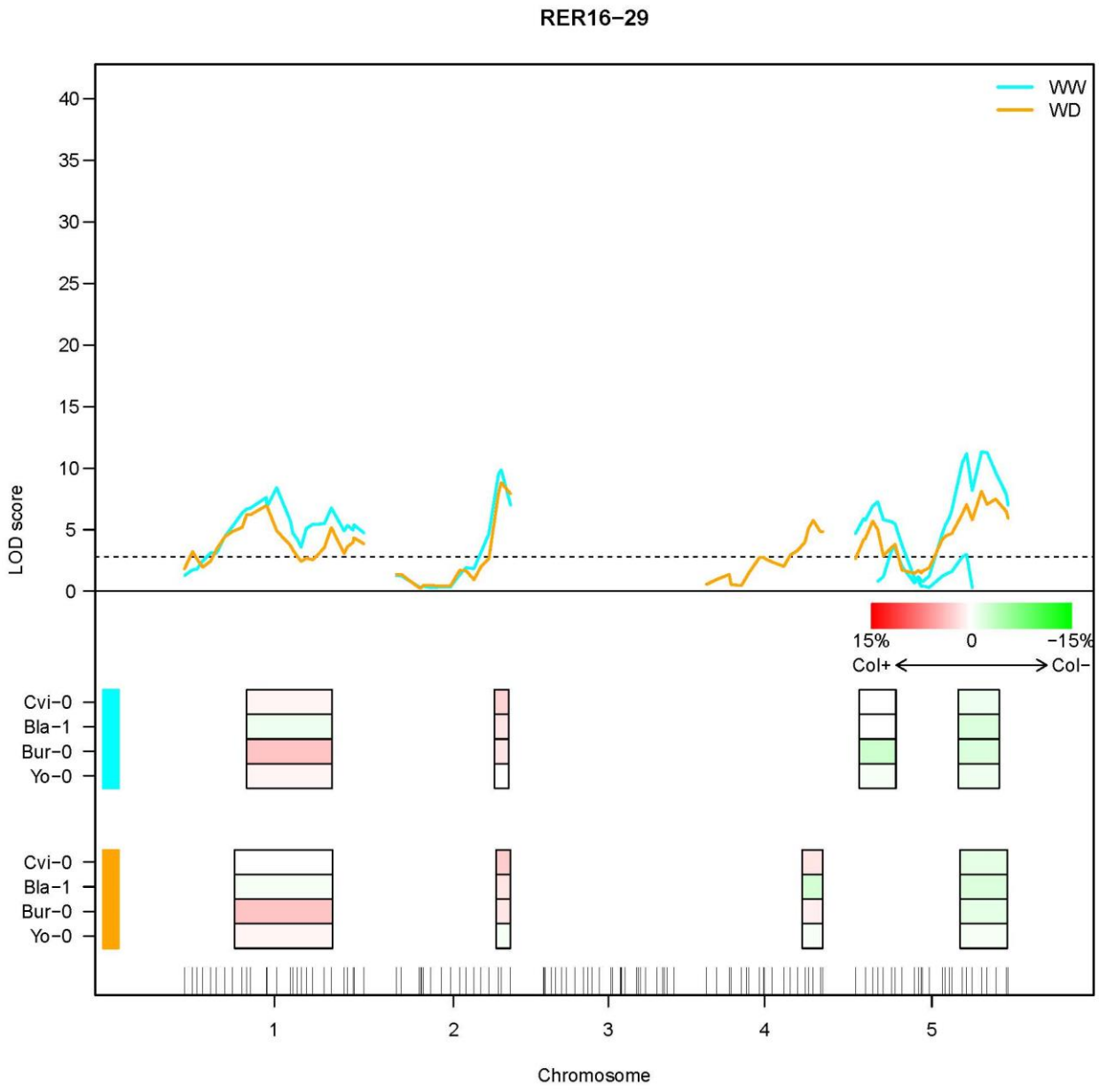

Supplementary Figure S3 [...]

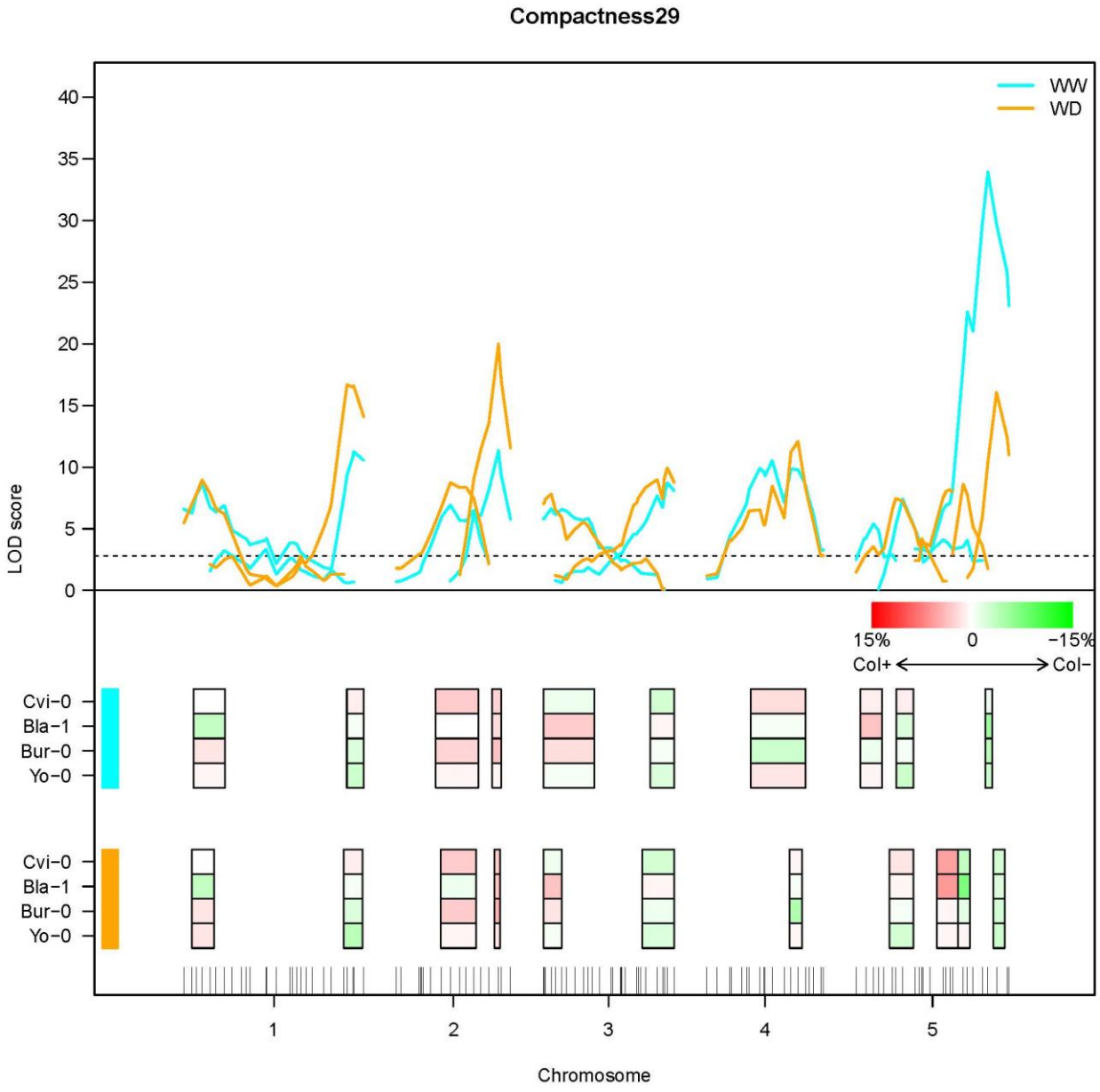

Supplementary Figure S3: Multi-cross QTL analysis for RER16-29 and Compactness29

Same legend as @Figure 5.

Chromosome 3 shows no significant combined QTLs for RER16-29.

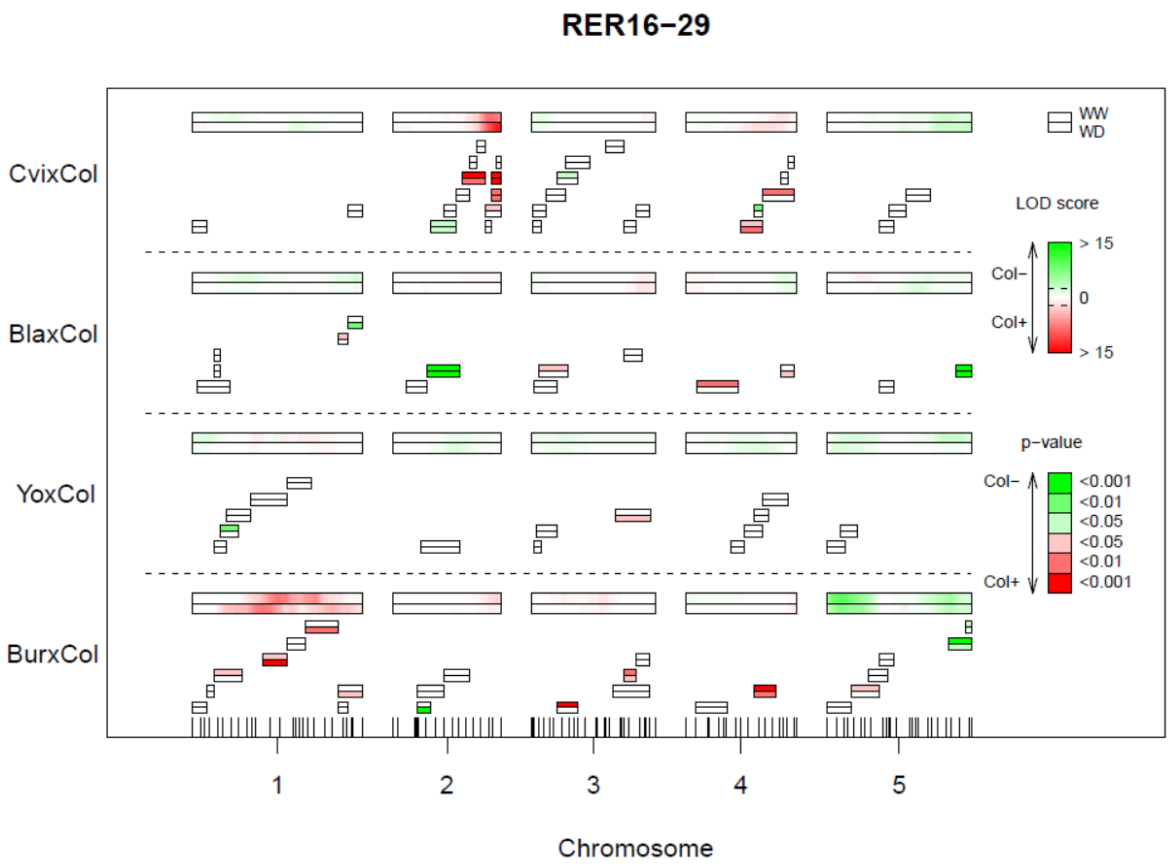

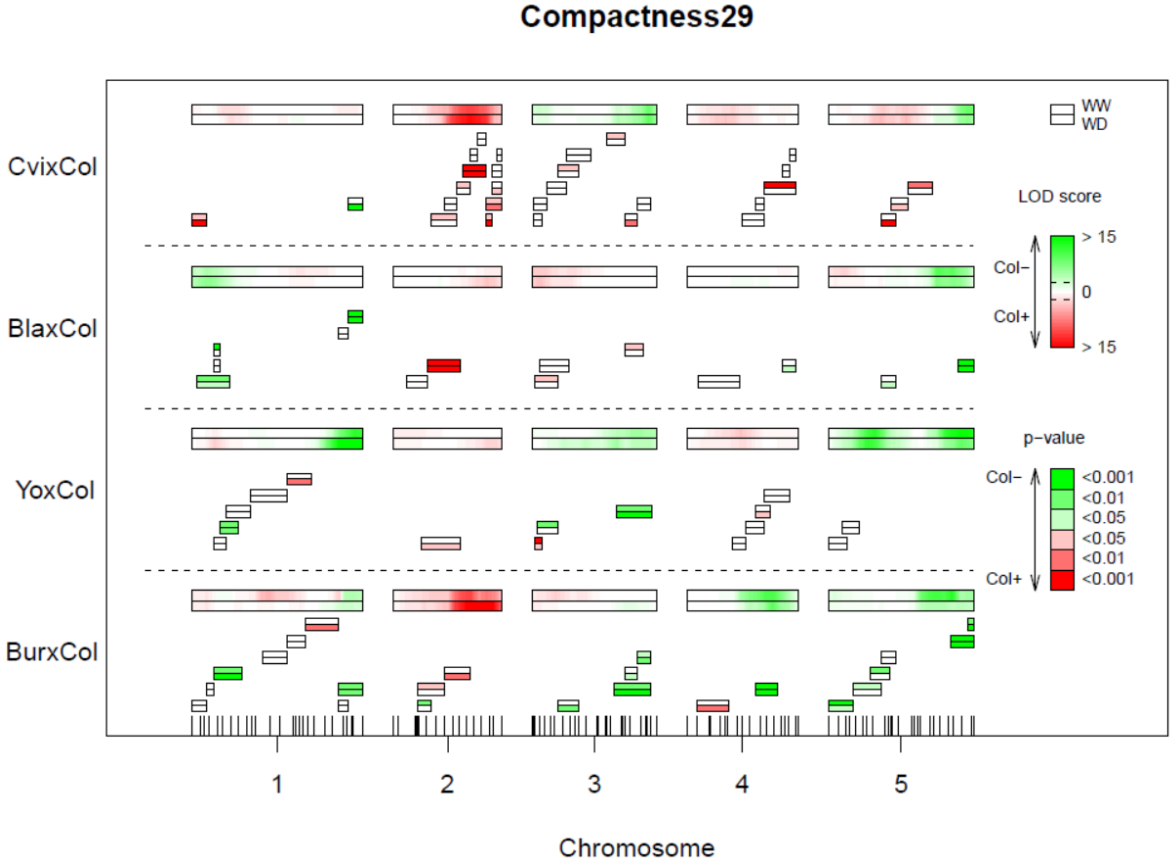

Supplementary Figure S4: Near isogenic lines-based validation of QTLs for RER16-29 and Compactness29. Same legend as @Figure 6

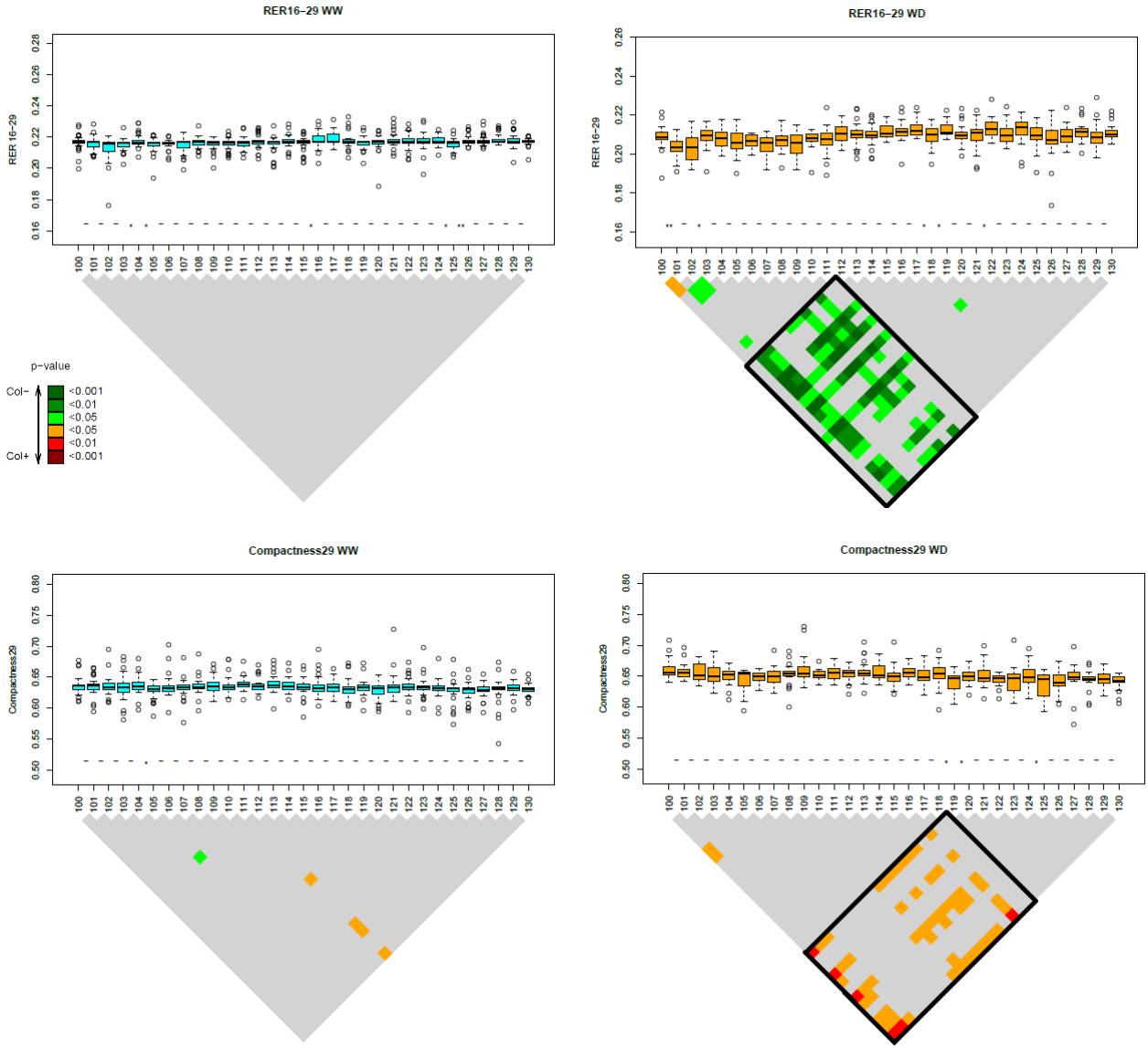

Supplementary Figure S5: Dissection of a genomic region in CvixCol for RER16-29 and Compactness29 ('microStairs' approach)

Same legend as @Figure 7

Supplementary Table S1: Heritabilities of the observed phenotypes

Broad-sense heritabilities (h2) in the 4 RIL sets (BlaxCol, CvixCol, BurxCol and YoxCol) for PRA29, RER16-29 and Compactness29 in WW and WD conditions. H2 > 0.4 are highlighted in bold. Broad-sense heritabilities were calculated with the following equation h2 = Var(G)/Var(P) with Var(P)=Var(G)+Var(E)

	BlaxCol	CvixCol	BurxCol	YoxCol
PRA29 WW	0.23	**0.67**	**0.62**	**0.48**
PRA29 WD	0.12	**0.45**	**0.55**	0.26
RER16-29 WW	0.17	0.13	**0.66**	NA
RER16-29 WD	0.22	NA	**0.42**	NA
Compactness29 WW	**0.75**	**0.60**	**0.65**	**0.54**
Compactness29 WD	**0.50**	**0.40**	0.37	0.34

Supplementary Table S2: Analyses of variance for genotype, experiment and condition factors, and their interactions

For each RIL set, -log(p values) of main and interaction effects calculated by the analysis of variance (ANOVA) from the following model :

$Yijkl \sim \mu+\alpha i+\beta j+\gamma k+\delta ij+\lambda jk+\sigma ik+\varepsilon ijkl$

where

Yijkl: phenotype; μ: mean; αi: effect of the condition; βj: effect of the experiment; γk: effect of the genotype; δij: effect of the interaction condition*experiment; λjk: effect of the interaction experiment*genotype; σik: effect of the interaction condition*genotype; εijkl: residuals

NS = Not Significant

RIL set	Phenotype	Condition	Experiment	Genotype	Condition * Experiment	Experiment * Genotype	Condition * Genotype
CvixCol	PRA29	726,57	26,33	526,59	75,81	51,37	16,87
CvixCol	Compactness29	57,54	212,95	378,58	50,64	13,01	NS
CvixCol	RER16-29	555,13	499,28	138,67	69,48	8,13	3,06
YoxCol	PRA29	450,11	27,20	185,91	20,90	47,28	3,30
YoxCol	Compactness29	12,03	96,39	151,05	25,42	NS	NS
YoxCol	RER16-29	482,02	355,28	84,52	8,39	6,57	NS
BlaxCol	PRA29	211,83	10,96	212,99	NS	184,35	9,44
BlaxCol	Compactness29	NS	4,27	183,33	NS	4,85	4,96
BlaxCol	RER16-29	161,24	47,86	112,12	NS	73,21	3,69
BurxCol	PRA29	402,90	14,73	168,74	7,37	4,92	11,24
BurxCol	Compactness29	34,46	8,21	91,88	NS	NS	NS
BurxCol	RER16-29	407,91	22,25	149,56	NS	11,60	13,24

Supplementary Table S3: Mapped QTL parameters across RIL sets, traits and conditions

For each RIL set, trait and condition (or GxE interaction term: 'inter'): every independent QTL peak is a row in the table, indicating its localisation (chromosome and position on the genetic map), its significance (maximum LOD score) and its effect (direction of the allelic effect: 'sign' indicates the sign of the allelic effect estimated as [Col – Xxx], where Xxx is the alternate parental allele; R2 %). Independent QTLs peaks are considered when the LOD score curve returns below threshold between 2 peaks, to ensure the loci are not too genetically linked.

RIL set	Phenotype	Condition	Chromosome	Position (cM)	LOD score	sign	R2 (%)
BurxCol	PRA29	WD	1	5	4,1	-1	1
BurxCol	PRA29	WD	1	50	11,2	1	11
BurxCol	PRA29	WD	5	93	2,6	-1	3
BurxCol	PRA29	WW	1	11	9,1	-1	4
BurxCol	PRA29	WW	1	50	19,8	1	12
BurxCol	PRA29	WW	4	0	8,3	-1	9
BurxCol	PRA29	WW	5	14	2,8	-1	2
BurxCol	PRA29	WW	5	93	3,2	-1	3
BurxCol	PRA29	inter	1	20	9	-1	7
BurxCol	PRA29	inter	1	50	6,6	1	4
BurxCol	PRA29	inter	2	70	3,9	1	3
BurxCol	PRA29	inter	4	0	5,3	-1	6
BurxCol	RER16-29	WD	1	50	9,3	1	11
BurxCol	RER16-29	WD	1	74	3,1	1	4
BurxCol	RER16-29	WD	1	90	2,9	1	8
BurxCol	RER16-29	WD	5	11	9,3	-1	6
BurxCol	RER16-29	WD	5	86	4,3	-1	3
BurxCol	RER16-29	WW	1	56	12,4	1	9
BurxCol	RER16-29	WW	2	64	2,9	1	2
BurxCol	RER16-29	WW	5	11	16	-1	12
BurxCol	RER16-29	WW	5	80	8	-1	4
BurxCol	RER16-29	inter	1	25	3,2	-1	5
BurxCol	Compactness29	WD	1	110	4,1	-1	3
BurxCol	Compactness29	WD	2	56	16,4	1	11
BurxCol	Compactness29	WD	4	56	12	-1	8
BurxCol	Compactness29	WD	5	86	7,4	-1	3
BurxCol	Compactness29	WW	1	104	7,2	-1	3
BurxCol	Compactness29	WW	1	50	2,8	1	1
BurxCol	Compactness29	WW	1	65	2,9	1	1
BurxCol	Compactness29	WW	2	47	14,6	1	11
BurxCol	Compactness29	WW	3	14	3,7	1	3
BurxCol	Compactness29	WW	4	56	13,7	-1	6
BurxCol	Compactness29	WW	5	6	4	-1	1
BurxCol	Compactness29	WW	5	80	17	-1	8
BurxCol	Compactness29	inter	3	59	2,7	1	4
YoxCol	PRA29	WD	1	20	4	-1	4

YoxCol	PRA29	WD	1	56	3,6	-1	5
YoxCol	PRA29	WD	2	33	4,2	-1	3
YoxCol	PRA29	WD	4	21	2,7	-1	3
YoxCol	PRA29	WD	4	47	2,9	-1	4
YoxCol	PRA29	WD	4	60	2,5	-1	4
YoxCol	PRA29	WD	5	80	11,6	-1	9
YoxCol	PRA29	WD	5	6	3,9	1	3
YoxCol	PRA29	WW	1	16	3,1	-1	4
YoxCol	PRA29	WW	1	35	5,7	-1	7
YoxCol	PRA29	WW	2	39	3	-1	4
YoxCol	PRA29	WW	4	15	6,2	-1	4
YoxCol	PRA29	WW	5	77	16,8	-1	12
YoxCol	PRA29	WW	5	11	9,6	1	6
YoxCol	PRA29	inter	4	0	3,6	-1	3
YoxCol	PRA29	inter	4	71	2,6	1	3
YoxCol	PRA29	inter	5	68	5,6	-1	4
YoxCol	PRA29	inter	5	11	4,9	1	4
YoxCol	RER16-29	WD	4	35	3,6	-1	4
YoxCol	RER16-29	WD	4	51	2,9	-1	5
YoxCol	RER16-29	WD	5	6	3	-1	4
YoxCol	RER16-29	WD	5	65	5,3	-1	5
YoxCol	RER16-29	WW	1	11	3,6	-1	3
YoxCol	RER16-29	WW	3	19	2,6	-1	4
YoxCol	RER16-29	WW	5	14	3,2	-1	4
YoxCol	RER16-29	WW	5	71	9,7	-1	11
YoxCol	RER16-29	inter	4	65	4,9	1	6
YoxCol	RER16-29	inter	5	92	3	-1	3
YoxCol	Compactness29	WD	1	104	27,6	-1	18
YoxCol	Compactness29	WD	1	11	2,4	1	5
YoxCol	Compactness29	WD	2	64	4,9	1	5
YoxCol	Compactness29	WD	3	69	6,6	-1	5
YoxCol	Compactness29	WD	4	32	4,7	1	3
YoxCol	Compactness29	WD	5	24	18,2	-1	10
YoxCol	Compactness29	WD	5	86	15,8	-1	13
YoxCol	Compactness29	WW	1	35	2,8	-1	1
YoxCol	Compactness29	WW	1	104	14,6	-1	10
YoxCol	Compactness29	WW	1	11	2,8	1	3
YoxCol	Compactness29	WW	3	69	8,2	-1	7
YoxCol	Compactness29	WW	4	35	6	1	3
YoxCol	Compactness29	WW	4	71	3,3	1	3
YoxCol	Compactness29	WW	5	28	16,8	-1	10
YoxCol	Compactness29	WW	5	86	24,7	-1	19
YoxCol	Compactness29	inter	1	85	5,1	1	7
YoxCol	Compactness29	inter	2	64	2,6	-1	3
BlaxCol	PRA29	WD	1	20	3,8	-1	6
BlaxCol	PRA29	WW	1	16	4,5	-1	7
BlaxCol	PRA29	WW	1	110	5,8	-1	6
BlaxCol	PRA29	inter	1	110	3,5	-1	6
BlaxCol	RER16-29	WD	3	69	2,8	1	4
BlaxCol	RER16-29	WD	4	65	2,5	-1	4
BlaxCol	RER16-29	WW	1	104	2,7	-1	3
BlaxCol	RER16-29	WW	3	76	3,5	1	4

BlaxCol	RER16-29	WW	5	65	2,5	-1	5
BlaxCol	RER16-29	WW	5	80	3,2	-1	4
BlaxCol	Compactness29	WD	1	11	6,8	-1	8
BlaxCol	Compactness29	WD	2	64	8,2	1	6
BlaxCol	Compactness29	WD	3	0	9,6	1	9
BlaxCol	Compactness29	WD	5	77	12,2	-1	10
BlaxCol	Compactness29	WW	1	11	6,3	-1	8
BlaxCol	Compactness29	WW	1	74	2,7	1	5
BlaxCol	Compactness29	WW	2	64	3,8	1	2
BlaxCol	Compactness29	WW	3	0	5,5	1	4
BlaxCol	Compactness29	WW	5	77	22,4	-1	20
BlaxCol	Compactness29	WW	5	11	5,6	1	4
CvixCol	PRA29	WD	1	20	4,5	-1	4
CvixCol	PRA29	WD	2	70	29,6	1	30
CvixCol	PRA29	WD	4	47	2,6	-1	1
CvixCol	PRA29	WD	5	86	6,3	-1	4
CvixCol	PRA29	WW	1	16	9,4	-1	7
CvixCol	PRA29	WW	1	104	3	-1	4
CvixCol	PRA29	WW	2	64	27,3	1	24
CvixCol	PRA29	WW	4	47	6,9	-1	3
CvixCol	PRA29	WW	5	86	9,4	-1	4
CvixCol	PRA29	inter	1	0	7,5	-1	8
CvixCol	PRA29	inter	2	42	3,4	1	4
CvixCol	PRA29	inter	4	47	4,9	-1	4
CvixCol	RER16-29	WD	2	70	32	1	27
CvixCol	RER16-29	WD	5	71	7	-1	4
CvixCol	RER16-29	WW	2	64	23,3	1	22
CvixCol	RER16-29	WW	5	80	4,8	-1	4
CvixCol	RER16-29	inter	1	5	2,7	-1	3
CvixCol	Compactness29	WD	2	47	14,2	1	8
CvixCol	Compactness29	WD	3	80	9,4	-1	7
CvixCol	Compactness29	WD	4	21	2,9	1	2
CvixCol	Compactness29	WD	5	86	7,8	-1	4
CvixCol	Compactness29	WD	5	36	2,5	1	1
CvixCol	Compactness29	WD	5	55	2,6	1	2
CvixCol	Compactness29	WW	1	29	2,5	1	2
CvixCol	Compactness29	WW	2	47	11,6	1	8
CvixCol	Compactness29	WW	3	5	3	-1	2
CvixCol	Compactness29	WW	3	80	9,4	-1	7
CvixCol	Compactness29	WW	4	15	3,5	1	3
CvixCol	Compactness29	WW	4	32	2,8	1	4
CvixCol	Compactness29	WW	5	92	8,4	-1	4
CvixCol	Compactness29	WW	5	55	2,6	1	2

Supplementary Table S4: microStairs; genotypic description of recombinant lines

The genotypes of the 31 lines selected for the microStairs experiment are indicated along this 3Mb region of the top of chromosome 1 with markers localised on the physical map (kb).

Marker name	Marker pos. (kb, Chrom 1)	Min Bin size (kb)	Max Bin size (kb)	Rough position	recomb. name	8HV294100	8HV294101	8HV294102	8HV294103	8HV294104	8HV294105	8HV294106	8HV294107	8HV294108	8HV294109	8HV294110	8HV294111	8HV294112	8HV294113	8HV294114	8HV294115	8HV294116	8HV294117	8HV294118	8HV294119	8HV294120	8HV294121	8HV294122	8HV294123	8HV294124	8HV294125	8HV294126	8HV294127	8HV294128	8HV294129	8HV294130	< Names on Figure 7 & S5
						100	101	102	103	104	105	106	107	108	109	110	111	112	113	114	115	116	117	118	119	120	121	122	123	124	125	126	127	128	129	130	
MSAT1.00008	8 639			0		Col	Cvi	Cvi	Cvi	Cvi	Cvi	Cvi	Cvi	Cvi	Cvi	Cvi	Cvi	Cvi	Cvi	Cvi	Cvi	Cvi	Cvi	Cvi	Cvi	Cvi	Cvi	Cvi	Cvi	Cvi	Cvi	Cvi	Cvi	Cvi	Cvi	Cvi	
HRM1.00084.F1b/R1b	84 908	76 269	161 913	0,1		Col	Cvi	Cvi	Cvi	Cvi	Cvi	Cvi	Cvi	Cvi	Cvi	Cvi	Cvi	Cvi	Cvi	Cvi	Cvi	Cvi	Cvi	Cvi	Cvi	Cvi	Cvi	Cvi	Cvi	Cvi	Cvi	Cvi	Cvi	Cvi	Cvi	Cvi	
IND1.00171	170 552	85 644	213 230	0,2		Col	Col	Cvi	Cvi	Cvi	Cvi	Cvi	Cvi	Cvi	Cvi	Cvi	Cvi	Cvi	Cvi	Cvi	Cvi	Cvi	Cvi	Cvi	Cvi	Cvi	Cvi	Cvi	Cvi	Cvi	Cvi	Cvi	Cvi	Cvi	Cvi	Cvi	
IND1.00298	298 138	127 586	256 791	0,3		Col	Col	Col	Cvi	Cvi	Cvi	Cvi	Cvi	Cvi	Cvi	Cvi	Cvi	Cvi	Cvi	Cvi	Cvi	Cvi	Cvi	Cvi	Cvi	Cvi	Cvi	Cvi	Cvi	Cvi	Cvi	Cvi	Cvi	Cvi	Cvi	Cvi	
T7I23	427 343	129 205	215 153	0,4		Col	Col	Col	Col	Cvi	Cvi	Cvi	Cvi	Cvi	Cvi	Cvi	Cvi	Cvi	Cvi	Cvi	Cvi	Cvi	Cvi	Cvi	Cvi	Cvi	Cvi	Cvi	Cvi	Cvi	Cvi	Cvi	Cvi	Cvi	Cvi	Cvi	
IND1.00513	513 291	85 948	189 488	0,5		Col	Col	Col	Col	Col	Cvi	Cvi	Cvi	Cvi	Cvi	Cvi	Cvi	Cvi	Cvi	Cvi	Cvi	Cvi	Cvi	Cvi	Cvi	Cvi	Cvi	Cvi	Cvi	Cvi	Cvi	Cvi	Cvi	Cvi	Cvi	Cvi	
HRM1.000616.F2b/R2	616 831	103 540	186 219	0,6		Col	Col	Col	Col	Col	Col	Cvi	Cvi	Cvi	Cvi	Cvi	Cvi	Cvi	Cvi	Cvi	Cvi	Cvi	Cvi	Cvi	Cvi	Cvi	Cvi	Cvi	Cvi	Cvi	Cvi	Cvi	Cvi	Cvi	Cvi	Cvi	
HRM1.00699	699 510	82 679	189 317	0,7		Col	Col	Col	Col	Col	Col	Col	Cvi	Cvi	Cvi	Cvi	Cvi	Cvi	Cvi	Cvi	Cvi	Cvi	Cvi	Cvi	Cvi	Cvi	Cvi	Cvi	Cvi	Cvi	Cvi	Cvi	Cvi	Cvi	Cvi	Cvi	
HRM1.00806	806 148	106 638	199 053	0,8		Col	Col	Col	Col	Col	Col	Col	Col	Cvi	Cvi	Cvi	Cvi	Cvi	Cvi	Cvi	Cvi	Cvi	Cvi	Cvi	Cvi	Cvi	Cvi	Cvi	Cvi	Cvi	Cvi	Cvi	Cvi	Cvi	Cvi	Cvi	
IND1.00899	898 563	92 415	200 402	0,9		Col	Col	Col	Col	Col	Col	Col	Col	Col	Cvi	Cvi	Cvi	Cvi	Cvi	Cvi	Cvi	Cvi	Cvi	Cvi	Cvi	Cvi	Cvi	Cvi	Cvi	Cvi	Cvi	Cvi	Cvi	Cvi	Cvi	Cvi	
HRM1.01007	1 006 550	107 987	172 012	1		Col	Col	Col	Col	Col	Col	Col	Col	Col	Col	Cvi	Cvi	Cvi	Cvi	Cvi	Cvi	Cvi	Cvi	Cvi	Cvi	Cvi	Cvi	Cvi	Cvi	Cvi	Cvi	Cvi	Cvi	Cvi	Cvi	Cvi	
F20D22#2	1 070 575	64 025	208 869	1,1		Col	Col	Col	Col	Col	Col	Col	Col	Col	Col	Col	Cvi	Cvi	Cvi	Cvi	Cvi	Cvi	Cvi	Cvi	Cvi	Cvi	Cvi	Cvi	Cvi	Cvi	Cvi	Cvi	Cvi	Cvi	Cvi	Cvi	
IND1.01215bR	1 215 419	144 844	221 028	1,2		Col	Col	Col	Col	Col	Col	Col	Col	Col	Col	Col	Col	Cvi	Cvi	Cvi	Cvi	Cvi	Cvi	Cvi	Cvi	Cvi	Cvi	Cvi	Cvi	Cvi	Cvi	Cvi	Cvi	Cvi	Cvi	Cvi	
HRM1.01292	1 291 603	76 184	203 857	1,3		Col	Col	Col	Col	Col	Col	Col	Col	Col	Col	Col	Col	Col	Cvi	Cvi	Cvi	Cvi	Cvi	Cvi	Cvi	Cvi	Cvi	Cvi	Cvi	Cvi	Cvi	Cvi	Cvi	Cvi	Cvi	Cvi	
IND1.01419	1 419 276	127 673	203 953	1,4		Col	Col	Col	Col	Col	Col	Col	Col	Col	Col	Col	Col	Col	Col	Cvi	Cvi	Cvi	Cvi	Cvi	Cvi	Cvi	Cvi	Cvi	Cvi	Cvi	Cvi	Cvi	Cvi	Cvi	Cvi	Cvi	
EMIND1.01496	1 495 556	76 280	184 549	1,5		Col	Col	Col	Col	Col	Col	Col	Col	Col	Col	Col	Col	Col	Col	Col	Cvi	Cvi	Cvi	Cvi	Cvi	Cvi	Cvi	Cvi	Cvi	Cvi	Cvi	Cvi	Cvi	Cvi	Cvi	Cvi	
EMIND1.01604	1 603 825	108 269	208 045	1,6		Col	Col	Col	Col	Col	Col	Col	Col	Col	Col	Col	Col	Col	Col	Col	Col	Cvi	Cvi	Cvi	Cvi	Cvi	Cvi	Cvi	Cvi	Cvi	Cvi	Cvi	Cvi	Cvi	Cvi	Cvi	
HRM1.01704	1 703 601	99 776	197 220	1,7		Col	Col	Col	Col	Col	Col	Col	Col	Col	Col	Col	Col	Col	Col	Col	Col	Col	Cvi	Cvi	Cvi	Cvi	Cvi	Cvi	Cvi	Cvi	Cvi	Cvi	Cvi	Cvi	Cvi	Cvi	
HRM1.01801	1 801 045	97 444	218 397	1,8		Col	Col	Col	Col	Col	Col	Col	Col	Col	Col	Col	Col	Col	Col	Col	Col	Col	Col	Cvi	Cvi	Cvi	Cvi	Cvi	Cvi	Cvi	Cvi	Cvi	Cvi	Cvi	Cvi	Cvi	
HRM1.01922	1 921 998	120 953	225 955	1,9		Col	Col	Col	Col	Col	Col	Col	Col	Col	Col	Col	Col	Col	Col	Col	Col	Col	Col	Col	Cvi	Cvi	Cvi	Cvi	Cvi	Cvi	Cvi	Cvi	Cvi	Cvi	Cvi	Cvi	
HRM1.02027 F1/R1b	2 027 000	105 002	183 086	2		Col	Col	Col	Col	Col	Col	Col	Col	Col	Col	Col	Col	Col	Col	Col	Col	Col	Col	Col	Col	Cvi	Cvi	Cvi	Cvi	Cvi	Cvi	Cvi	Cvi	Cvi	Cvi	Cvi	
MSAT1.02105	2 105 084	78 084	169 604	2,1		Col	Col	Col	Col	Col	Col	Col	Col	Col	Col	Col	Col	Col	Col	Col	Col	Col	Col	Col	Col	Col	Cvi	Cvi	Cvi	Cvi	Cvi	Cvi	Cvi	Cvi	Cvi	Cvi	
HRM1.02197	2 196 604	91 520	179 307	2,2		Col	Col	Col	Col	Col	Col	Col	Col	Col	Col	Col	Col	Col	Col	Col	Col	Col	Col	Col	Col	Col	Col	Cvi	Cvi	Cvi	Cvi	Cvi	Cvi	Cvi	Cvi	Cvi	
HRM1.02284	2 284 391	87 787	209 037	2,3		Col	Col	Col	Col	Col	Col	Col	Col	Col	Col	Col	Col	Col	Col	Col	Col	Col	Col	Col	Col	Col	Col	Col	Cvi	Cvi	Cvi	Cvi	Cvi	Cvi	Cvi	Cvi	
AT1G07790_HRM2_FW	2 405 641	121 250	225 462	2,4		Col	Col	Col	Col	Col	Col	Col	Col	Col	Col	Col	Col	Col	Col	Col	Col	Col	Col	Col	Col	Col	Col	Col	Col	Cvi	Cvi	Cvi	Cvi	Cvi	Cvi	Cvi	
HRM1.02509	2 509 853	104 212	181 070	2,5		Col	Col	Col	Col	Col	Col	Col	Col	Col	Col	Col	Col	Col	Col	Col	Col	Col	Col	Col	Col	Col	Col	Col	Col	Col	Cvi	Cvi	Cvi	Cvi	Cvi	Cvi	
HRM1.02586.F2/R2	2 586 711	76 858	200 432	2,6		Col	Col	Col	Col	Col	Col	Col	Col	Col	Col	Col	Col	Col	Col	Col	Col	Col	Col	Col	Col	Col	Col	Col	Col	Col	Col	Cvi	Cvi	Cvi	Cvi	Cvi	
HRM1.02710	2 710 285	123 574	223 966	2,7		Col	Col	Col	Col	Col	Col	Col	Col	Col	Col	Col	Col	Col	Col	Col	Col	Col	Col	Col	Col	Col	Col	Col	Col	Col	Col	Col	Cvi	Cvi	Cvi	Cvi	
HRM1.02811b	2 810 677	100 392	204 895	2,8		Col	Col	Col	Col	Col	Col	Col	Col	Col	Col	Col	Col	Col	Col	Col	Col	Col	Col	Col	Col	Col	Col	Col	Col	Col	Col	Col	Col	Cvi	Cvi	Cvi	
HRM1.02915	2 915 180	104 503	198 440	2,9		Col	Col	Col	Col	Col	Col	Col	Col	Col	Col	Col	Col	Col	Col	Col	Col	Col	Col	Col	Col	Col	Col	Col	Col	Col	Col	Col	Col	Col	Cvi	Cvi	
HRM1.03009	3 009 117	93 937	181 820	3		Col	Col	Col	Col	Col	Col	Col	Col	Col	Col	Col	Col	Col	Col	Col	Col	Col	Col	Col	Col	Col	Col	Col	Col	Col	Col	Col	Col	Col	Col	Cvi	
HRM1.03097	3 097 000	87 883	130 943	3,1		Col	Col	Col	Col	Col	Col	Col	Col	Col	Col	Col	Col	Col	Col	Col	Col	Col	Col	Col	Col	Col	Col	Col	Col	Col	Col	Col	Col	Col	Col	Cvi	
mHIND1.03140	3 140 060	43 060				Cvi	Cvi	Cvi	Cvi	Cvi	Cvi	Cvi	Cvi	Cvi	Cvi	Cvi	Cvi	Cvi	Cvi	Cvi	Cvi	Cvi	Cvi	Cvi	Cvi	Cvi	Cvi	Cvi	Cvi	Cvi	Cvi	Cvi	Cvi	Cvi	Cvi	Cvi	

Supplementary Table S5: microStairs; polymorphisms segregating in different bins

This table lists all known polymorphisms between Col-0 and Cvi-0 that can potentially affect gene function (according to 1001Genomes data) within PRA29-significant bins only: in the selected physical interval, genes with more than 3 non-synonymous SNP or a high-impact polymorphism are highlighted in yellow and orange respectively. CRY2 candidate gene is highlighted in red.

intervals microStairs	gene id	region	funct_consequence	chr	pos	Col allele	Cvi allele	Gene generic name
101/102	AT1G01220	exonic	nonsynonymous SNV	Chr1	95386	A	C	
101/102	AT1G01260	exonic	nonsynonymous SNV	Chr1	111074	T	G	
101/102	AT1G01260	exonic	nonsynonymous SNV	Chr1	111321	G	C	
101/102	AT1G01300	exonic	nonsynonymous SNV	Chr1	117329	G	C	Eukaryotic aspartyl protease family protein
101/102	AT1G01300	exonic	nonsynonymous SNV	Chr1	117331	C	A	
101/102	AT1G01300	exonic	nonsynonymous SNV	Chr1	117375	A	G	
101/102	AT1G01300	exonic	nonsynonymous SNV	Chr1	117675	G	T	
101/102	AT1G01300	exonic	nonsynonymous SNV	Chr1	118006	C	G	
101/102	AT1G01310	exonic	nonsynonymous SNV	Chr1	120661	C	G	
101/102	AT1G01320	exonic	nonsynonymous SNV	Chr1	123313	G	C	REC1, REDUCED CHLOROPLAST COVERAGE
101/102	AT1G01320	exonic	nonsynonymous SNV	Chr1	127093	T	C	
101/102	AT1G01320	exonic	nonsynonymous SNV	Chr1	127891	C	T	
101/102	AT1G01320	exonic	nonsynonymous SNV	Chr1	129003	T	G	
101/102	AT1G01340	exonic	nonsynonymous SNV	Chr1	134470	T	G	
101/102	AT1G01350	exonic	nonsynonymous SNV	Chr1	137008	C	G	
101/102	AT1G01350	exonic	nonsynonymous SNV	Chr1	137115	C	T	
101/102	AT1G01355	exonic	nonsynonymous SNV	Chr1	138608	C	G	
101/102	AT1G01370	exonic	nonsynonymous SNV	Chr1	144331	C	A	
101/102	AT1G01390	exonic	nonsynonymous SNV	Chr1	148357	T	C	
101/102	AT1G01390	exonic	nonsynonymous SNV	Chr1	149437	T	G	
101/102	AT1G01400	exonic	nonsynonymous SNV	Chr1	151491	C	T	hypothetical protein
101/102	AT1G01400	exonic	nonsynonymous SNV	Chr1	151494	C	T	
101/102	AT1G01400	exonic	nonsynonymous SNV	Chr1	151617	A	G	
101/102	AT1G01400	exonic	nonsynonymous SNV	Chr1	151942	A	C	
101/102	AT1G01410	exonic	frameshift deletion	Chr1	154016	AT	A	APUM22, PUM22, PUMILIO 22

101/102	AT1G01410	exonic	nonsynonymous SNV	Chr1	153232	T	A	
101/102	AT1G01420	exonic	nonsynonymous SNV	Chr1	154679	A	C	UDP-GLUCOSYL TRANSFERASE 72B3
101/102	AT1G01420	exonic	nonsynonymous SNV	Chr1	155442	T	G	
101/102	AT1G01420	exonic	nonsynonymous SNV	Chr1	155626	T	A	
101/102	AT1G01420	exonic	nonsynonymous SNV	Chr1	155678	C	A	
101/102	AT1G01420	exonic	nonsynonymous SNV	Chr1	155809	A	G	
101/102	AT1G01420	exonic	nonsynonymous SNV	Chr1	155921	G	C	
101/102	AT1G01420	exonic	nonsynonymous SNV	Chr1	155984	C	A	
101/102	AT1G01430	exonic	nonsynonymous SNV	Chr1	157407	T	C	TBL25, TRICHOME BIREFRINGENCE-LIKE 25
101/102	AT1G01430	exonic	nonsynonymous SNV	Chr1	157974	C	T	
101/102	AT1G01430	exonic	nonsynonymous SNV	Chr1	158305	A	G	
101/102	AT1G01430	exonic	nonsynonymous SNV	Chr1	158355	G	A	
101/102	AT1G01450	exonic	frameshift deletion	Chr1	164164	CTATATA	CTATA	Protein kinase superfamily protein
101/102	AT1G01450	exonic	nonsynonymous SNV	Chr1	164638	A	C	
101/102	AT1G01450	exonic	nonsynonymous SNV	Chr1	165105	T	G	
101/102	AT1G01450	exonic	stopgain	Chr1	165397	G	A	
101/102	AT1G01453	exonic	nonsynonymous SNV	Chr1	167692	T	G	
101/102	AT1G01460	exonic	nonsynonymous SNV	Chr1	169429	A	T	ATPIPK11, PIPK11
101/102	AT1G01460	exonic	nonsynonymous SNV	Chr1	170271	A	G	
101/102	AT1G01460	exonic	nonsynonymous SNV	Chr1	170284	T	G	
101/102 & 102/103	AT1G01471	exonic	nonsynonymous SNV	Chr1	173351	C	T	
101/102 & 102/103	AT1G01471	exonic	nonsynonymous SNV	Chr1	173359	C	A	
101/102 & 102/103	AT1G01471	exonic	nonsynonymous SNV	Chr1	173387	T	A	
101/102 & 102/103	AT1G01471	exonic	nonsynonymous SNV	Chr1	173392	G	A	
101/102 & 102/103	AT1G01471	exonic	nonsynonymous SNV	Chr1	173417	A	C	
101/102 & 102/103	AT1G01471	exonic	nonsynonymous SNV	Chr1	173428	C	A	
101/102 & 102/103	AT1G01480	exonic	nonsynonymous SNV	Chr1	176276	A	G	1-AMINO-CYCLOPROPANE-1-CARBOXYLATE SYNTHASE 2, ACS2, AT-ACC2
101/102 & 102/103	AT1G01480	exonic	nonsynonymous SNV	Chr1	177089	G	A	
101/102 & 102/103	AT1G01480	exonic	nonsynonymous SNV	Chr1	177090	A	G	
101/102 & 102/103	AT1G01480	exonic	nonsynonymous SNV	Chr1	177112	C	G	
101/102 & 102/103	AT1G01480	exonic	nonsynonymous SNV	Chr1	177117	C	T	
101/102 & 102/103	AT1G01480	exonic	nonsynonymous SNV	Chr1	177121	A	C	
101/102 & 102/103	AT1G01480	exonic	nonsynonymous SNV	Chr1	177611	A	C	

101/102 & 102/103	AT1G01480	exonic	nonsynonymous SNV	Chr1	177741	G	A	
101/102 & 102/103	AT1G01480	exonic	nonsynonymous SNV	Chr1	177909	A	T	
101/102 & 102/103	AT1G01500	exonic	nonsynonymous SNV	Chr1	185783	T	C	
101/102 & 102/103	AT1G01510	exonic	nonsynonymous SNV	Chr1	187761	G	C	AN, ANGUSTIFOLIA, DETORQUEO, DOQ
101/102 & 102/103	AT1G01510	exonic	nonsynonymous SNV	Chr1	187763	T	G	
101/102 & 102/103	AT1G01510	exonic	nonsynonymous SNV	Chr1	187768	A	T	
101/102 & 102/103	AT1G01530	exonic	nonsynonymous SNV	Chr1	193553	C	G	
101/102 & 102/103	AT1G01540	exonic	frameshift insertion	Chr1	197912	A	AT	Protein kinase superfamily protein;(source:Araport11)
101/102 & 102/103	AT1G01540	exonic	nonsynonymous SNV	Chr1	197929	T	C	
101/102 & 102/103	AT1G01540	exonic	nonsynonymous SNV	Chr1	197947	T	G	
101/102 & 102/103	AT1G01540	exonic	nonsynonymous SNV	Chr1	197963	C	T	
101/102 & 102/103	AT1G01540	exonic	nonsynonymous SNV	Chr1	198347	G	C	
101/102 & 102/103	AT1G01540	exonic	nonsynonymous SNV	Chr1	198376	A	T	
101/102 & 102/103	AT1G01550	exonic	nonsynonymous SNV	Chr1	200533	G	C	BPS1, BYPASS 1
101/102 & 102/103	AT1G01550	exonic	nonsynonymous SNV	Chr1	200551	G	C	
101/102 & 102/103	AT1G01550	exonic	stopgain	Chr1	200568	G	T	
101/102 & 102/103	AT1G01570	exonic	nonsynonymous SNV	Chr1	205393	A	G	transferring glycosyl group transferase (DUF604);(source:Araport11)
101/102 & 102/103	AT1G01570	exonic	nonsynonymous SNV	Chr1	205710	A	G	
101/102 & 102/103	AT1G01570	exonic	nonsynonymous SNV	Chr1	207187	T	A	
101/102 & 102/103	AT1G01570	exonic	nonsynonymous SNV	Chr1	207196	G	C	
101/102 & 102/103	AT1G01580	exonic	nonsynonymous SNV	Chr1	210438	T	C	ATFRO2, FERRIC CHELATE REDUCTASE DEFECTIVE 1, FERRIC REDUCTION OXIDASE 2, FRD
101/102 & 102/103	AT1G01580	exonic	nonsynonymous SNV	Chr1	210543	A	C	
101/102 & 102/103	AT1G01580	exonic	nonsynonymous SNV	Chr1	211861	A	C	
101/102 & 102/103	AT1G01590	exonic	nonsynonymous SNV	Chr1	214515	C	G	ATFRO1, FERRIC REDUCTION OXIDASE 1, FRO1
101/102 & 102/103	AT1G01590	exonic	nonsynonymous SNV	Chr1	215411	T	G	
101/102 & 102/103	AT1G01590	exonic	nonsynonymous SNV	Chr1	215414	T	G	
101/102 & 102/103	AT1G01590	exonic	nonsynonymous SNV	Chr1	215421	C	G	
101/102 & 102/103	AT1G01590	exonic	nonsynonymous SNV	Chr1	215427	T	G	
101/102 & 102/103	AT1G01590	exonic	nonsynonymous SNV	Chr1	215432	C	G	
101/102 & 102/103	AT1G01590	exonic	nonsynonymous SNV	Chr1	215435	A	T	
101/102 & 102/103	AT1G01590	exonic	nonsynonymous SNV	Chr1	215444	T	G	
101/102 & 102/103	AT1G01590	exonic	nonsynonymous SNV	Chr1	215677	G	T	
101/102 & 102/103	AT1G01590	exonic	nonsynonymous SNV	Chr1	215760	G	C	

101/102 & 102/103	AT1G01590	exonic	nonsynonymous SNV	Chr1	215890	C	A	
101/102 & 102/103	AT1G01590	exonic	nonsynonymous SNV	Chr1	216643	G	A	
101/102 & 102/103	AT1G01590	exonic	nonsynonymous SNV	Chr1	216875	A	C	
101/102 & 102/103	AT1G01600	exonic	nonsynonymous SNV	Chr1	220860	T	C	"CYTOCHROME P450, FAMILY 86, SUBFAMILY A, POLYPEPTIDE 4", CYP86A4
101/102 & 102/103	AT1G01600	exonic	nonsynonymous SNV	Chr1	220937	C	G	
101/102 & 102/103	AT1G01600	exonic	nonsynonymous SNV	Chr1	220968	T	A	
101/102 & 102/103	AT1G01650	exonic	nonsynonymous SNV	Chr1	233581	A	C	
101/102 & 102/103	AT1G01670	exonic	nonsynonymous SNV	Chr1	244174	C	T	
101/102 & 102/103	AT1G01670	exonic	nonsynonymous SNV	Chr1	244584	C	T	
101/102 & 102/103	AT1G01680	exonic	nonsynonymous SNV	Chr1	247400	G	C	
101/102 & 102/103	AT1G01680	exonic	nonsynonymous SNV	Chr1	247410	A	T	
101/102 & 102/103	AT1G01690	exonic	nonsynonymous SNV	Chr1	249795	G	T	
101/102 & 102/103	AT1G01690	exonic	nonsynonymous SNV	Chr1	249796	A	C	
101/102 & 102/103	AT1G01695	exonic	nonsynonymous SNV	Chr1	252953	G	A	TON1 RECRUITING MOTIF 33, TRM33
101/102 & 102/103	AT1G01695	exonic	nonsynonymous SNV	Chr1	253606	G	A	
101/102 & 102/103	AT1G01695	exonic	nonsynonymous SNV	Chr1	254004	C	G	
101/102 & 102/103	AT1G01700	exonic	nonsynonymous SNV	Chr1	259953	G	C	ATROPGEF2, ROP (RHO OF PLANTS) GUANINE NUCLEOTIDE EXCHANGE FACTOR 2, ROPG
101/102 & 102/103	AT1G01700	exonic	nonsynonymous SNV	Chr1	260010	C	A	
101/102 & 102/103	AT1G01700	exonic	nonsynonymous SNV	Chr1	260158	T	C	
101/102 & 102/103	AT1G01710	exonic	nonsynonymous SNV	Chr1	265611	G	C	
101/102 & 102/103	AT1G01720	exonic	nonsynonymous SNV	Chr1	268852	T	G	
101/102 & 102/103	AT1G01730	exonic	nonsynonymous SNV	Chr1	271050	G	C	
101/102 & 102/103	AT1G01730	exonic	nonsynonymous SNV	Chr1	271416	T	C	
101/102 & 102/103	AT1G01740	exonic	nonsynonymous SNV	Chr1	272826	G	A	
101/102 & 102/103	AT1G01770	exonic	nonsynonymous SNV	Chr1	281313	G	A	
101/102 & 102/103	AT1G01770	exonic	nonsynonymous SNV	Chr1	281933	G	C	
101/102 & 102/103	AT1G01790	exonic	nonsynonymous SNV	Chr1	284989	A	G	ATKEA1, K+ EFFLUX ANTIPORTER 1, KEA1
101/102 & 102/103	AT1G01790	exonic	nonsynonymous SNV	Chr1	285111	G	A	
101/102 & 102/103	AT1G01790	exonic	nonsynonymous SNV	Chr1	285729	A	G	
101/102 & 102/103	AT1G01790	exonic	nonsynonymous SNV	Chr1	286029	A	C	
101/102 & 102/103	AT1G01800	exonic	nonsynonymous SNV	Chr1	294545	G	C	
101/102 & 102/103	AT1G01800	exonic	nonsynonymous SNV	Chr1	294704	C	G	
101/102 & 102/103	AT1G01820	exonic	nonsynonymous SNV	Chr1	296955	T	A	PEROXIN 11C, PEX11C

101/102 & 102/103	AT1G01820	exonic	nonsynonymous SNV	Chr1	296959	T	C	
101/102 & 102/103	AT1G01820	exonic	nonsynonymous SNV	Chr1	296965	T	C	
102/103 & 103/104	AT1G01830	exonic	nonsynonymous SNV	Chr1	299439	T	C	ARM repeat superfamily protein
102/103 & 103/104	AT1G01830	exonic	nonsynonymous SNV	Chr1	299440	T	C	
102/103 & 103/104	AT1G01830	exonic	nonsynonymous SNV	Chr1	300023	C	A	
102/103 & 103/104	AT1G01830	exonic	nonsynonymous SNV	Chr1	300024	C	T	
102/103 & 103/104	AT1G01830	exonic	nonsynonymous SNV	Chr1	300277	C	A	
102/103 & 103/104	AT1G01880	exonic	nonsynonymous SNV	Chr1	306651	A	C	ATGEN1, GEN1, ORTHOLOG OF HSGEN1
102/103 & 103/104	AT1G01880	exonic	nonsynonymous SNV	Chr1	306653	T	C	
102/103 & 103/104	AT1G01880	exonic	nonsynonymous SNV	Chr1	307266	C	T	
102/103 & 103/104	AT1G01900	exonic	nonsynonymous SNV	Chr1	310748	G	T	
102/103 & 103/104	AT1G01930	exonic	nonsynonymous SNV	Chr1	321016	G	A	
102/103 & 103/104	AT1G01930	exonic	nonsynonymous SNV	Chr1	321370	C	A	
102/103 & 103/104	AT1G01950	exonic	nonsynonymous SNV	Chr1	326964	T	G	ARABIDOPSIS THALIANA KINESIN UNGROUPED CLADE, GENE B, ARK2, ARMADILLO REPE
102/103 & 103/104	AT1G01950	exonic	nonsynonymous SNV	Chr1	326965	T	A	
102/103 & 103/104	AT1G01950	exonic	nonsynonymous SNV	Chr1	328445	A	T	
102/103 & 103/104	AT1G01960	exonic	nonsynonymous SNV	Chr1	331269	A	G	BIG3, EDA10, EMBRYO SAC DEVELOPMENT ARREST 10
102/103 & 103/104	AT1G01960	exonic	nonsynonymous SNV	Chr1	331736	A	C	
102/103 & 103/104	AT1G01960	exonic	nonsynonymous SNV	Chr1	332347	A	T	
102/103 & 103/104	AT1G01970	exonic	nonsynonymous SNV	Chr1	338744	T	G	
102/103 & 103/104	AT1G01980	exonic	nonsynonymous SNV	Chr1	340810	C	A	ATBBE1
102/103 & 103/104	AT1G01980	exonic	nonsynonymous SNV	Chr1	341545	G	A	
102/103 & 103/104	AT1G01980	exonic	nonsynonymous SNV	Chr1	341924	T	C	
102/103 & 103/104	AT1G01980	exonic	nonsynonymous SNV	Chr1	341969	C	A	
102/103 & 103/104	AT1G01980	exonic	nonsynonymous SNV	Chr1	341982	C	A	
102/103 & 103/104	AT1G01980	exonic	nonsynonymous SNV	Chr1	341990	A	C	
102/103 & 103/104	AT1G01990	exonic	nonsynonymous SNV	Chr1	344075	G	A	
102/103 & 103/104	AT1G02010	exonic	nonsynonymous SNV	Chr1	349310	C	A	
102/103 & 103/104	AT1G02020	exonic	frameshift insertion	Chr1	354813	T	TACTT	nitroreductase family protein
102/103 & 103/104	AT1G02020	exonic	nonsynonymous SNV	Chr1	353491	A	T	
102/103 & 103/104	AT1G02020	exonic	nonsynonymous SNV	Chr1	354413	G	C	
102/103 & 103/104	AT1G02020	exonic	nonsynonymous SNV	Chr1	354473	C	T	
102/103 & 103/104	AT1G02020	exonic	nonsynonymous SNV	Chr1	354700	G	A	

102/103 & 103/104	AT1G02020	exonic	nonsynonymous SNV	Chr1	354701	A	C	
102/103 & 103/104	AT1G02020	exonic	nonsynonymous SNV	Chr1	354727	A	G	
102/103 & 103/104	AT1G02020	exonic	nonsynonymous SNV	Chr1	354746	G	A	
102/103 & 103/104	AT1G02030	exonic	nonsynonymous SNV	Chr1	356127	C	T	
102/103 & 103/104	AT1G02040	exonic	nonsynonymous SNV	Chr1	358397	T	G	C2H2-type zinc finger family protein
102/103 & 103/104	AT1G02040	exonic	nonsynonymous SNV	Chr1	358570	G	T	
102/103 & 103/104	AT1G02040	exonic	nonsynonymous SNV	Chr1	358639	G	C	
102/103 & 103/104	AT1G02050	exonic	nonsynonymous SNV	Chr1	359566	C	G	
102/103 & 103/104	AT1G02060	exonic	frameshift deletion	Chr1	361050	GT	G	Tetratricopeptide repeat (TPR)-like superfamily protein
102/103 & 103/104	AT1G02060	exonic	nonsynonymous SNV	Chr1	361859	G	C	
102/103 & 103/104	AT1G02060	exonic	nonsynonymous SNV	Chr1	362150	C	A	
102/103 & 103/104	AT1G02065	exonic	nonsynonymous SNV	Chr1	365823	C	T	
102/103 & 103/104	AT1G02065	exonic	nonsynonymous SNV	Chr1	366788	A	C	
102/103 & 103/104	AT1G02080	exonic	nonsynonymous SNV	Chr1	373680	G	T	transcription regulator
102/103 & 103/104	AT1G02080	exonic	nonsynonymous SNV	Chr1	375346	G	A	
102/103 & 103/104	AT1G02080	exonic	nonsynonymous SNV	Chr1	381773	A	T	
102/103 & 103/104	AT1G02080	exonic	nonsynonymous SNV	Chr1	384704	A	T	
102/103 & 103/104	AT1G02110	exonic	nonsynonymous SNV	Chr1	393497	C	T	bZIP domain class transcription factor (DUF630 and DUF632)
102/103 & 103/104	AT1G02110	exonic	nonsynonymous SNV	Chr1	395265	T	G	
102/103 & 103/104	AT1G02110	exonic	nonsynonymous SNV	Chr1	395277	T	G	
102/103 & 103/104	AT1G02120	exonic	nonsynonymous SNV	Chr1	395878	A	G	
102/103 & 103/104	AT1G02120	exonic	nonsynonymous SNV	Chr1	399654	A	T	
102/103 & 103/104	AT1G02140	exonic	nonsynonymous SNV	Chr1	404233	T	G	
102/103 & 103/104	AT1G02145	exonic	nonsynonymous SNV	Chr1	405652	A	G	
102/103 & 103/104	AT1G02150	exonic	nonsynonymous SNV	Chr1	408849	T	G	
102/103 & 103/104	AT1G02180	exonic	nonsynonymous SNV	Chr1	413624	A	G	ferredoxin-like protein
102/103 & 103/104	AT1G02180	exonic	nonsynonymous SNV	Chr1	414477	A	G	
102/103 & 103/104	AT1G02180	exonic	nonsynonymous SNV	Chr1	414481	C	T	
102/103 & 103/104	AT1G02180	exonic	nonsynonymous SNV	Chr1	414484	A	T	
102/103 & 103/104	AT1G02180	exonic	nonsynonymous SNV	Chr1	414487	T	A	
102/103 & 103/104	AT1G02190	exonic	nonsynonymous SNV	Chr1	416141	C	G	Fatty acid hydroxylase superfamily
102/103 & 103/104	AT1G02190	exonic	nonsynonymous SNV	Chr1	417318	C	G	
102/103 & 103/104	AT1G02190	exonic	nonsynonymous SNV	Chr1	417642	T	G	

102/103 & 103/104	AT1G02190	exonic	nonsynonymous SNV	Chr1	417789	C	A	
102/103 & 103/104	AT1G02205	exonic	nonsynonymous SNV	Chr1	420807	A	C	CER1, CER22, ECERIFERUM 1, ECERIFERUM 22
102/103 & 103/104	AT1G02205	exonic	nonsynonymous SNV	Chr1	420866	G	A	
102/103 & 103/104	AT1G02205	exonic	nonsynonymous SNV	Chr1	421745	T	G	
102/103 & 103/104	AT1G02205	exonic	nonsynonymous SNV	Chr1	422054	T	C	
102/103 & 103/104	AT1G02205	exonic	nonsynonymous SNV	Chr1	422095	C	A	
111/112	AT1G04130	exonic	nonsynonymous SNV	Chr1	1073941	C	G	
111/112	AT1G04140	exonic	nonsynonymous SNV	Chr1	1077510	C	T	
111/112	AT1G04140	exonic	nonsynonymous SNV	Chr1	1080239	C	T	
111/112	AT1G04160	exonic	nonsynonymous SNV	Chr1	1087192	G	T	
111/112	AT1G04160	exonic	nonsynonymous SNV	Chr1	1088730	C	A	
111/112	AT1G04160	exonic	nonsynonymous SNV	Chr1	1089125	A	G	
111/112	AT1G04160	exonic	nonsynonymous SNV	Chr1	1092049	T	C	
111/112	AT1G04160	exonic	nonsynonymous SNV	Chr1	1092888	C	T	
111/112	AT1G04160	exonic	nonsynonymous SNV	Chr1	1093364	A	G	
111/112	AT1G04160	exonic	nonsynonymous SNV	Chr1	1093415	T	A	
111/112	AT1G04160	exonic	nonsynonymous SNV	Chr1	1093442	A	G	
111/112	AT1G04160	exonic	nonsynonymous SNV	Chr1	1093696	T	C	
111/112	AT1G04160	exonic	nonsynonymous SNV	Chr1	1094402	G	A	
111/112	AT1G04171	exonic	nonsynonymous SNV	Chr1	1100483	C	G	
111/112	AT1G04171	exonic	stoploss	Chr1	1100445	T	C	
111/112	AT1G04180	exonic	nonsynonymous SNV	Chr1	1105035	A	C	
111/112	AT1G04180	exonic	nonsynonymous SNV	Chr1	1105284	G	A	
111/112	AT1G04180	exonic	nonsynonymous SNV	Chr1	1105473	G	C	
111/112	AT1G04180	exonic	nonsynonymous SNV	Chr1	1105494	T	A	
111/112	AT1G04190	exonic	nonsynonymous SNV	Chr1	1108545	C	A	
111/112	AT1G04200	exonic	nonsynonymous SNV	Chr1	1112557	G	T	
111/112	AT1G04210	exonic	nonsynonymous SNV	Chr1	1114803	C	G	
111/112	AT1G04210	exonic	nonsynonymous SNV	Chr1	1115603	G	A	
111/112	AT1G04210	exonic	nonsynonymous SNV	Chr1	1116274	G	T	
111/112	AT1G04210	exonic	nonsynonymous SNV	Chr1	1116487	G	T	

111/112	AT1G04210	exonic	nonsynonymous SNV	Chr1	1116814	G	A	
111/112	AT1G04220	exonic	nonsynonymous SNV	Chr1	1121987	A	G	
111/112	AT1G04230	exonic	nonsynonymous SNV	Chr1	1126079	T	G	
111/112	AT1G04280	exonic	nonsynonymous SNV	Chr1	1143832	A	C	
111/112	AT1G04280	exonic	nonsynonymous SNV	Chr1	1144374	C	G	
111/112	AT1G04280	exonic	nonsynonymous SNV	Chr1	1144388	T	G	
111/112	AT1G04280	exonic	nonsynonymous SNV	Chr1	1144395	T	A	
111/112	AT1G04280	exonic	nonsynonymous SNV	Chr1	1144396	T	G	
111/112	AT1G04300	exonic	nonsynonymous SNV	Chr1	1149308	T	G	
111/112	AT1G04300	exonic	nonsynonymous SNV	Chr1	1149464	C	A	
111/112	AT1G04300	exonic	nonsynonymous SNV	Chr1	1149753	C	G	
111/112	AT1G04310	exonic	nonsynonymous SNV	Chr1	1155448	T	C	
111/112	AT1G04310	exonic	nonsynonymous SNV	Chr1	1155536	G	C	
111/112	AT1G04310	exonic	nonsynonymous SNV	Chr1	1155601	G	T	
111/112	AT1G04310	exonic	nonsynonymous SNV	Chr1	1155940	A	G	
111/112	AT1G04330	exonic	nonsynonymous SNV	Chr1	1161615	G	A	
111/112	AT1G04350	exonic	nonsynonymous SNV	Chr1	1165444	T	C	
111/112	AT1G04360	exonic	nonsynonymous SNV	Chr1	1167844	C	T	
111/112	AT1G04360	exonic	nonsynonymous SNV	Chr1	1168048	T	C	
111/112	AT1G04370	exonic	nonsynonymous SNV	Chr1	1175414	T	A	
111/112	AT1G04380	exonic	frameshift insertion	Chr1	1177257	A	AG	
111/112	AT1G04380	exonic	nonsynonymous SNV	Chr1	1177976	C	A	
111/112	AT1G04380	exonic	nonsynonymous SNV	Chr1	1178065	T	A	
111/112	AT1G04380	exonic	nonsynonymous SNV	Chr1	1178252	C	T	
111/112	AT1G04380	exonic	nonsynonymous SNV	Chr1	1178349	C	G	
111/112	AT1G04390	exonic	nonsynonymous SNV	Chr1	1182175	G	A	
111/112	AT1G04390	exonic	nonsynonymous SNV	Chr1	1183153	T	A	
111/112	AT1G04400	exonic	nonsynonymous SNV	Chr1	1186131	G	A	
111/112	AT1G04400	exonic	nonsynonymous SNV	Chr1	1186604	C	T	CRY2
111/112	AT1G04440	exonic	nonsynonymous SNV	Chr1	1205599	G	A	
111/112	AT1G04445	exonic	nonsynonymous SNV	Chr1	1207461	T	C	
111/112	AT1G04445	exonic	nonsynonymous SNV	Chr1	1207631	T	G	
111/112	AT1G04470	exonic	nonsynonymous SNV	Chr1	1211516	C	G	

111/112	AT1G04470	exonic	nonsynonymous SNV	Chr1	1211716	G	T
111/112	AT1G04470	exonic	nonsynonymous SNV	Chr1	1212827	A	C
111/112	AT1G04470	exonic	nonsynonymous SNV	Chr1	1213602	G	T
111/112	AT1G04500	exonic	nonsynonymous SNV	Chr1	1221994	G	T
111/112	AT1G04500	exonic	nonsynonymous SNV	Chr1	1222002	G	T
111/112	AT1G04500	exonic	nonsynonymous SNV	Chr1	1222664	G	A
111/112	AT1G04500	exonic	nonsynonymous SNV	Chr1	1222848	G	A
111/112	AT1G04500	exonic	nonsynonymous SNV	Chr1	1222849	T	A
111/112	AT1G04501	exonic	frameshift insertion	Chr1	1224678	T	TG
111/112	AT1G04510	exonic	nonsynonymous SNV	Chr1	1230313	G	A
111/112	AT1G04510	exonic	nonsynonymous SNV	Chr1	1230476	A	T
111/112	AT1G04530	exonic	nonsynonymous SNV	Chr1	1234740	C	T
111/112	AT1G04540	exonic	nonsynonymous SNV	Chr1	1238041	G	T
111/112	AT1G04540	exonic	nonsynonymous SNV	Chr1	1238146	C	A
111/112	AT1G04540	exonic	nonsynonymous SNV	Chr1	1238148	A	C
111/112	AT1G04540	exonic	nonsynonymous SNV	Chr1	1238210	A	T
111/112	AT1G04550	exonic	nonsynonymous SNV	Chr1	1241208	C	G
111/112	AT1G04580	exonic	nonsynonymous SNV	Chr1	1252247	T	C
111/112	AT1G04580	exonic	nonsynonymous SNV	Chr1	1252557	C	T
111/112	AT1G04580	exonic	nonsynonymous SNV	Chr1	1253047	C	T
111/112	AT1G04580	exonic	nonsynonymous SNV	Chr1	1253643	C	T
111/112	AT1G04580	exonic	nonsynonymous SNV	Chr1	1253963	G	A
111/112	AT1G04580	exonic	nonsynonymous SNV	Chr1	1253964	A	T
111/112	AT1G04580	exonic	nonsynonymous SNV	Chr1	1253977	A	T
111/112	AT1G04580	exonic	nonsynonymous SNV	Chr1	1253989	G	C
111/112	AT1G04580	exonic	nonsynonymous SNV	Chr1	1256134	T	C
111/112	AT1G04580	exonic	nonsynonymous SNV	Chr1	1256399	T	C
111/112	AT1G04580	exonic	nonsynonymous SNV	Chr1	1256409	C	A
111/112	AT1G04580	exonic	nonsynonymous SNV	Chr1	1257491	A	C
111/112	AT1G04590	exonic	nonsynonymous SNV	Chr1	1258774	C	T
111/112	AT1G04590	exonic	nonsynonymous SNV	Chr1	1258830	C	A
111/112	AT1G04590	exonic	nonsynonymous SNV	Chr1	1258841	G	C
111/112	AT1G04590	exonic	nonsynonymous SNV	Chr1	1258843	T	A

111/112	AT1G04590	exonic	nonsynonymous SNV	Chr1	1259468	C	T	
111/112	AT1G04590	exonic	nonsynonymous SNV	Chr1	1260778	C	A	
111/112	AT1G04590	exonic	nonsynonymous SNV	Chr1	1260784	C	T	
111/112	AT1G04590	exonic	nonsynonymous SNV	Chr1	1260793	C	T	
111/112	AT1G04600	exonic	nonsynonymous SNV	Chr1	1262584	C	G	
111/112	AT1G04600	exonic	nonsynonymous SNV	Chr1	1264578	G	A	
111/112	AT1G04600	exonic	nonsynonymous SNV	Chr1	1265645	G	T	
111/112	AT1G04600	exonic	nonsynonymous SNV	Chr1	1265875	G	A	
111/112	AT1G04600	exonic	nonsynonymous SNV	Chr1	1266414	C	T	
111/112	AT1G04600	exonic	nonsynonymous SNV	Chr1	1268742	A	C	
111/112	AT1G04600	exonic	nonsynonymous SNV	Chr1	1269300	G	A	
111/112	AT1G04600	exonic	nonsynonymous SNV	Chr1	1270934	T	C	
111/112	AT1G04600	exonic	nonsynonymous SNV	Chr1	1270935	C	T	
111/112	AT1G04600	exonic	nonsynonymous SNV	Chr1	1270940	A	G	
111/112	AT1G04600	exonic	nonsynonymous SNV	Chr1	1270941	A	C	
111/112	AT1G04600	exonic	nonsynonymous SNV	Chr1	1270942	G	T	
111/112	AT1G04600	exonic	nonsynonymous SNV	Chr1	1270943	A	G	
111/112	AT1G04600	exonic	nonsynonymous SNV	Chr1	1270953	A	G	
111/112	AT1G04600	exonic	nonsynonymous SNV	Chr1	1270957	G	T	
111/112	AT1G04600	exonic	nonsynonymous SNV	Chr1	1271564	G	A	
111/112	AT1G04600	exonic	nonsynonymous SNV	Chr1	1271577	C	A	
111/112	AT1G04610	exonic	nonsynonymous SNV	Chr1	1279957	T	G	
111/112	AT1G04625	exonic	nonsynonymous SNV	Chr1	1288684	T	C	
111/112	AT1G04630	exonic	nonsynonymous SNV	Chr1	1290815	C	A	
115/116	AT1G05180	exonic	nonsynonymous SNV	Chr1	1498549	A	G	
115/116	AT1G05180	exonic	nonsynonymous SNV	Chr1	1500228	C	T	
115/116	AT1G05200	exonic	nonsynonymous SNV	Chr1	1505708	G	C	ATGLR3.4, GLR3.4, GLUR3, GLUTAMATE RECEPTOR 3.4
115/116	AT1G05200	exonic	nonsynonymous SNV	Chr1	1505757	T	A	
115/116	AT1G05200	exonic	nonsynonymous SNV	Chr1	1505796	G	C	
115/116	AT1G05200	exonic	nonsynonymous SNV	Chr1	1505805	G	C	
115/116	AT1G05200	exonic	nonsynonymous SNV	Chr1	1505919	G	C	

115/116	AT1G05220	exonic	nonsynonymous SNV	Chr1	1512531	G	A	
115/116	AT1G05220	exonic	nonsynonymous SNV	Chr1	1512630	G	C	
115/116	AT1G05230	exonic	nonsynonymous SNV	Chr1	1515063	T	C	
115/116	AT1G05260	exonic	nonsynonymous SNV	Chr1	1529880	T	G	
115/116	AT1G05270	exonic	nonsynonymous SNV	Chr1	1532755	A	C	TraB family protein
115/116	AT1G05270	exonic	nonsynonymous SNV	Chr1	1534106	T	C	
115/116	AT1G05270	exonic	nonsynonymous SNV	Chr1	1534298	A	T	
115/116	AT1G05280	exonic	nonsynonymous SNV	Chr1	1535468	A	C	ERV-F (C)1 provirus ancestral Env polyprotein, putative (DUF604)
115/116	AT1G05280	exonic	nonsynonymous SNV	Chr1	1536067	G	C	
115/116	AT1G05280	exonic	nonsynonymous SNV	Chr1	1536136	C	A	
115/116	AT1G05280	exonic	nonsynonymous SNV	Chr1	1537170	A	T	
115/116	AT1G05290	exonic	nonsynonymous SNV	Chr1	1539258	G	C	CCT motif family protein
115/116	AT1G05290	exonic	nonsynonymous SNV	Chr1	1539465	G	A	
115/116	AT1G05290	exonic	nonsynonymous SNV	Chr1	1539666	G	A	
115/116	AT1G05290	exonic	nonsynonymous SNV	Chr1	1539810	C	T	
115/116	AT1G05290	exonic	nonsynonymous SNV	Chr1	1539823	C	G	
115/116	AT1G05290	exonic	nonsynonymous SNV	Chr1	1540311	C	A	
115/116	AT1G05290	exonic	nonsynonymous SNV	Chr1	1540545	A	T	
115/116	AT1G05300	exonic	nonsynonymous SNV	Chr1	1545548	T	C	
115/116	AT1G05300	exonic	nonsynonymous SNV	Chr1	1547262	C	A	
115/116	AT1G05310	exonic	nonsynonymous SNV	Chr1	1550655	A	T	Pectin lyase-like superfamily protein
115/116	AT1G05310	exonic	nonsynonymous SNV	Chr1	1552172	G	A	
115/116	AT1G05310	exonic	nonsynonymous SNV	Chr1	1552179	C	T	
115/116	AT1G05320	exonic	nonsynonymous SNV	Chr1	1555291	C	T	
115/116	AT1G05320	exonic	nonsynonymous SNV	Chr1	1556199	C	G	
115/116	AT1G05320	exonic	nonsynonymous SNV	Chr1	1557299	A	G	
115/116	AT1G05320	exonic	nonsynonymous SNV	Chr1	1557641	G	C	
115/116	AT1G05350	exonic	nonsynonymous SNV	Chr1	1563930	T	G	
115/116	AT1G05360	exonic	nonsynonymous SNV	Chr1	1565881	T	C	KILLING ME SLOWLY 2, KMS2
115/116	AT1G05360	exonic	nonsynonymous SNV	Chr1	1565916	A	G	
115/116	AT1G05360	exonic	nonsynonymous SNV	Chr1	1566911	G	A	
115/116	AT1G05360	exonic	nonsynonymous SNV	Chr1	1567259	C	G	
115/116	AT1G05370	exonic	nonsynonymous SNV	Chr1	1569615	T	C	myosin heavy chain, embryonic smooth protein

115/116	AT1G05370	exonic	nonsynonymous SNV	Chr1	1569666	T	G	
115/116	AT1G05370	exonic	nonsynonymous SNV	Chr1	1569677	T	G	
115/116	AT1G05370	exonic	nonsynonymous SNV	Chr1	1569687	T	G	
115/116	AT1G05380	exonic	nonsynonymous SNV	Chr1	1578543	C	G	Acyl-CoA N-acyltransferase with RING/FYVE/PHD-type zinc finger protein
115/116	AT1G05380	exonic	nonsynonymous SNV	Chr1	1579543	T	C	
115/116	AT1G05380	exonic	nonsynonymous SNV	Chr1	1580237	G	A	
115/116	AT1G05380	exonic	nonsynonymous SNV	Chr1	1581606	G	A	
115/116	AT1G05410	exonic	nonsynonymous SNV	Chr1	1585517	T	C	CDPK adapter, putative (DUF1423)
115/116	AT1G05410	exonic	nonsynonymous SNV	Chr1	1585637	T	G	
115/116	AT1G05410	exonic	nonsynonymous SNV	Chr1	1586313	A	C	
115/116	AT1G05410	exonic	nonsynonymous SNV	Chr1	1586415	T	C	
115/116	AT1G05410	exonic	nonsynonymous SNV	Chr1	1586980	G	T	
115/116	AT1G05420	exonic	nonsynonymous SNV	Chr1	1590148	G	A	ARABIDOPSIS THALIANA OVATE FAMILY PROTEIN 12, ATOFP12, OFP12, OVATE FAMILY P
115/116	AT1G05420	exonic	nonsynonymous SNV	Chr1	1590175	C	A	
115/116	AT1G05420	exonic	nonsynonymous SNV	Chr1	1590233	A	C	
115/116	AT1G05420	exonic	nonsynonymous SNV	Chr1	1590409	T	C	
115/116	AT1G05420	exonic	nonsynonymous SNV	Chr1	1590589	A	C	
115/116	AT1G05430	exonic	nonsynonymous SNV	Chr1	1594587	C	T	hypothetical protein
115/116	AT1G05430	exonic	nonsynonymous SNV	Chr1	1594594	T	G	
115/116	AT1G05430	exonic	nonsynonymous SNV	Chr1	1594628	T	A	
115/116	AT1G05430	exonic	nonsynonymous SNV	Chr1	1595032	A	T	
115/116	AT1G05440	exonic	nonsynonymous SNV	Chr1	1596493	C	T	
115/116	AT1G05440	exonic	nonsynonymous SNV	Chr1	1597764	G	A	
115/116	AT1G05460	exonic	nonsynonymous SNV	Chr1	1602829	G	A	SDE3, SILENCING DEFECTIVE
115/116	AT1G05460	exonic	nonsynonymous SNV	Chr1	1603341	T	C	
115/116	AT1G05460	exonic	nonsynonymous SNV	Chr1	1603459	A	G	
115/116	AT1G05460	exonic	nonsynonymous SNV	Chr1	1603471	T	A	
115/116	AT1G05470	exonic	nonsynonymous SNV	Chr1	1610192	T	C	
115/116	AT1G05490	exonic	nonsynonymous SNV	Chr1	1620624	T	C	
115/116	AT1G05490	exonic	nonsynonymous SNV	Chr1	1621838	T	A	
115/116	AT1G05500	exonic	nonsynonymous SNV	Chr1	1625751	A	C	
115/116	AT1G05520	exonic	nonsynonymous SNV	Chr1	1631841	A	C	
115/116	AT1G05550	exonic	nonsynonymous SNV	Chr1	1641504	C	T	

115/116	AT1G05550	exonic	nonsynonymous SNV	Chr1	1642614	G	A	
115/116	AT1G05570	exonic	nonsynonymous SNV	Chr1	1650886	A	C	
115/116	AT1G05570	exonic	nonsynonymous SNV	Chr1	1655859	A	T	
115/116	AT1G05575	exonic	nonsynonymous SNV	Chr1	1662071	T	C	
115/116	AT1G05590	exonic	nonsynonymous SNV	Chr1	1670227	A	C	ATHEX3, BETA-HEXOSAMINIDASE 2, BETA-HEXOSAMINIDASE 3, HEXO2
115/116	AT1G05590	exonic	nonsynonymous SNV	Chr1	1670564	G	C	
115/116	AT1G05590	exonic	nonsynonymous SNV	Chr1	1671273	T	G	
115/116	AT1G05610	exonic	nonsynonymous SNV	Chr1	1674739	T	A	
115/116	AT1G05610	exonic	nonsynonymous SNV	Chr1	1675823	T	C	
115/116	AT1G05615	exonic	nonsynonymous SNV	Chr1	1677548	T	A	B3 domain protein
115/116	AT1G05615	exonic	nonsynonymous SNV	Chr1	1677914	A	C	
115/116	AT1G05615	exonic	nonsynonymous SNV	Chr1	1678264	C	T	
115/116	AT1G05620	exonic	nonsynonymous SNV	Chr1	1680254	G	A	
115/116	AT1G05630	exonic	nonsynonymous SNV	Chr1	1682798	A	C	5PTASE13, ARABIDOPSIS THALIANA INOSITOL-POLYPHOSPHATE 5-PHOSPHATASE 13, AT
115/116	AT1G05630	exonic	nonsynonymous SNV	Chr1	1683963	T	G	
115/116	AT1G05630	exonic	nonsynonymous SNV	Chr1	1686860	T	A	
115/116	AT1G05640	exonic	nonsynonymous SNV	Chr1	1688098	C	T	
115/116	AT1G05650	exonic	nonsynonymous SNV	Chr1	1690472	G	C	
115/116	AT1G05650	exonic	nonsynonymous SNV	Chr1	1691013	A	T	
115/116	AT1G05660	exonic	nonsynonymous SNV	Chr1	1695029	G	A	
115/116	AT1G05660	exonic	nonsynonymous SNV	Chr1	1695902	C	T	
115/116	AT1G05670	exonic	nonsynonymous SNV	Chr1	1698662	T	C	Pentatricopeptide repeat (PPR-like) superfamily protein
115/116	AT1G05670	exonic	nonsynonymous SNV	Chr1	1699068	C	T	
115/116	AT1G05670	exonic	nonsynonymous SNV	Chr1	1699680	A	G	
115/116	AT1G05675	exonic	nonsynonymous SNV	Chr1	1701334	G	C	UDP-Glycosyltransferase superfamily protein
115/116	AT1G05675	exonic	nonsynonymous SNV	Chr1	1701577	G	C	
115/116	AT1G05675	exonic	nonsynonymous SNV	Chr1	1702443	C	G	
115/116	AT1G05680	exonic	nonsynonymous SNV	Chr1	1703332	T	C	UGT74E2, URIDINE DIPHOSPHATE GLYCOSYLTRANSFERASE 74E2
115/116	AT1G05680	exonic	nonsynonymous SNV	Chr1	1703338	C	G	
115/116	AT1G05680	exonic	nonsynonymous SNV	Chr1	1703345	T	C	
125/126	AT1G08060	exonic	nonsynonymous SNV	Chr1	2509854	G	A	

125/126	AT1G08065	exonic	nonsynonymous SNV	Chr1	2512212	A	T	ACA5, ALPHA CARBONIC ANHYDRASE 5, ATACA5
125/126	AT1G08065	exonic	nonsynonymous SNV	Chr1	2512258	C	T	
125/126	AT1G08065	exonic	nonsynonymous SNV	Chr1	2512977	C	A	
125/126	AT1G08065	exonic	nonsynonymous SNV	Chr1	2512993	C	T	
125/126	AT1G08070	exonic	nonsynonymous SNV	Chr1	2515041	C	T	EMB3102, EMBRYO DEFECTIVE 3102, ORGANELLE TRANSCRIPT PROCESSING 82, OTP82
125/126	AT1G08070	exonic	nonsynonymous SNV	Chr1	2515968	G	A	
125/126	AT1G08070	exonic	nonsynonymous SNV	Chr1	2516044	C	T	
125/126	AT1G08070	exonic	nonsynonymous SNV	Chr1	2516326	T	C	
125/126	AT1G08070	exonic	nonsynonymous SNV	Chr1	2516397	A	C	
125/126	AT1G08080	exonic	nonsynonymous SNV	Chr1	2518362	C	T	A. THALIANA ALPHA CARBONIC ANHYDRASE 7, ACA7, ALPHA CARBONIC ANHYDRASE 7, A
125/126	AT1G08080	exonic	nonsynonymous SNV	Chr1	2518462	A	T	
125/126	AT1G08080	exonic	nonsynonymous SNV	Chr1	2518485	A	G	
125/126	AT1G08080	exonic	nonsynonymous SNV	Chr1	2518514	G	C	
125/126	AT1G08080	exonic	nonsynonymous SNV	Chr1	2518523	A	T	
125/126	AT1G08100	exonic	nonsynonymous SNV	Chr1	2527436	G	C	
125/126	AT1G08110	exonic	nonsynonymous SNV	Chr1	2535690	T	C	ATGLYI2, GLYOXALASE12
125/126	AT1G08110	exonic	nonsynonymous SNV	Chr1	2535699	T	C	
125/126	AT1G08110	exonic	nonsynonymous SNV	Chr1	2535714	G	T	
125/126	AT1G08110	exonic	nonsynonymous SNV	Chr1	2535715	C	T	
125/126	AT1G08125	exonic	nonsynonymous SNV	Chr1	2540106	C	G	S-adenosyl-L-methionine-dependent methyltransferases superfamily protein
125/126	AT1G08125	exonic	nonsynonymous SNV	Chr1	2542131	A	G	
125/126	AT1G08125	exonic	nonsynonymous SNV	Chr1	2542161	A	C	
125/126	AT1G08130	exonic	nonsynonymous SNV	Chr1	2543632	G	A	ATLIG1, DNA LIGASE 1, LIG1
125/126	AT1G08130	exonic	nonsynonymous SNV	Chr1	2546066	C	A	
125/126	AT1G08130	exonic	nonsynonymous SNV	Chr1	2546069	C	G	
125/126	AT1G08130	exonic	nonsynonymous SNV	Chr1	2547316	G	C	
125/126	AT1G08130	exonic	nonsynonymous SNV	Chr1	2547317	A	T	
125/126	AT1G08130	exonic	nonsynonymous SNV	Chr1	2547318	C	A	
125/126	AT1G08130	exonic	nonsynonymous SNV	Chr1	2547320	T	C	
125/126	AT1G08130	exonic	nonsynonymous SNV	Chr1	2547459	A	T	
125/126	AT1G08130	exonic	nonsynonymous SNV	Chr1	2547485	G	C	
125/126	AT1G08130	exonic	nonsynonymous SNV	Chr1	2547487	A	G	
125/126	AT1G08130	exonic	nonsynonymous SNV	Chr1	2547506	G	A	

125/126	AT1G08130	exonic	nonsynonymous SNV	Chr1	2547518	A	G	
125/126	AT1G08130	exonic	nonsynonymous SNV	Chr1	2547688	G	A	
125/126	AT1G08130	exonic	nonsynonymous SNV	Chr1	2547721	A	C	
125/126	AT1G08130	exonic	nonsynonymous SNV	Chr1	2547728	T	G	
125/126	AT1G08130	exonic	nonsynonymous SNV	Chr1	2547743	A	C	
125/126	AT1G08130	exonic	nonsynonymous SNV	Chr1	2547759	T	G	
125/126	AT1G08135	exonic	nonsynonymous SNV	Chr1	2548992	A	C	ATCHX6B, CATION/H+ EXCHANGER 6B, CHX6B
125/126	AT1G08135	exonic	nonsynonymous SNV	Chr1	2549136	A	G	
125/126	AT1G08135	exonic	nonsynonymous SNV	Chr1	2549711	G	T	
125/126	AT1G08135	exonic	nonsynonymous SNV	Chr1	2549914	A	T	
125/126	AT1G08135	exonic	nonsynonymous SNV	Chr1	2550447	G	T	
125/126	AT1G08135	exonic	nonsynonymous SNV	Chr1	2550594	T	G	
125/126	AT1G08135	exonic	nonsynonymous SNV	Chr1	2551032	A	C	
125/126	AT1G08135	exonic	nonsynonymous SNV	Chr1	2551048	C	A	
125/126	AT1G08135	exonic	nonsynonymous SNV	Chr1	2551440	A	G	
125/126	AT1G08140	exonic	nonsynonymous SNV	Chr1	2552226	G	C	ATCHX6A, CATION/H+ EXCHANGER 6A, CHX6A
125/126	AT1G08140	exonic	nonsynonymous SNV	Chr1	2552246	T	C	
125/126	AT1G08140	exonic	nonsynonymous SNV	Chr1	2553324	T	G	
125/126	AT1G08140	exonic	nonsynonymous SNV	Chr1	2553380	G	T	
125/126	AT1G08140	exonic	nonsynonymous SNV	Chr1	2553393	G	A	
125/126	AT1G08140	exonic	nonsynonymous SNV	Chr1	2554146	C	G	
125/126	AT1G08140	exonic	nonsynonymous SNV	Chr1	2554217	C	A	
125/126	AT1G08140	exonic	nonsynonymous SNV	Chr1	2554240	T	C	
125/126	AT1G08150	exonic	nonsynonymous SNV	Chr1	2556911	A	T	ATCHX5, CATION/H+ EXCHANGER 5, CHX5
125/126	AT1G08150	exonic	nonsynonymous SNV	Chr1	2557414	C	G	
125/126	AT1G08150	exonic	nonsynonymous SNV	Chr1	2558213	G	T	
125/126	AT1G08150	exonic	nonsynonymous SNV	Chr1	2558221	A	C	
125/126	AT1G08150	exonic	nonsynonymous SNV	Chr1	2558270	C	T	
125/126	AT1G08150	exonic	nonsynonymous SNV	Chr1	2558300	T	G	
125/126	AT1G08150	exonic	nonsynonymous SNV	Chr1	2558827	T	A	
125/126	AT1G08150	exonic	nonsynonymous SNV	Chr1	2559028	A	T	
125/126	AT1G08150	exonic	nonsynonymous SNV	Chr1	2559048	C	G	
125/126	AT1G08150	exonic	nonsynonymous SNV	Chr1	2559065	G	T	

125/126	AT1G08170	exonic	nonsynonymous SNV	Chr1	2563240	C	T	Histone superfamily protein
125/126	AT1G08170	exonic	nonsynonymous SNV	Chr1	2563458	A	G	
125/126	AT1G08170	exonic	nonsynonymous SNV	Chr1	2563473	G	C	
125/126	AT1G08170	exonic	nonsynonymous SNV	Chr1	2563515	A	G	
125/126	AT1G08170	exonic	nonsynonymous SNV	Chr1	2563569	A	G	
125/126	AT1G08170	exonic	nonsynonymous SNV	Chr1	2563606	T	C	
125/126	AT1G08190	exonic	nonsynonymous SNV	Chr1	2571385	G	C	
125/126	AT1G08210	exonic	nonsynonymous SNV	Chr1	2577153	A	G	Eukaryotic aspartyl protease family protein
125/126	AT1G08210	exonic	nonsynonymous SNV	Chr1	2577192	T	A	
125/126	AT1G08210	exonic	nonsynonymous SNV	Chr1	2579650	A	C	
125/126	AT1G08220	exonic	nonsynonymous SNV	Chr1	2581872	C	T	ATPase complex subunit
125/126	AT1G08220	exonic	nonsynonymous SNV	Chr1	2582456	C	T	
125/126	AT1G08220	exonic	nonsynonymous SNV	Chr1	2582551	G	A	
125/126	AT1G08230	exonic	nonsynonymous SNV	Chr1	2584326	T	A	Codes for a H+-driven, high affinity gamma-aminobutyric acid (GABA) transporter
125/126	AT1G08230	exonic	nonsynonymous SNV	Chr1	2584662	G	T	
125/126	AT1G08230	exonic	nonsynonymous SNV	Chr1	2584663	G	T	
125/126	AT1G08230	exonic	nonsynonymous SNV	Chr1	2584702	G	A	
125/126	AT1G08230	exonic	nonsynonymous SNV	Chr1	2584705	C	T	
125/126	AT1G08230	exonic	nonsynonymous SNV	Chr1	2586289	T	C	
125/126	AT1G08230	exonic	nonsynonymous SNV	Chr1	2586414	G	T	
125/126	AT1G08250	exonic	nonsynonymous SNV	Chr1	2590091	C	T	
125/126	AT1G08260	exonic	nonsynonymous SNV	Chr1	2604067	A	G	ABA OVERLY SENSITIVE 4, ABO4, EARLY IN SHORT DAYS 7, EMB142, EMB2284, EMB529,
125/126	AT1G08260	exonic	nonsynonymous SNV	Chr1	2605196	C	G	
125/126	AT1G08260	exonic	nonsynonymous SNV	Chr1	2606695	G	C	
125/126	AT1G08270	exonic	nonsynonymous SNV	Chr1	2607078	T	A	
125/126	AT1G08280	exonic	nonsynonymous SNV	Chr1	2608462	G	A	GALT29A, GLYCOSYLTRANSFERASE 29A
125/126	AT1G08280	exonic	nonsynonymous SNV	Chr1	2608534	T	A	
125/126	AT1G08280	exonic	nonsynonymous SNV	Chr1	2608969	A	G	
125/126	AT1G08280	exonic	nonsynonymous SNV	Chr1	2609119	A	G	
125/126	AT1G08280	exonic	nonsynonymous SNV	Chr1	2609290	A	G	
125/126	AT1G08280	exonic	nonsynonymous SNV	Chr1	2609540	G	A	
125/126	AT1G08290	exonic	nonsynonymous SNV	Chr1	2611044	A	G	
125/126	AT1G08290	exonic	nonsynonymous SNV	Chr1	2612922	G	T	

125/126	AT1G08300	exonic	frameshift insertion	Chr1	2616190	C	CT	NO VEIN-LIKE, NVL
125/126	AT1G08300	exonic	frameshift insertion	Chr1	2618749	G	GA	
125/126	AT1G08300	exonic	nonsynonymous SNV	Chr1	2615541	C	A	
125/126	AT1G08300	exonic	nonsynonymous SNV	Chr1	2615681	A	C	
125/126	AT1G08300	exonic	nonsynonymous SNV	Chr1	2616091	T	C	
125/126	AT1G08300	exonic	nonsynonymous SNV	Chr1	2616190	C	T	
125/126	AT1G08300	exonic	nonsynonymous SNV	Chr1	2617758	A	C	
125/126	AT1G08300	exonic	nonsynonymous SNV	Chr1	2617809	T	A	
125/126	AT1G08300	exonic	nonsynonymous SNV	Chr1	2617815	A	G	
125/126	AT1G08300	exonic	nonsynonymous SNV	Chr1	2617873	C	A	
125/126	AT1G08300	exonic	nonsynonymous SNV	Chr1	2617914	A	G	
125/126	AT1G08300	exonic	nonsynonymous SNV	Chr1	2617980	C	T	
125/126	AT1G08300	exonic	nonsynonymous SNV	Chr1	2618297	C	T	
125/126	AT1G08300	exonic	nonsynonymous SNV	Chr1	2618641	T	A	
125/126	AT1G08310	exonic	nonsynonymous SNV	Chr1	2619464	C	A	
125/126	AT1G08320	exonic	nonsynonymous SNV	Chr1	2625734	C	T	
125/126	AT1G08340	exonic	frameshift insertion	Chr1	2632664	C	CA	Rho GTPase activating protein with PAK-box/P21-Rho-binding domain-containing protei
125/126	AT1G08340	exonic	nonsynonymous SNV	Chr1	2632486	T	A	
125/126	AT1G08340	exonic	nonsynonymous SNV	Chr1	2632613	G	T	
125/126	AT1G08350	exonic	nonsynonymous SNV	Chr1	2633817	G	A	
125/126	AT1G08350	exonic	nonsynonymous SNV	Chr1	2635515	C	T	
125/126	AT1G08370	exonic	frameshift insertion	Chr1	2639859	C	CCTCACCAA	
125/126	AT1G08370	exonic	nonsynonymous SNV	Chr1	2639845	A	C	
125/126	AT1G08370	exonic	nonsynonymous SNV	Chr1	2640076	C	G	
125/126	AT1G08390	exonic	nonsynonymous SNV	Chr1	2642583	A	C	
125/126	AT1G08400	exonic	nonsynonymous SNV	Chr1	2644262	A	T	RINT-1 / TIP-1 family
125/126	AT1G08400	exonic	nonsynonymous SNV	Chr1	2644442	G	A	
125/126	AT1G08400	exonic	nonsynonymous SNV	Chr1	2645038	C	T	
125/126	AT1G08400	exonic	nonsynonymous SNV	Chr1	2645213	C	T	
125/126	AT1G08410	exonic	nonsynonymous SNV	Chr1	2646460	A	T	DIG6, DROUGHT INHIBITED GROWTH OF LATERAL ROOTS 6, LSG1-2, YEAST LSG1 ORTHO
125/126	AT1G08410	exonic	nonsynonymous SNV	Chr1	2648160	G	A	
125/126	AT1G08410	exonic	nonsynonymous SNV	Chr1	2648581	A	C	
125/126	AT1G08410	exonic	nonsynonymous SNV	Chr1	2648588	A	C	

125/126	AT1G08420	exonic	nonsynonymous SNV	Chr1	2650127	C	T	
125/126	AT1G08420	exonic	nonsynonymous SNV	Chr1	2653619	A	T	
125/126	AT1G08430	exonic	nonsynonymous SNV	Chr1	2658847	T	G	
125/126	AT1G08430	exonic	nonsynonymous SNV	Chr1	2660670	G	A	
125/126	AT1G08440	exonic	nonsynonymous SNV	Chr1	2664419	C	T	aluminum activated malate transporter family protein
125/126	AT1G08440	exonic	nonsynonymous SNV	Chr1	2664489	C	G	
125/126	AT1G08440	exonic	nonsynonymous SNV	Chr1	2664744	A	T	
125/126	AT1G08440	exonic	nonsynonymous SNV	Chr1	2664756	T	G	
125/126	AT1G08440	exonic	nonsynonymous SNV	Chr1	2664772	C	T	
125/126	AT1G08440	exonic	nonsynonymous SNV	Chr1	2664818	C	A	
125/126	AT1G08440	exonic	nonsynonymous SNV	Chr1	2664873	A	G	
125/126	AT1G08440	exonic	nonsynonymous SNV	Chr1	2665107	G	C	
125/126	AT1G08440	exonic	nonsynonymous SNV	Chr1	2665295	T	G	
125/126	AT1G08460	exonic	nonsynonymous SNV	Chr1	2672698	A	G	ATHDA8, HDA08, HDA8, HISTONE DEACETYLASE 8
125/126	AT1G08460	exonic	nonsynonymous SNV	Chr1	2672729	T	G	
125/126	AT1G08460	exonic	nonsynonymous SNV	Chr1	2673048	G	T	
125/126	AT1G08460	exonic	nonsynonymous SNV	Chr1	2674228	T	C	
125/126	AT1G08460	exonic	nonsynonymous SNV	Chr1	2674356	C	T	
125/126	AT1G08460	exonic	nonsynonymous SNV	Chr1	2674392	G	C	
125/126	AT1G08460	exonic	nonsynonymous SNV	Chr1	2674399	A	T	
125/126	AT1G08460	exonic	nonsynonymous SNV	Chr1	2674429	C	G	
125/126	AT1G08460	exonic	nonsynonymous SNV	Chr1	2674437	A	T	
125/126	AT1G08470	exonic	nonsynonymous SNV	Chr1	2683834	C	A	
125/126	AT1G08470	exonic	nonsynonymous SNV	Chr1	2683974	C	T	
125/126	AT1G08480	exonic	nonsynonymous SNV	Chr1	2684443	G	C	
125/126	AT1G08490	exonic	nonsynonymous SNV	Chr1	2686021	C	A	
125/126	AT1G08490	exonic	nonsynonymous SNV	Chr1	2687526	C	A	
125/126	AT1G08500	exonic	nonsynonymous SNV	Chr1	2689634	C	G	
125/126	AT1G08520	exonic	nonsynonymous SNV	Chr1	2696747	T	A	ALB-1V, ALB1, ALBINA 1, CHLD, PDE166, PIGMENT DEFECTIVE EMBRYO 166, V157
125/126	AT1G08520	exonic	nonsynonymous SNV	Chr1	2697959	A	T	
125/126	AT1G08520	exonic	nonsynonymous SNV	Chr1	2699081	A	C	
125/126	AT1G08530	exonic	frameshift insertion	Chr1	2701364	A	ACT	chitinase-like protein
125/126	AT1G08530	exonic	frameshift insertion	Chr1	2702948	A	AT	

125/126	AT1G08530	exonic	nonsynonymous SNV	Chr1	2701294	T	C	
125/126	AT1G08530	exonic	nonsynonymous SNV	Chr1	2701297	C	T	
125/126	AT1G08530	exonic	nonsynonymous SNV	Chr1	2701309	G	C	
125/126	AT1G08530	exonic	nonsynonymous SNV	Chr1	2701319	C	G	
125/126	AT1G08530	exonic	nonsynonymous SNV	Chr1	2701340	C	A	
125/126	AT1G08530	exonic	nonsynonymous SNV	Chr1	2701366	G	C	
125/126	AT1G08530	exonic	nonsynonymous SNV	Chr1	2701366	G	T	
125/126	AT1G08530	exonic	nonsynonymous SNV	Chr1	2701369	T	A	
125/126	AT1G08530	exonic	nonsynonymous SNV	Chr1	2701370	C	A	
125/126	AT1G08530	exonic	nonsynonymous SNV	Chr1	2701372	C	A	
125/126	AT1G08530	exonic	nonsynonymous SNV	Chr1	2701373	A	T	
125/126	AT1G08530	exonic	nonsynonymous SNV	Chr1	2701376	C	T	
125/126	AT1G08530	exonic	nonsynonymous SNV	Chr1	2701423	A	G	
125/126	AT1G08530	exonic	nonsynonymous SNV	Chr1	2701522	T	G	
125/126	AT1G08530	exonic	nonsynonymous SNV	Chr1	2702918	A	C	
125/126	AT1G08540	exonic	nonsynonymous SNV	Chr1	2703512	A	C	ABC1, ATSIG1, ATSIG2, RNA POLYMERASE SIGMA SUBUNIT 1, RNAPOLYMERASE SIGMA S
125/126	AT1G08540	exonic	nonsynonymous SNV	Chr1	2704774	T	C	
125/126	AT1G08540	exonic	nonsynonymous SNV	Chr1	2704795	A	T	
125/126	AT1G08540	exonic	nonsynonymous SNV	Chr1	2704796	T	C	
125/126	AT1G08540	exonic	nonsynonymous SNV	Chr1	2704832	A	T	
125/126	AT1G08550	exonic	nonsynonymous SNV	Chr1	2707640	C	T	ARABIDOPSIS VIOLAXANTHIN DE-EPOXIDASE 1, AVDE1, NON-PHOTOCHEMICAL QUENCH
125/126	AT1G08550	exonic	nonsynonymous SNV	Chr1	2707773	C	G	
125/126	AT1G08550	exonic	nonsynonymous SNV	Chr1	2709007	A	G	

Supplementary Table S6: microStairs; differentially expressed genes controlled in cis

List of Cvi/Col differentially expressed genes in an allele-specific fashion ([log2]>0.8 in at least one condition; from Cubillos *et al.*, 2014) across the whole region.

	ASE Control (WW)				ASE Stress (WD)					
Gene ID	Col reads	Cvi reads	Col/Cvi(log2)	q-value	Col reads	Cvi reads	Col/Cvi(log2)	q_value	**intervals microStairs**	**Gene generic name**
AT1G01650	81	108	-0,402639894	0,07560446	108	194	-0,845655158	3,65713E-06	101/102 &102/103	ARABIDOPSIS THALIANA SIGNAL PEPTIDE PEPTIDASE-LIKE 4, ATSPPL4
AT1G02330	349	138	1,337279936	6,97655E-21	332	134	1,307526862	2,08595E-19	103/104 &104/105	COP1 SUPPRESSOR 2, CSU2
AT1G02820	187	90	1,056044642	1,7085E-08	209	120	0,80043073	6,11044E-06	105/106 & 106/107	ATLEA3, LATE EMBRYOGENESIS ABUNDANT 3, LEA3
AT1G04270	1232	589	1,064582504	1,12091E-50	1095	562	0,960855303	2,26474E-38	110/111 & 111/112	CYTOSOLIC RIBOSOMAL PROTEIN S15, RPS15
AT1G04590	151	95	0,665060862	0,001028409	238	120	0,984119372	2,61273E-09	111/112 & 112/113	PPR containing-like protein;(source:Araport11)
AT1G04820	946	158	2,579042003	5,8722E-135	1261	267	2,240487717	1,7323E-152	112/113 & 113/114	TOR2, TORTIFOLIA 2, TUA4, TUBULIN ALPHA-4 CHAIN
AT1G05190	757	1326	-0,808945186	8,83925E-35	1285	1744	-0,440815502	7,13456E-16	114/115 & 115/116	EMB2394, EMBRYO DEFECTIVE 2394, RPL6
AT1G05200	387	256	0,600150477	1,02508E-06	274	149	0,880791484	7,1714E-09	114/115 & 115/116	ATGLR3.4, GLR3.4, GLUR3, GLUTAMATE RECEPTOR 3.4
AT1G05830	322	185	0,801618342	6,04279E-09	242	147	0,720931695	5,31431E-06	116/117 & 117/118	ATX2, SDG30, SET DOMAIN PROTEIN 30, TRITHORAX-LIKE PROTEIN 2
AT1G05940	314	169	0,896291292	2,26578E-10	287	184	0,645465342	9,71077E-06	117/118 & 118/119	CAT9, CATIONIC AMINO ACID TRANSPORTER 9
AT1G06010	316	122	1,369212951	1,11664E-19	116	55	1,076416631	1,41487E-05	117/118 & 118/119	basic leucine zipper/W2 domain protein;(source:Araport11)
AT1G06550	128	238	-0,893177584	5,53467E-08	136	215	-0,657481446	8,27649E-05	118/119 & 119/120	ATP-dependent caseinolytic (Clp) protease/crotonase family protein;(source:Araport11)
AT1G06640	849	75	3,500514393	5,4528E-165	1317	119	3,465373996	9,1562E-254	119/120 & 120/121	similar to a 2-oxoglutarate-dependent dioxygenase
AT1G06645	317	185	0,77935644	1,92031E-08	298	114	1,384912101	4,99852E-19	119/120 & 120/121	2-oxoglutarate (2OG) and Fe(II)-dependent oxygenase superfamily protein
AT1G07110	439	267	0,718500344	7,06647E-10	392	221	0,831349133	3,3311E-11	120/121 & 121/122	"FRUCTOSE-2,6-BISPHOSPHATASE", ATF2KP, F2KP, FKFBP
AT1G07140	586	205	1,516955755	5,29432E-42	392	188	1,063211171	1,59872E-16	120/121 & 121/122	SIRANBP
AT1G07470	430	165	1,383568313	4,19265E-27	432	173	1,320547496	2,32775E-25	122/123 & 123/124	Transcription factor IIA, alpha/beta subunit;(source:Araport11)
AT1G07670	481	261	0,88332755	4,14228E-15	443	234	0,917972643	6,87879E-15	122/123 & 123/124	ATECA4, ECA4, ENDOMEMBRANE-TYPE CA-ATPASE 4
AT1G07790	114	308	-1,438891813	1,055E-20	73	131	-0,842002787	0,000195055	123/124 & 124/125	HTB1
AT1G08000	419	211	0,986977656	6,69742E-16	335	265	0,337338638	0,009191087	123/124 & 124/125	GATA TRANSCRIPTION FACTOR 10, GATA10
AT1G08650	670	401	0,738737387	1,41887E-15	1019	383	1,412385267	2,80763E-65	126/127 & 127/128	ATPPCK1, PHOSPHOENOLPYRUVATE CARBOXYLASE KINASE 1, PPCK1
AT1G09200	743	241	1,626965603	1,2041E-58	1115	306	1,866440723	2,2682E-106	128/129 & 129/130	H3.1, HISTONE 3.1
AT1G09590	4894	2357	1,054069628	4,3167E-197	4069	1539	1,402271696	5,0292E-257	128/129 & 129/130	Translation protein SH3-like family protein;(source:Araport11)

Extracted from Cubillos et al., The Plant Cell, 2014
Genes that were also identified as local eQTL (Cubillos et al., BMC Genomics, 2012) are in bold